VLT/ERIS

ERIS User Manual

Doc. No.: ESO-476500

Issue: 117.1

Date: 08/12/2025

Prepared . . . .
            Name   Date   Signature

Approved . . . .
            Name   Date   Signature

Released . . . .
            Name   Date   Signature

Original authors: Y. Dallilar, K. Kravchenko, W. Taylor, S. Esposito, R. Davies, E. Sturm

This page was intentionally left blank

Change Record

Version	Date	Section	Comment
111.0	25/08/2022	–	Initial release for P111
111.1	24/01/2023	2.4.1.1	Updated readout noise values (NIX)
		2.4.1.3	Added recommendation for jitter box size
		2.5.6.1	Updated readout noise values (SPIFFIER)
		3.4	Added offsets between SPIFFIER FoVs
		4.2.3.1	PA of North for APP observations
		4.3.1.2	Updated bright limits for IFS
		6.4	Instrument overheads updated
		7.1.2	PA of North for APP, FPC, SAM observations
		7.2	Telescope guide star now mandatory
		7.3	Revised SPIFFIER acquisition procedure
		7.4.2	Changed `DETECTOR` offset convention
		7.7.1	Added information about telluric standards
112.0	28/02/2023	2.4.1.2	Modification to windows, added figure
		3.2	Non-sidereal and differential tracking
		3.3	Seeing enhancer mode
		3.5.3	Updated with new NIX modes
		4.2.3.1	Updated peak intensities of the APP PSF
		4.2.3.2	Added information for SAM
		4.3.1.1	Added restriction on NDITs for long DIT
		4.3.2	Updated SPIFFIER line profiles
		5.1, 5.2	New modes offered in P112
		5.5, 6.2, 7.1.1	New NGS and LGS limiting magnitudes
		6.4	New and updated overhead estimates
		7.2.1	New section describing P2 for non-sidereal and differential tracking
		7.3	Updated acquisition positions
		7.8.2.1	New IFS templates
		7.8.2.2	New NIX templates
112.1	30/06/2023	4.2.1.3	Updated bright limit table
		4.2.1.4	Added description of file transfer overheads
		4.2.3.1	Added recommendation for unsaturated APP calibration
		4.2.3.2	Added rotator angle for SAM observations
		5.5	Reduced maximum off-axis limit to 59″
		6.5.2	Updates to calibration plan
		7.1.2	Added recommendation for unsaturated APP calibration
		7.2.1	Further details for P2 for non-sidereal acquisitions
		7.9.2.2	Added recommendation for unsaturated APP calibration
		7.10	Added OB naming rules
113.0	25/08/2023	3	Added new modes offered in P113
		3.5.3	Added new modes offered in P113
		4.2.1.2	Reduced maximum number of NDITs allowed in cube mode
		4.2.1.3	Added more information about saturation with up-the-ramp sampling
		4.2.3.3	Added information about NIX FPC
		4.2.3.4	Added information about NIX LSS
		4.3.1.2	Added more information about saturation with up-the-ramp sampling
		5.1	Added new modes offered in P113
		5.5	Added coherence time to table of constraints
		5.6.9	Added faint limit for NIX FPC observations
		6.5.2	Reduced the number of standards observed at start of operations with NIX
		6.5.3	Added NIX LSS telluric standards
		7.1.2	Added notes for NIX FPC and LSS observations
		7.3	Added NIX FPC, LSS acquisition positions

		7.5	Updated blind offset section
		7.7.3	Added placeholder for NIX LSS telluric standards
		7.8	Added NIX LSS telluric standards
		7.8.2.2	Added example templates for NIX FPC and LSS
		7.9.2.3	Added NIX LSS telluric standards
113.1	24/11/2023	6.4	Updated detector overheads for IFS and NIX
		7.1, 7.2.1	Added information regarding EXTENDED and EXTENDED_FULL keywords
		7.1.2, 7.1.3	Added more information for NIX/IFS OB preparation
114.0	01/02/2024	5.5, 5.6.1	NGS TCAT limit now 70%
114.1	14/04/2024	2.4.1.1	Added information about fast mode overheads
		4.2.1.2	Updated NDIT limits in cube mode for NIX
		4.2.3.3	Extensive modifications to the FPC section
		4.3.1.1	Added 180s, 450s to list of allowed DITs for SPIFFIER
		7.1.3	Added recommendation to image tip-tilt star to measure drift induced by differential flexure in SPIFFIER observations
115.0	24/11/2024	4.2.3.3	Added reference to off-axis PSF measurement procedure
		7.1.2	Recommendation for precision photometry with standard imaging, description of off-axis PSF measurement with nixFPC_GenericOffset template, and description of the offset issue for OBs with multiple nixFPC observing templates.
116.0	01/03/2025	3.4, 3.5, 5.1 5.2, 7.1	Pupil tracking offered for IFS and nixIMG observations.
		7.4.2	Added section describing the calculation of the position angle of North.
116.1	07/05/2025	4.2.3.3	Updating DIT below which overheads may affect QACITS performance
		7.1.2.4	Updated advice for off-axis PSF measurement
		7.1.4	Restrictions when using pupil tracking
117.0	01/09/2025	3.0	Added length of long slit to Table 6
		7.1.2.4	Software bug affecting FPC offsets has been fixed
		7.4.2	Corrected equation for PA of North for 13mas-JHK/LM cameras.
117.1	08/12/2025	2.4.1.2	Documented bug in position of detector window in fast readout.
		4.2.1.2	Increased NDIT limits in cube mode
		4.2.3.3	Moved description of FPC acquisition and observation to 7.2.1.4.
		7	Major re-organisation of this section.
		7.1.3, 7.2.2	Described acquire on NGS/TTS functionality.
		8.2.3	Long-slit data reduction.
		8.3	Useful FITS header keywords.

Contents

1 Introduction

1.1 Scope

The ERIS User Manual provides comprehensive information about the technical characteristics of the instrument, the observations procedures and the reduction of ERIS data. The intended audience is Paranal staff who are new to ERIS and will be supporting observations, and also the science users in the community. This is a draft version presented for PAE and is based on the ERIS OCD as well as the SINFONI and NACO user manuals.

In addition to this User Manual, complementary information about ERIS will also be provided on the ERIS web page at `http://www.eso.org/sci/facilities/paranal/instruments/eris/` which you are invited to visit regularly for any last-minute updates.

1.2 Contents of this manual

This document gives an overview of the ERIS instrument and its subsystems. Necessary information will be provided for observation planning and performing observations with ERIS. Additional details will be given on the instrument software and on the operation modes offered during the corresponding period including example observing runs for guidance.

1.3 Latest news and changes

1.4 Reference documents

	Document Number	Document Title	Issue	Date
RD1	ESO-476948	ERIS Calibration Plan	111.0	25/08/2022
RD2	ESO-476499	ERIS Template Manual	111.1	14/12/2022

1.5 Abbreviations and Acronyms

4LGSF	4 Laser Guide Star Facility (a sub-system of the AOF)
ADI	Angular Differential Imaging
AGPM	Annular Groove Phase Mask
AO	Adaptive Optics
AOF	Adaptive Optics Facility
APP	Apodizing Phase Plate
CU	Calibration Unit
DL	Diffraction Limit
DSM	Deformable Secondary Mirror
ESO	European Southern Observatory
FPC	Focal Plane Coronagraphy
IFU	integral Field Unit
LSS	Long Slit Spectroscopy
PAE	Preliminary Acceptance Europe
SAM	Sparse Aperture Mask(ing)
SF	Spatial Filter
SPARTA	Standard Platform for Adaptive Optics Real Time Applications
UT	Unit Telescope
VC	Vortex Coronagraph
VLT	Very Large Telescope
WFS	WaveFront Sensor

ERIS, NACO, SINFONI, NIX, SPIFFI, SPIFFIER, XSHOOTER, VISIR, and SPHERE are names of instruments or cameras.

2 Technical instrument description

2.1 Instrument overview

ERIS is a Cassegrain instrument that will take over the fundamental adaptive optics capabilities at the VLT previously provided by NACO and SINFONI (and operationally has many similarities to those instruments). ERIS instrument has two science cameras; SPIFFIER, an integral field spectrograph covering J to K bands, and NIX, an imager covering J to M bands.

During science operations, users will select either ERIS-NIX or ERIS-SPIFFIER for their observations. ERIS is mounted on UT4 and makes use of the AOF: any one of the four lasers in the 4LGSF can be used to generate a LGS when required (but only one laser at the time), the real-time computer uses SPARTA, and the wavefront correction is done by the DSM.
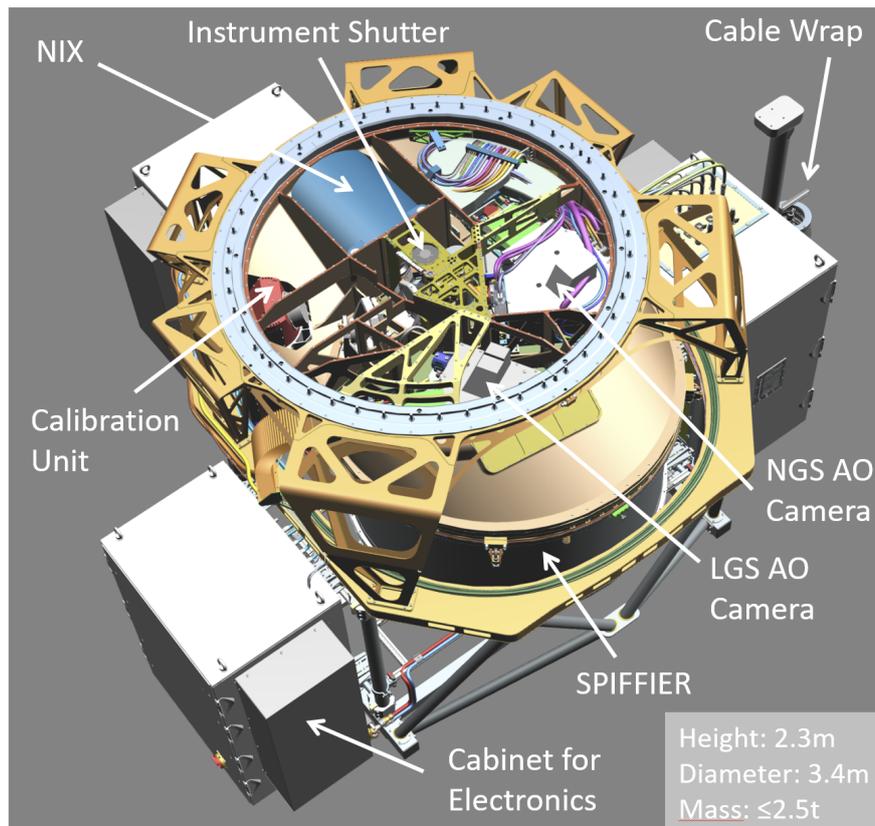
Figure 1: Overview of ERIS as it will appear when mounted on the Cassegrain focus of the UT. The main sub-systems are labelled: the central structure with the LGS and NGS WFS, the NIX imager, the upgraded IFU SPIFFIER, the Calibration Unit, and the Electronics.

As shown in Figure 1, ERIS comprises several distinct sub-systems:

- The **central structure** mounts to the Cassegrain adaptor/rotator. The structure contains the warm relay optics and an optical/infrared dichroic that reflects the visible light to the two wavefront sensors while transmitting the infrared light to either SPIFFIER or NIX. There are two switchable fold mirrors. One of them is used to select either telescope or calibration unit beam (for internal calibrations). The other mirror reflects the incoming beam to either SPIFFIER or NIX, noting that the instruments cannot be used simultaneously. This sub-system also houses a shutter that blocks the surrounding light during internal calibrations.

- The **Adaptive Optics (AO)** system provides corrected wavefronts in the J-M bands to NIX and SPIFFIER using the AOF. Its components are housed in the central structure.

- The **NIX** imager is a replacement for NACO. It provides diffraction limited imaging from J- to M-band over a field of up to 1 arcmin, as well as high contrast capabilities with coronagraphs and sparse aperture masks. It also includes a long-slit spectroscopic mode, covering L-band at a resolution of R~900.

- **SPIFFIER** is an upgrade and refurbishment of SPIFFI, which was the IFU spectrometer of SINFONI. This subsystem provides integral field spectroscopy, with selectable pixel scale on the sky (25, 100, or 250mas) and spectral resolution (J, H, K bands or subsets thereof at R∼5000 and ∼10000 respectively).

- The **Calibration Unit (CU)** provides various internal sources up to 2.5 μm for daily calibrations and technical activities. Long wavelength (L & M band) calibrations with NIX are performed exclusively on-sky.

2.2 Adaptive optics system

The AO module of ERIS provides two main adaptive modes:

1. NGS mode with on/off axis reference star. The search field for the NGS WFS reference star is a radius of 59″. The NGS WFS patrols this FoV by using translation stages in conjunction with a periscope arm. The maximum Zenith distance is 70 degrees.

2. LGS mode with on axis LGS and off axis NGS for tip tilt sensing and truth sensing. The LGS WFS is fixed on axis and translates along the optical axis to accommodate for LGS source focus variable position at different Zenith pointing. The maximum Zenith angles is 60 degrees.

The AO module developed for the ERIS instrument is part of the warm optics, which comprises the relay optics from telescope input beam and the two AO WFSs for LGS and NGS respectively.

2.2.1 Warm optics
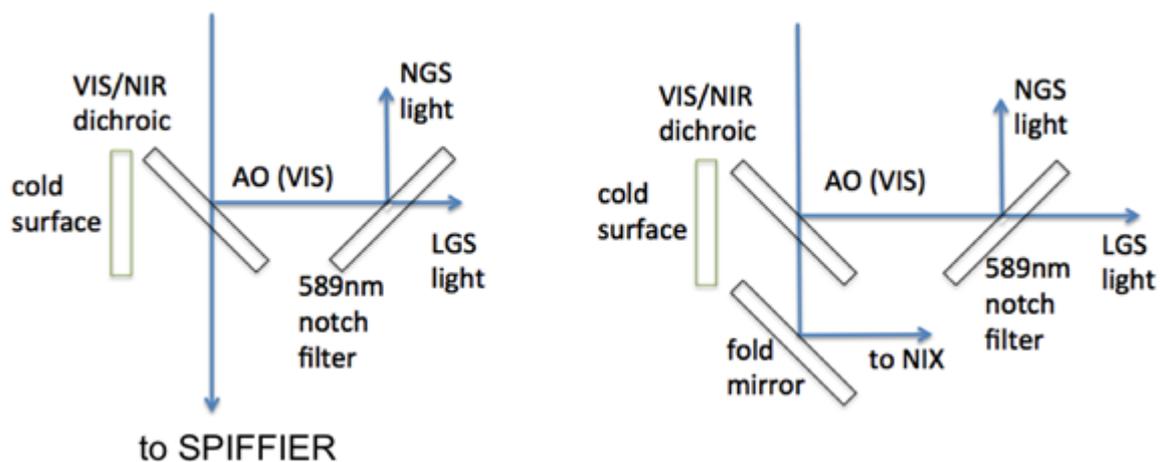
Figure 2: A sketch of the optical path and elements of the warm optics (in black) used to provide IR and VIS light to scientific instruments (NIX, SPIFFIER) and to the AO module. Left: configuration for SPIFFIER operation, right: configuration for NIX operation.

The warm optics feeds the light from the telescope to the AO WFSs. A sketch of the warm optics arrangement and components is shown in Figure 2 where the optical relay configuration for NIX and SPIFFIER observations are reported. The main optical components of the relay include: (a) a 45 degree tilted dichroic separating VIS and NIR light, sending the first to the WFS and the second towards the science instruments; (b) a retractable mirror that is deployed to feed the NIR light to the camera NIX; (c) a notch filter transmitting Sodium Laser light to the LGS WFS and reflecting other visible wavelengths to NGS WFS. In addition a cold window facing part (a) is introduced to reduce background light injected in the science instruments. A detailed picture of the warm optics showing all opto-mechanical components is reported in Figure 3.

2.2.2 NGS wavefront sensor

The NGS WFS is a configurable Shack-Hartmann sensor with 40x40 subapertures for high-order correction, and 5x5 subapertures for low-order & truth sensing for LGS operation. The two configurations respectively referred as HO WFS and LO WFS and are achieved by exchanging two lenslets arrays using a translation stage. The main characteristics of the two SH configurations are reported in the following table.
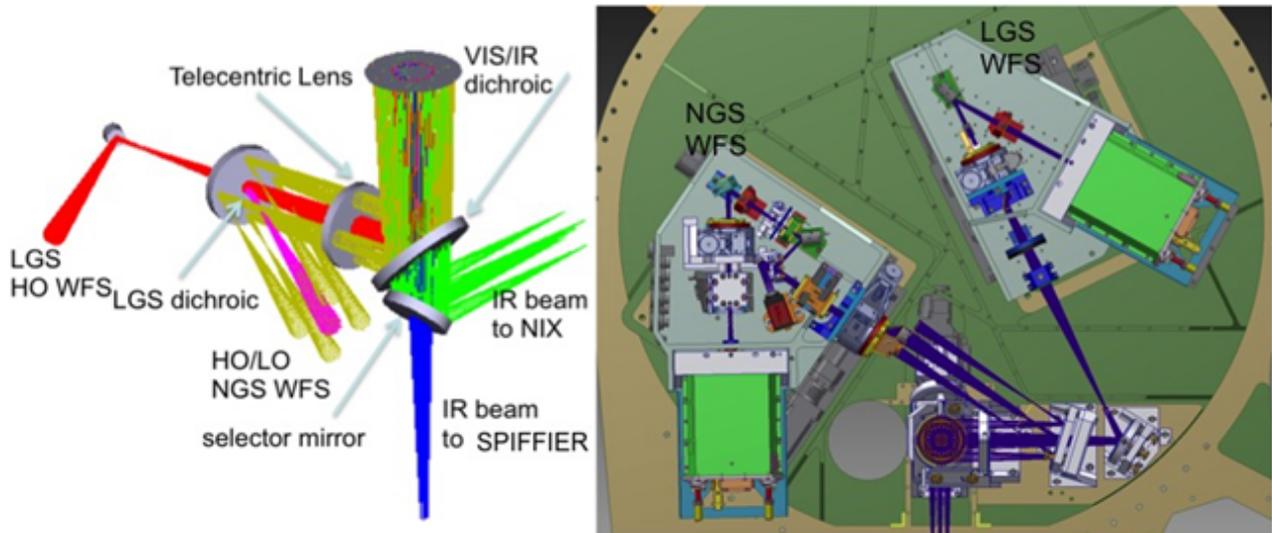
Figure 3: The arrangement of the AO module warm optics. Left: the optical components, right: the opto-mechanical arrangement as mounted on the ERIS optical plate. The figure shows the two ERIS WFSs, the NGS WFS (left) and the LGS WFS (right).
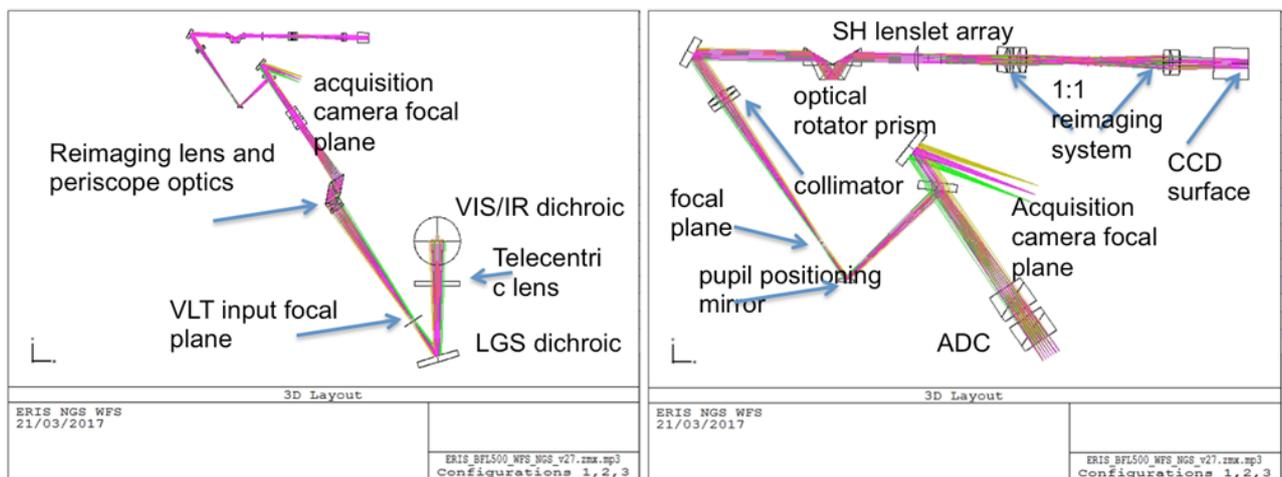
Figure 4: The optical layout of the NGS WFS. Left: optical path from VIS/NIR dichroic, right: zooming into the upper part of the left figure illustrating the optical path from the pupil image to the final spots pattern.

NGS SH sensor main parameters	FoV (arcsec)	Pixel scale (arcsec/pixel)	Pixel per subaperture
HO conf.	2.5	0.41	6x6
LO conf.	2.5	0.21	12x12

The optical layout of the SH WFS path is reported in the Figure 4. In addition, the NGS WFS features an acquisition camera that uses light below 600 nm reflected off-plane by the first folding mirror located after the optical rotator prism. The acquisition camera has a FoV of 15 arcsec and a pixel scale of 0.19 arcsec (when binned by 20 pixels). As labelled in the optical layout the NGS WFS is equipped with:

1. a reimaging lens and periscopic optics that allows to search a radius of $59''$ by rotating the periscope and translating the WFS stages.

2. a derotator used in field tracking mode. It is an optical prism derotator which keeps the pupil image fixed on the CCD.

3. a pupil positioning mirror which keeps the pupil aligned on the SH. It can move the pupil by $\pm$ 8 subapertures on the array.

4. an atmospheric dispersion corrector made up of two equal double prisms that compensate for atmospheric dispersion in the range 0-70 deg.

5. a 1:1 reimaging system made up of two equal lenses that create the final image of the spot pattern onto the CCD.

2.2.3   LGS wavefront sensor
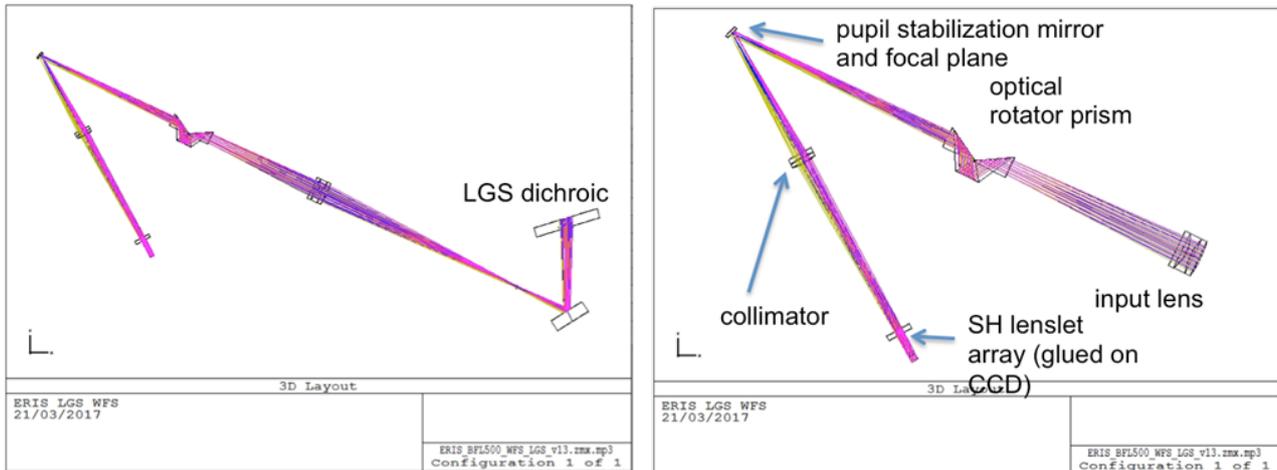
Figure 5: The optical layout of the LGS WFS.

The LGS WFS is a SH sensor with 40x40 subapertures. The main characteristics of the SH configuration are reported in the following table.

LGS SH sensor main parameters	FoV (arcsec)	Pixel scale (arcsec/pixel)	Pixel per subaperture
	5.0	0.83	6x6

The optical layout of the LGS SH sensor is reported in Figure 5. The LGS WFS does not have an acquisition camera so the reference spot is placed in the centre of the FoV by using the 4LGSF acquisition camera.

As labelled in the optical layout the LGS WFS is equipped with: (1) an optical prism rotator to keep the pupil image fixed on the CCD pixel grid while the Cassegrain rotator is moving for field derotation (2) a pupil positioning mirror located close to the focal plane to adjust the pupil image on the SH lenslet array in the range of $\pm$ 8 subapertures.

2.3 Calibration Unit
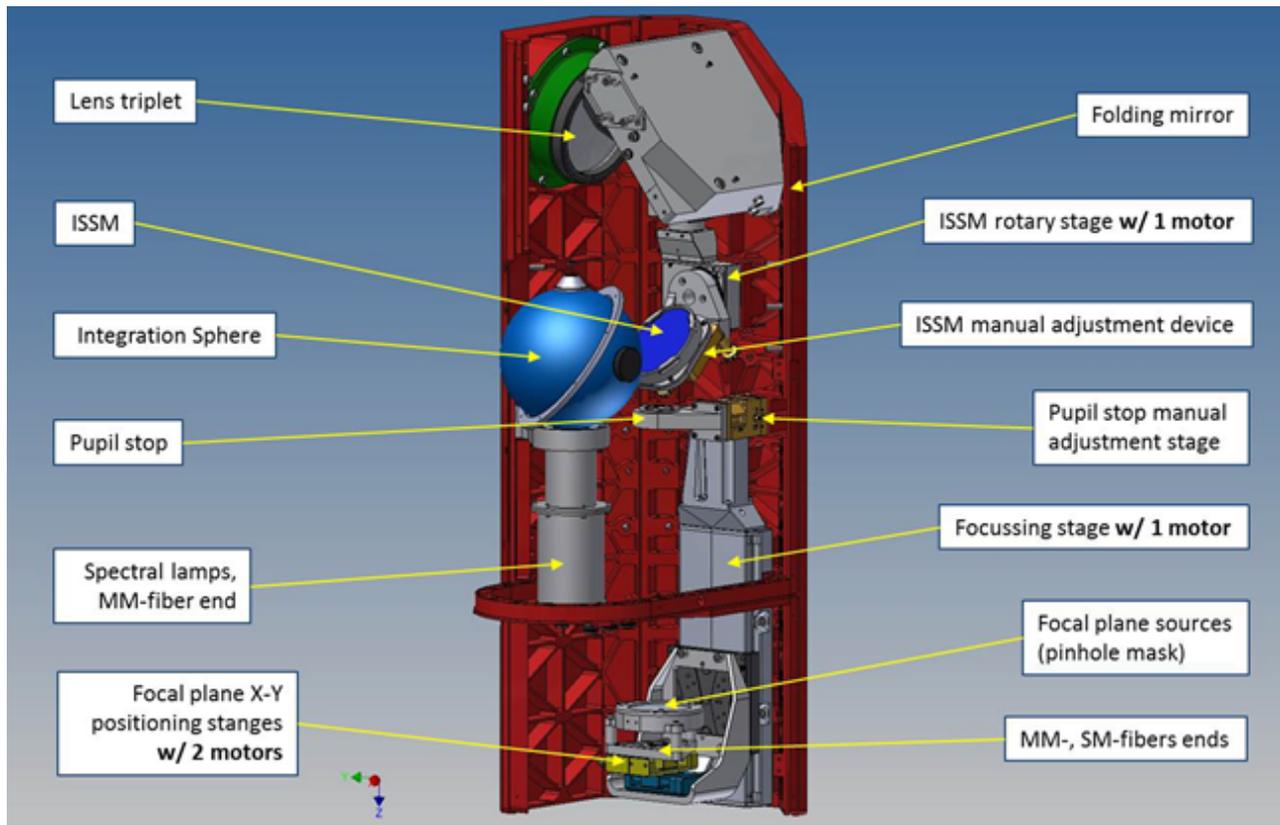
Figure 6: CUMB main components and devices.

The Calibration Unit (CU) is a subsystem of ERIS that provides calibration capabilities for the ERIS instruments (NIX, SPIFFI and AO WFS). It is composed of two separate units.

The first unit, the Calibration Unit Main Bench (CUMB), is optically and mechanically interfaced with ERIS optical plate, the main components can be seen in Figure 6. It is equipped with an objective transmitting from visible to 2.5 μm that operates with a magnification of 1:1.296 in order to project point sources of various sizes onto the Cassegrain focal plane and to deliver a projected virtual position of the pupil that coincides with the telescope secondary mirror. Alternatively, the integrating sphere selector mirror (ISSM) is inserted in the beam to deliver spatially uniform illumination. The second unit, the Calibration Unit Fiber Switchyard (CUFS), is hosted inside one of the ERIS cabinets and interfaced to the CU only. It hosts light sources for flat field capabilities and pinhole mask sources.

The CU includes a selection of light sources: (1) a Quartz-Tungsten Halogen lamp (QTH), (2) four pencil-ray lamps (Ne, Xe, Kr, Ar), (3) a Laser Driven Light Source (LDLS). The QTH lamp provides flat-fielding capabilities during day-time, and covers all possible configurations of SPIFFIER, as well as standard narrow/broad imaging with NIX from J to K bands. In L and M bands, flat-fielding is performed during night-time and on-sky as part of the standard calibration plan. Pre-defined combinations of pencil-ray lamps are used for SPIFFIER wavelength calibrations depending on the instrument configuration. These lamps are all used with the integrating sphere.

The LDLS serves different purposes with a selected pattern of masks placed onto the back focal plane of the objective, which is used to generate artificial optical/infrared point and extended sources and the back-lit triple-slit. There are two mechanisms associated with the configuration: one allowing adjustment along the beam for focusing purposes and other lateral adjustment, i.e. position on the NIX/SPIFFIER detector. The triple-slit configuration is exclusively used for distortion correction with SPIFFIER. Other options are only available for technical day-time activities.

This is the only configuration of the CU in which the beam passes through a fixed pupil which imitates the secondary mirror of the telescope and the spiders. An artificial point source is used, in this case, for the internal alignment of ERIS subsystems. Positioning of a variable neutral density (ND) filter allows adjusting light levels in the instrument software within the range of 12 magnitudes.

2.4 NIX
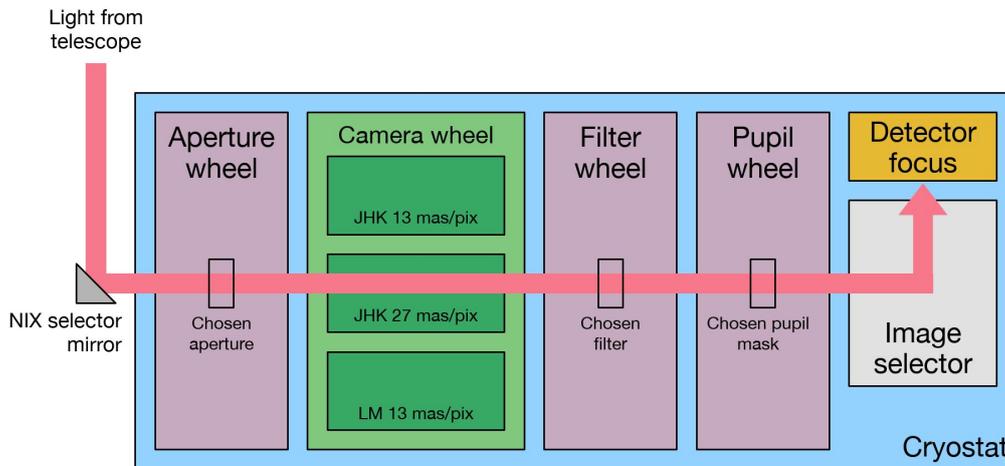
Figure 7: NIX mechanism layout.

The NIX imager provides diffraction-limited observing capabilities from 1-5 microns, with a range of high contrast observing modes. Full details of the ERIS observing modes are given in Section 3 of the document. This section provides a brief overview of the optical layout to explain the aspects of the design that are relevant to the astronomer.

The primary elements of NIX are indicated in Figure 7. As is described in Section 2.2.1 light from the ERIS warm optics is directed into NIX by the NIX selector mirror. The light passes through the aperture window into the cryostat of NIX, indicated by the blue region in the figure. Nearly all components and mechanisms inside the cryostat are cooled to 75K to limit thermal background radiation; the detector is the only item cooled further to ~35K.

The aperture wheel houses various field masks that are used depending on the observing mode. The aperture wheel has eight possible slots, including a blank position, and is driven by stepper motors providing high positional repeatability of order 50 microns. The design and performance of the other wheels is very similar. Its position will be set automatically for a given observing mode.

The next mechanism is the camera wheel, which contains three different camera barrels. Two are optimised for the shorter wavelengths (J, H and K), providing spatial scales of 13 mas/pix or 27 mas/pix. The third camera barrel is for the longer wavelengths (L and M) delivering 13 mas/pix.

The filter wheel and the pupil wheel are identical mechanisms housed within a single unit. Both wheels can house up to 20 elements that can be combined in various ways for the different science cases. As its name suggests the filter wheel houses all the optical filters – more details of which are given in Section 3.5. The pupil wheel contains a mixture of different elements that include pupil masks, but also a grism and additional filters.

The image selector has four positions one for each of the two field sizes, and one to allow the pupil to be imaged. There are also several blocking positions for this mechanism to fully prevent light reaching to detector. This configuration is either used to instrumental dark frames for calibration or to minimise persistence issues during instrument setup.

Finally, the detector focus stage is used to adjust internal focus of NIX detector. It is left in a static configuration for all observing modes (only for technical pupil imaging is a different internal focus position used). In noAO modes, pre-defined best focus offsets are sent to DSM.

2.4.1 Detector

2.4.1.1 Characteristics NIX is equipped with a science grade Teledyne Hawaii 2RG detector (2Kx2K). The characteristics of detector are summarised in Table 3. Two readout modes are supported:

- In slow mode, up the ramp (UTR) readout scheme is used as in SPIFFIER. The readnoise as a function of DIT is shown in Figure 8.

- In fast mode, an uncorrelated readout scheme is used. The purpose of this mode is either high background observations in L and M bands or special observing modes requiring fast data acquisition (without special

timing requirements).

In fast mode, raw images have ∼10-11k ADU bias level which varies depending on the channels for the most part. This subtracts out well, and is only noted here to avoid confusion. The fast readout can also have a significant overhead at the start of each exposure if the `DIT` is more than a few tenths of a second. The sequencer performs ten integrations (each of length `DIT`) before starting the integration that will be saved to disk. This alone leads to an overhead of $10 \times$ `DIT` at the start of each exposure, regardless of whether cube mode is used or not. This overhead becomes very significant for `DIT`> 2 s.

Operating Temperature	∼35K
Pixel size	18 microns
Dark Current	∼0.1 e-/s
Well Depth	∼85k e-
Slow Mode `SLOW_GR_UTR`	
Detector Gain	5.2 e-/ADU
Readout Noise	∼17 e- (2 s)
	∼9 e- (60 s)
	∼12 e- (600 s)
Minimum DIT	1.97 s (`windowF`)
	1.39 s (`window1`)
	1.19 s (`window2`)
	0.79 s (`window3,4,5`)
Non-linearity	∼ 3% (@ 5k ADU)
Fast Mode `FAST_UNCORR`	
Detector Gain	2.6 e-/ADU
Readout Noise	∼50 e-
Minimum DIT	0.0336 s (`windowF`)
	0.0215 s (`window1`)
	0.0171 s (`window2`)
	0.0087 s (`window3,4,5`)
Non-linearity	∼ 4% (@ 20k ADU)

Table 3: NIX detector parameters
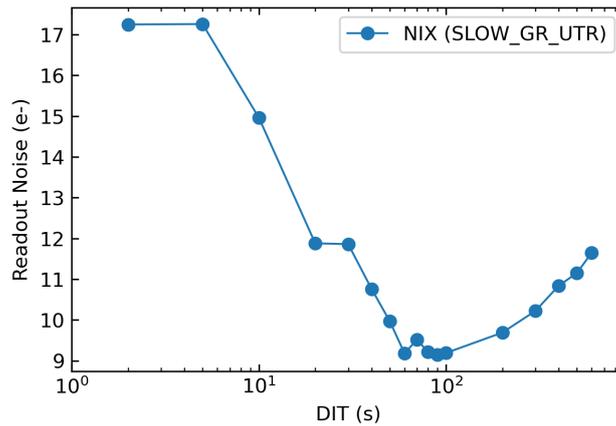
Figure 8: Detector readout noise as a function of detector integration time (DIT) for the the slow readout mode (`SLOW_GR_UTR`) of NIX. This curve is used by the ERIS ETC to estimate S/N of observations.

2.4.1.2 Sub-arrays NIX detector offers capabilities to increase the readout speed (with respect to that reported in Table 3) by restricting the readout to be done only between two selected rows. This applies only in the vertical direction (i.e. along the read channels); the horizontal width (i.e. across the read channels) is always kept full. Each window can be used with either the `SLOW_GR_UTR` or `FAST_UNCORR` readout modes.

In NIX templates, this feature is introduced via a set of predefined options for the `SEQ.NIX.DET.WINDOWING` parameter. The options are given in Table 4. Note that `window1` and `window3` are only to be used with FPC observations, and `window4` is strongly recommended for APP and SAM observations to reduce data volume.

Due to a bug in the detector control software the first row was one higher than requested for windowed data taken in the `FAST_UNCORR` readout mode before 2025 December 05 16:00 (MJD 61014.67). For the manual processing of windowed data taken in this mode before this date you should add one to the value of `DET.SEQ1.WIN.STRY` recorded in the header. The ERIS pipeline automatically corrects for this bug when processing such data.

DET.WINDOWING		First Row	No of Rows	IMG	APP	FPC	SAM	Comment
windowF	SLOW	1	2048	✓	✓		✓	
	FAST	1	2046	✓	✓		✓	
window1		751	1296			✓		FPC only, full FoV
window2		1025	1024	✓	✓		✓	
window3		1155	512			✓		FPC only, inner FoV
window4		1281	512	✓	✓		✓	Recommended for APP, SAM
window5		795	512					Observatory use only

Table 4: Pre-defined row selections for NIX readouts.
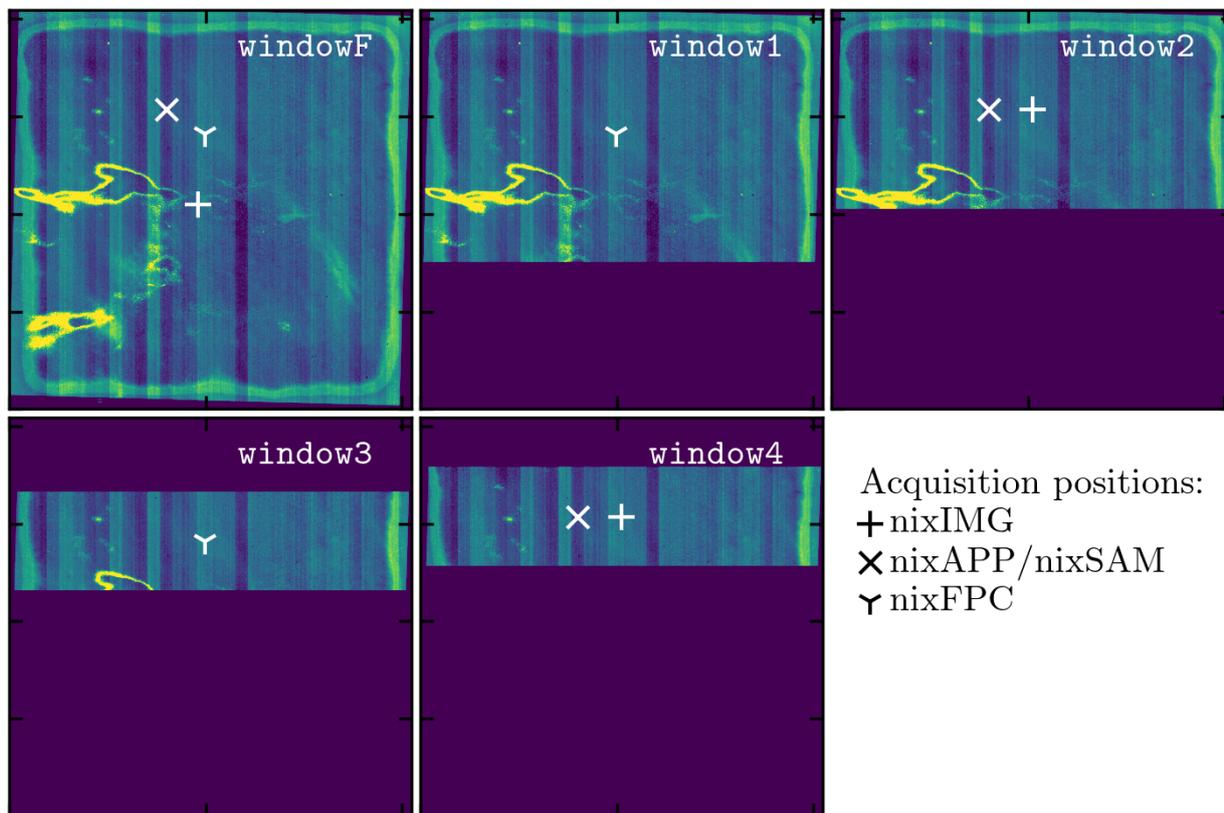
Figure 9: The five different windows that can be read on the NIX detector. The acquisition position for standard imaging (plus symbol) and APP and SAM (cross symbol) are indicated for each sub-array, see Section 7.1.4.

Note that while the `windowF` option is nominally full frame, the `FAST_UNCORR` readout mode provides frames with only 2046 rows. There is no loss in scientific pixels in this case, only two rows of reference pixels are removed in order to reduce detector glow.

2.4.1.3 Bad pixels Some regions on the NIX detector are densely populated by bad pixels, without any distinction on their type. These regions are represented in Figure 10 in terms of number of identified bad pixels neighbouring each pixel. In other words, for pixels marked in red in this figure, there will be very limited local
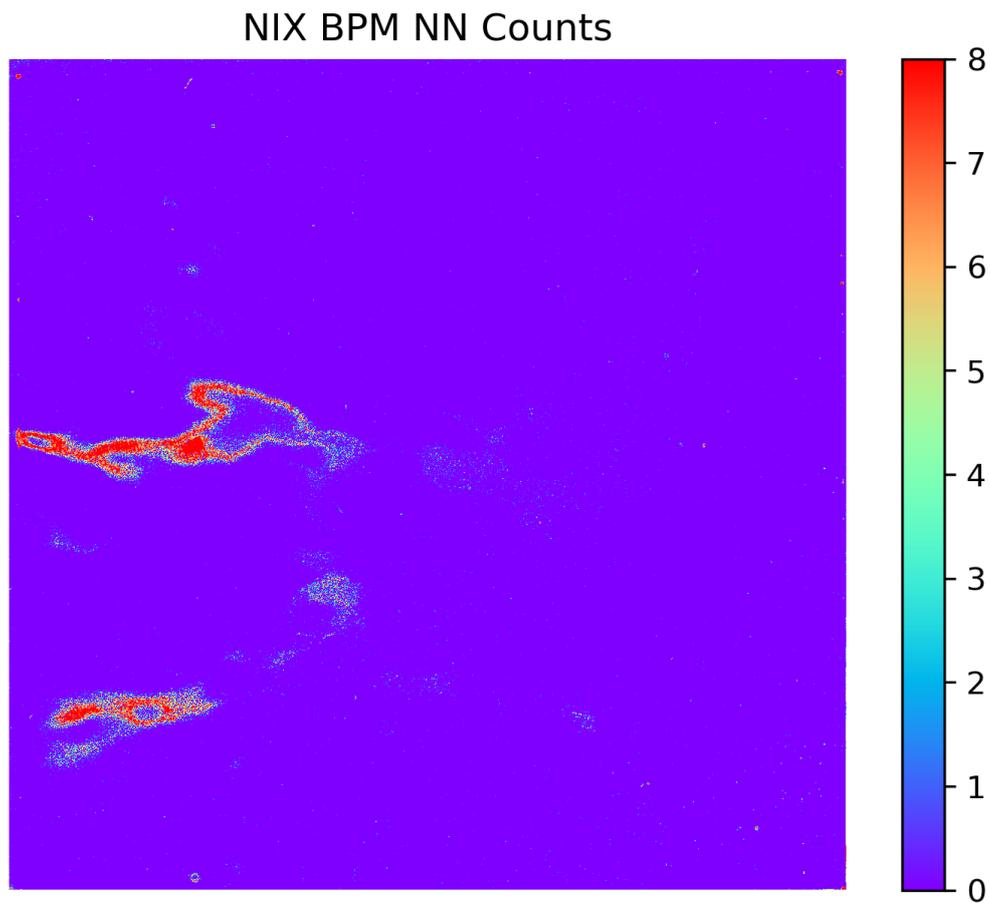
Figure 10: Number of identified bad pixels neighbouring each pixel in NIX detector. Pixels which are not identified as bad pixels have a value of 0.

information to recover their true values via simple interpolation methods within a single image. Therefore, high priority targets should avoid these regions. For field observations, dithering is strongly recommended as bad pixels can be replaced using the information from offset frames during aligning and stacking. For observations using the `nixIMG_obs_AutoJitter` template, a jitter width of more than $5''$ ($10''$) for the 13mas (27mas) camera is recommended. Note that the jitter pattern does not discriminate between good and bad regions of the detector. A representative bad pixel map can be found on the ERIS website[1] to help prepare observations with explicitly defined offset patterns to avoid these regions.

---

[1] `https://www.eso.org/sci/facilities/paranal/instruments/eris/inst.html`

2.5   SPIFFIER

The integral field spectrometer SPIFFIER is an upgraded/refurbished version of SPIFFI (SPectrometer for Infrared Faint Field Imaging) featuring a new HAWAII 2RG detector and four new gratings providing better spectral resolution. Figure 11 shows a view inside the cryostat. The light enters from the top, and passes through the sky-spider. The pre-optics with a filter wheel and interchangeable lenses provides three different image scales. The image slicer re-arranges the two-dimensional field into a pseudo-long slit, which is perpendicular to the base plate. Three diamond turned mirrors collimate the light onto the gratings. In total, four gratings are implemented on the grating drive. A multiple-lens system then focuses the spectra on the detector. All components are cooled in a bath cryostat to the temperature of liquid nitrogen (∼77 K). The liquid nitrogen reservoir sits below the instrument plate.
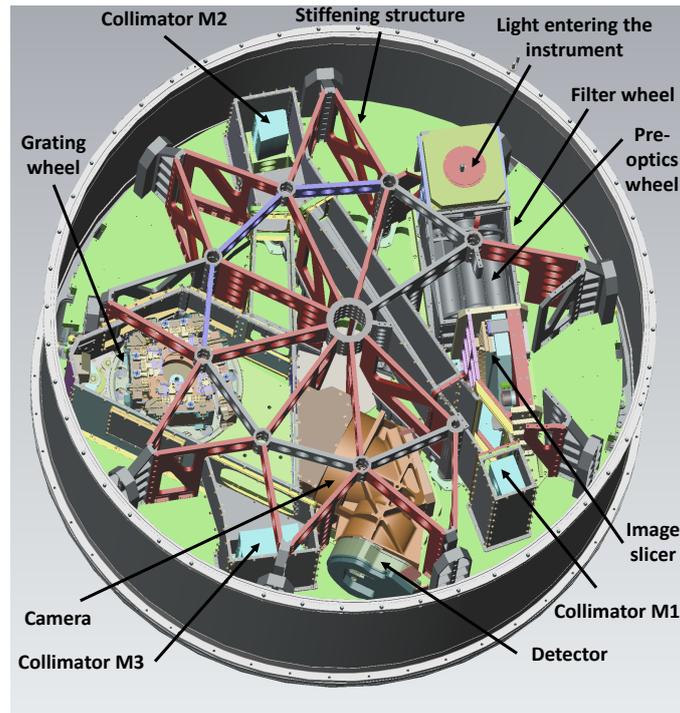
Figure 11: An inside view of the SPIFFIER cryostat with indications for the locations of various opto-mechanical elements. Some housing covers and parts of the stiffening structure are not shown for better illustration. The diameter of the instrument is 1.3m.

SPIFFIER provides simultaneous spectroscopy of 32x64 spatial pixels (spaxels) with a spectral resolution of either ∼5000 or ∼10000. Three pixel scales are available by rotating the optics wheel; 25, 100, 250 mas/pixel. A spaxel corresponds to a rectangular area on the sky, for example, 12.5x25mas^2 in the 25mas pixel scale. The 25 mas configuration is suited for use with adaptive optics since the angular resolution at 2.2 μm is 56 mas. To make optimal use of the spatial elements in seeing limited observations and at partial correction of the atmospheric turbulence with faint reference stars, SPIFFIER also provides image scales of 100 mas/pixel and 250 mas/pixel. These are associated with correspondingly larger fields of view.

Each of the atmospheric transmission bands J (1.1-1.4 μm), H (1.45-1.85 μm), and K (1.95-2.45 μm) is covered with single exposures at a resolution of ∼5000 as in SINFONI. With the addition of a new high resolution grating, only half wavelength range of the J, H, and K bands can be measured in a single exposure at a resolution of ∼10000 - refer to Table 9 for the full set of configurations.

A detailed description of the SPIFFI instrument design can be found in Eisenhauer et al. 2003 (Proc. SPIE 4841, 1686), with part of the upgrades to SPIFFIER described in George et al. 2017 (JATIS, 3, 1).

2.5.1   Pre-optics

Below the entrance focal plane baffle, a triplet lens unit collimates the light onto a cold stop for the suppression of the thermal background. The stop has a diameter of ∼6 mm, and is equipped with a central obscuration with the equivalent size of the telescope secondary mirror. Just in front of the cold stop is the motorised filter wheel, housing the band-pass filters, which are required to suppress the unwanted diffraction orders of the

gratings. After the cold stop, the motorised optics wheel provides the interchangeable lens systems for the three different image scales, and a pupil-imaging lens for alignment purposes. Each objective consists of two or three lenses. All moving functions are driven by two-phase stepper motors, which have been modified for use at cryogenic temperatures.

2.5.2 Image slicer
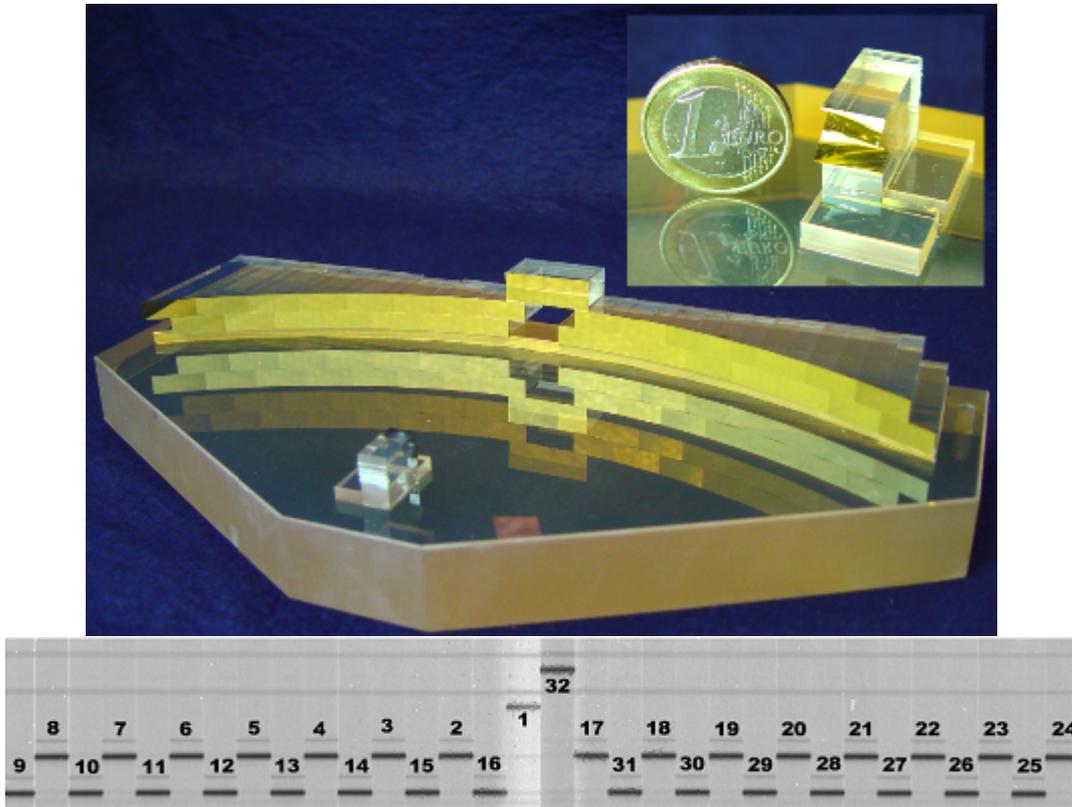
Figure 12: Top: SPIFFIER image slicer (a): The light enters through the hole in the big slicer. A stack of 32 small mirrors, the small slicer (also shown in the sub-panel), slices the image and redirects the light to-wards the 32 mirrors of the big slicer, which re-arranges the slitlets into a 31 cm long pseudo-slit. Bottom: Illustration of the slitlet layout in raw SPIFFIER images, light is dispersed vertically on the science detector.

The focus of the pre-optics is located at the small slicer. This part of the image slicer consists of a stack of 32 plane mirrors, which slices the image into slitlets, and separates the light from each slitlet in different directions. A second set of 32 mirrors, the big slicer, collects the light and forms the pseudo-slit, which appears as a *brick-wall pattern* on the detector. To avoid differential thermal contraction, the unit is completely made from a zero expansion glass, and all parts are optically contacted.

Figure 12 shows the image slicer and the positions of the slitlets on a raw SPIFFIER frame. The slitlets run horizontally across the imaging field-of-view and are numbered from top to bottom on the small slicer.

2.5.3 Spectrometer collimator

After the image has been sliced and re-arranged into a pseudo-slit, three diamond turned mirrors collimate the light onto the gratings. The first mirror is spherical, and the other two mirrors have an oblate elliptical shape. All mirrors are made from aluminium. The mirrors are gold-coated for higher reflectivity.

2.5.4 Grating wheel

In total, SPIFFIER has four gratings. Three of the gratings cover the J, H, and K atmospheric windows at a resolution of $R \sim 5000$ similar to SINFONI. The fourth grating is the high-resolution grating and replaces the H+K grating slot in SINFONI. This grating doubles the spectral resolution in a given band but reduces the

wavelength range by a factor of two. For each band, the instrument is pre-configured option to observe either short, middle or long wavelength regime. The options are detailed in Table 9.

Each low resolution grating is blazed to the centre of its band-pass, while the high resolution grating is blazed to optimise efficiency in all bands. In order to be able to move the spectrum on the detector with an accuracy of 1/5 of a pixel, the grating wheel is driven with a 1:647 gear, and controlled via an inductive encoder directly attached to the grating wheel.

2.5.5 Spectrometer camera

The camera is a five-lens + 1 folding mirror f/D∼1/2.8 design. The diameter of the three big lenses is 170 mm. All lenses have a multi-layer anti-reflection coating optimised for the wavelength range from 1.05-2.45 μm.

2.5.6 Detector

SPIFFIER is operated with a science grade Teledyne HAWAII 2RG detector (2k x 2k).

2.5.6.1 Characteristics The characteristics of the new detector are summarised in Table 5, and the readout noise is plotted as a function of the detector integration time in Figure 13.

Operating Temperature	77K
Pixel size	18 microns
Dark Current	0.19 e-/s
Well Depth	>80k e-
Detector Gain	2.0 e-/ADU
Readout Noise	12 e- (2s)
	7 e- (60s)
	11 e- (600s)
Minimum DIT	1.6 secs
Non-linearity	$\sim$ 3% (@ 20k ADU)

Table 5: SPIFFIER detector parameters
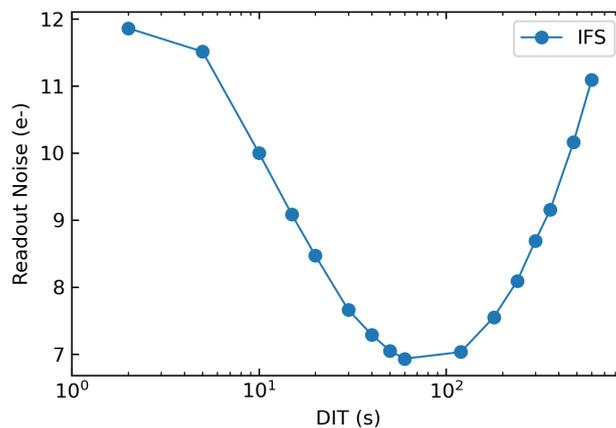
Figure 13: Detector readout noise as a function of detector integration time (DIT) for SPIFFIER. This curve is used by the ERIS ETC to estimate S/N of observations.

2.5.6.2 Bad pixels As commonly seen in infrared arrays, the SPIFFIER detector also has randomly distributed bad pixels. These can be easily interpolated over during data reduction. The only defect worth noting is a clump of cold pixels (not sensitive to light) about 10 pixels in diameter, marked with a dark blue circle in Figure 14. This spot falls into slitlet 16 in all configurations, i.e. in the middle of the reconstructed image.
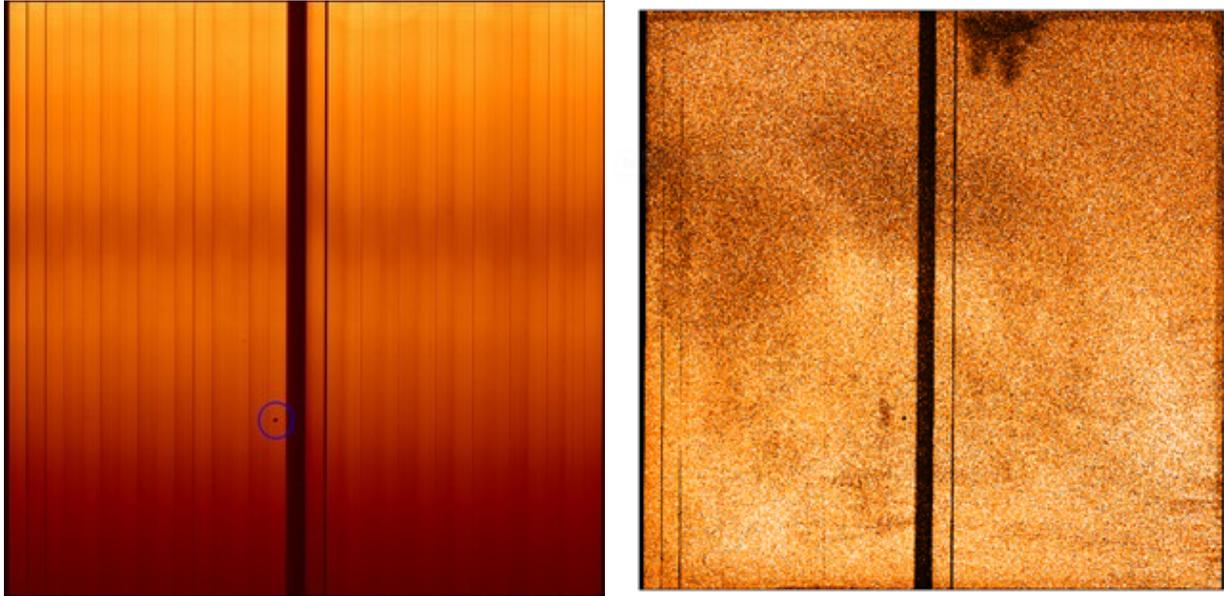
Figure 14: Left: SPIFFIER K_low flat at 25 mas pixel scale. A clump of cold pixels is marked with circle in the left panel. Right: 2D persistence map after a 5-minute long flat exposure.

2.5.6.3 Persistence In contrast to the old SINFONI detector, the new detector of SPIFFIER is less prone to persistence events -– in the worst cases, the duration is reduced from days to hours. However, the instrument still needs to be operated in a way that minimises persistence. Operationally, when not observing, the filter wheel always remains in the blocked configuration to avoid excessive flux reaching the detector and so-called persistence frames are continuously recorded during instrument setup. On the observational side, however, it is responsibility of users to follow persistence limits to avoid disturbing subsequent exposures.

Figure 14 shows a 2D persistence map after a long (5-minute) flat exposure near full well. As seen in the image, illuminated parts of the detector have almost uniform persistence background with the exception of low persistence anomaly - a thumb-like feature between slits 17 and 19 at the longest wavelengths. However, note that bright point-like sources or OH sky lines will still leave distinct persistence footprint on the detector.

In Figure 15, we report the persistence decay timescale with respect to peak illumination flux. In simple terms, exposures on the order of a minute reaching near 80% well-depth would require about an hour recovery time before the start of upcoming science OBs.
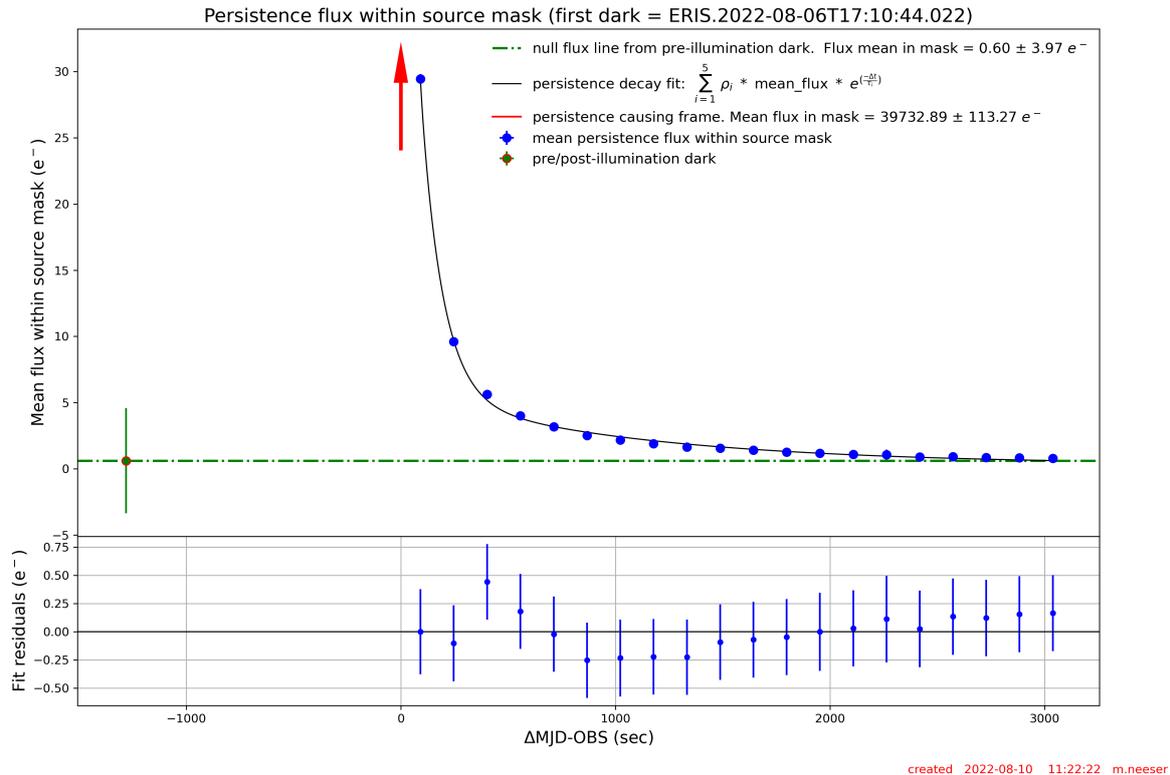
Figure 15: Persistence recovery time of SPIFFIER detector with respect to peak flux.

3 Observing modes and instrument configuration

Table 6 below summarises the different modes and configurations offered by ERIS. Observations with ERIS can only be carried out in combinations of these. But not all combinations are possible. For example, pupil tracking is associated with some instrument related restrictions, which are described in Section 3.1; and the seeing limited AO mode does not make sense to use with the high contrast imaging observing mode. So the possible combinations are limited by the available templates. The various tracking, AO, and observing modes are explained in more detail in the following subsections.

3.1 Focal plane rotation modes

This defines whether the orientation of the field or pupil in ERIS is fixed with respect to the detector focal plane.

Field tracking is the standard mode, and means that the orientation of the sky on the focal plane remains constant (so that ERIS rotates at a speed that depends on declination and hour angle). Pupil tracking means that the orientation of the pupil on the focal plane remains constant (i.e. ERIS is set at some predefined angle and then does not rotate). This is an important capability for high contrast imaging, in order to remove speckles in the PSF of the primary star. With pupil tracking, ERIS rotates to a pre-configured angle so that the pupil mask is aligned with the telescope spider arms. How this corresponds to the orientation on-sky depends on the declination and hour angle of the pointing.

Note that the use of off-axis guide stars with pupil tracking mode is not supported.

3.2 Differential tracking modes

This defines the rate at which the telescope, instrument, and AO system move across the sky in order to keep an object centred in the field of view.

- **Target**: sidereal, **AO**: sidereal. This applies to most science targets, which remain at a fixed right ascension and declination for the duration of an OB. The offset between the target and AO star is

Focal Plane Rotation Modes	
Field tracking	The standard focal plane rotation mode, in which the orientation of the field on the instrument focal plane remains constant.
Pupil tracking	In ERIS, this is used exclusively for Angular Differential Imaging (ADI), and means that the orientation of the pupil on the instrument focal plane remains constant. Its primary application is for high contrast imaging with NIX.
Differential Tracking Modes	
Sidereal tracking	The standard sky tracking mode, in which the telescope (+instrument) and AO system follow targets at a fixed right ascension and declination. This covers differential tracking, in which the AO guide (or tip-tilt) star is moving relative to the science target, as well as simple non-sidereal tracking, where the AO guide star is the non-sidereal science target.
Non-sidereal tracking	
Adaptive Optics modes	
NGS-AO	On-axis or off-axis
LGS-AO	With an on-axis or off-axis tip-tilt star
LGS Seeing Enhancer (SE)	With LGS but no tip-tilt star
Seeing Limited	No AO guide star
SPIFFIER Observing Modes	
Integral field spectroscopy	FOV: $0.8''$, $3.2''$, $8''$; R $\sim$5k or 10k; 1-2.5μm
NIX Observing Modes	
Short Imaging	13/27 mas/pix ($26''/55''$ FOV); *J-K* narrow/broad bands
Long Imaging	13 mas/pix ($26''$ FOV); *L-M* narrow/broad bands
Apodizing Phase Plate (APP)	*K-M* narrow bands; 13 mas/pix
Focal Plane Coronography (FPC)	*L-M* bands; 13 mas/pix
Sparse Aperture Mask (SAM)	*J-M* bands (narrow-band only for SAM-23); 13 mas/pix
Long Slit Spectroscopy (LSS)	*L* band only; R$\sim$900, slit width 86 mas, slit length $12''$

Table 6: Short summary of ERIS modes currently available.

constant throughput the OB.

- **Target**: non-sidereal, **AO**: the same non-sidereal object. This applies to bright non-sidereal objects that can also be used as the AO reference star. In this case the telescope tracking speed needs to be adjusted in both axes to keep the object centred. No differential tracking is performed as the target and AO reference star are the same.

- **Target**: non-sidereal, **AO**: sidereal. In this scenario the AO system will have to track differentially to the science instrument so that the science target remains fixed in the field of view. This is handled by continually updating the offset between AO guide star and science target. The maximum separation between these two must remain within the maximum $59''$ patrol radius of the AO system.

- **Target**: sidereal, **AO**: non-sidereal. As with the previous scenario, although in this case the AO system is differentially tacking to keep the AO star centred within the wavefront sensor.

- **Target**: non-sidereal, **AO**: a different non-sidereal target. As with the previous scenario. The telescope tracks the non-sidereal science target, while the AO system compensates for the differential motion between the two to keep the two objects centred in the science camera and AO wavefront sensor.

3.3   Adaptive optics modes

There are four AO modes, summarised in Table 6. Their combination with respective observing modes is limited by the available templates to only those that make sense.

- **NGS-AO**, a natural guide star (specified already in Phase 1 proposal preparation) is sensed at visible wavelengths to provide the AO correction. The guide star can be on axis or up to $59''$ off axis. Because ERIS uses only a single DM (the DSM of the AOF), the field of view over which there is a good AO correction is finite. This also means that in the off-axis configuration, anisoplanatism can significantly reduce the AO performance at the location of the science target.

- **LGS-AO**, any one of the lasers from the 4LGSF is used to generate an on-axis LGS that is used to correct high order aberrations. A second WFS senses a tip-tilt star at visible wavelengths simultaneously. The tip-tilt star can be on axis or up to 59″ off axis. Note that, when dithering, the LGS will always point to the centre of the observed field, while the science target will move to different positions in the field. The impact of the resulting high order anisoplanatism will usually be small (note that tilt anisoplanatism, which dominates the off-axis PSF shape, is unaffected by the location of the LGS). This mode of operation has advantages in improving the overall PSF for extended targets and fields.

- **Seeing enhancer (SE)**, this uses an LGS to correct the high order aberrations, but without a tip-tilt star (although with VLT field stabilization). As for the LGS-AO mode, when dithering the LGS is always in the centre of the observed field while the science target moves around it. No AO (tip-tilt) guide star is specified.

- **Seeing limited**, in this 'no AO' mode, the AO system is off (loops open) and so no guide star is specified. Instead VLT field stabilisation is used.

3.4 SPIFFIER modes

From an operational perspective, the use of SPIFFIER in ERIS is similar to SINFONI. There is only one mode: integral field spectroscopy. But this mode has a variety of fixed configuration options for the pixel scale (see Table 7 and Fig. 16) and the spectral setting (band/wavelength and resolution), see Table 9. An important difference to SINFONI is that during acquisition, the AO system goes first, after which one can expect that the SPIFFIER pointing should be reasonably precise. The offset between the centres of the three fields of view are given in Table 8. For observations at a non-zero position angle (i.e. `TEL.ROT.OFFANGLE` $\neq 0$ deg), it is strongly recommended to use `DETECTOR` offsets to move the telescope to re-centre an object if the plate scale is changed, otherwise you must apply the appropriate rotation to the `SKY` offsets to account for the instrument rotation.

Field of view	Spaxel size on-sky	Tag
0.8"x0.8"	12.5x25mas	`25mas`
3.2"x3.2"	50x100mas	`100mas`
8"x8"	125x250mas	`250mas`

Table 7: FOV and spaxel size for each pixel scale options of SPIFIER.
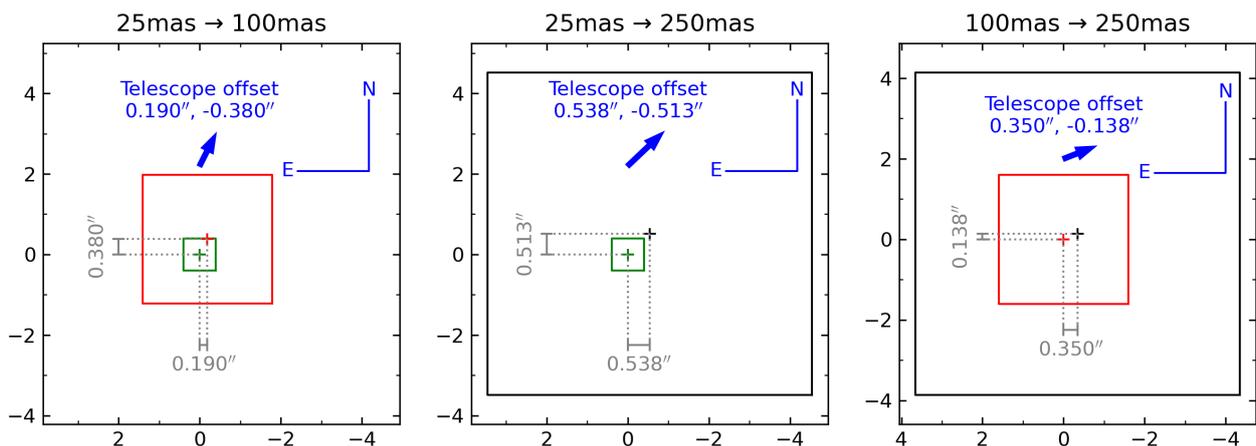
Figure 16: Relative centring of the SPIFFIER FoVs for the three allowed changes within a single OB; the pixel scale cannot be decreased between subsequent science templates. The telescope offset assuming `TEL.ROT.OFFANGLE`= 0 deg required to move an object from the centre of the smaller field of view to the centre of the larger field of view is shown.

There is no restriction between AO mode and the choice of pixel scale. Since the field of view of 25mas pixel scale configuration is <1 arcsec, the 100mas pixel scale configuration can be used during acquisition if the object coordinates are not precisely known. If this is done the target will be centred using the 100mas

Tag	25mas		100mas		250mas	
25mas	$(32.0, 32.0)$ px	$(0, 0)''$	$\cdots$	$\cdots$	$\cdots$	$\cdots$
100mas	$(28.2, 24.4)$ px	$(+0.190, -0.380)''$	$(32.0, 32.0)$ px	$(0, 0)''$	$\cdots$	$\cdots$
250mas	$(27.7, 27.9)$ px	$(+0.538, -0.513)''$	$(29.2, 30.9)$ px	$(+0.350, -0.138)''$	$(32.0, 32.0)$ px	$(0, 0)''$

Table 8: Pixel coordinates for the centre of each pixel scale (columns) within the other pixel scales (row), and the telescope offset (`SKY`) to move an object from the centre of one field of view to the centre of the other, assuming `TEL.ROT.OFFANGLE`$=0$ deg. As an example, the centre of the 25mas field of view is at pixel coordinate $(28.2, 24.4)$ in the 100mas field of view, and a telescope offset of $(+0.380, -0.760)''$ would be required to move an object from the centre of the 25mas field of view to the centre of the 100mas field of view.

pixel scale configuration and an offset must be applied within the first science template at the 25mas pixel scale configuration if precise centring for the science exposures is required (see Table 8, and the schematic in Figure 16). If the object coordinates are precisely known then it is highly recommended to use the desired pixel scale configuration for the science for the acquisition.

There are twelve options for the spectral configuration and these are detail in Table 9. Low resolution configurations roughly cover a full single broad band. Alternatively, short and long variants can be used in conjunction to observe a full band doubling spectral resolution at the expense of longer observing time. The middle configurations are useful if there is a spectral feature of interest in the middle of a given band and higher resolution is required.

SPIFFIER is offered with both field tracking and pupil tracking (i.e. ADI) options, the latter being specifically for high contrast observations. However, full pipeline processing is only available for field tracking; with pupil tracking, cubes will be reconstructed but no background subtraction or shifting and combining of individual cubes will be performed. This is because the algorithms required are highly specialized according to the specific science goal, and develop and change very quickly over time.

Configuration	Band	λ_c [μm]	λ range [μm]	Resolution
Low Resolution	`J_low`	1.25	1.09-1.42	$\sim$5000
	`H_low`	1.66	1.45-1.87	$\sim$5200
	`K_low`	2.21	1.93-2.48	$\sim$5600
High Resolution	`J_short`	1.18	1.10-1.27	$\sim$10000
	`J_middle`	1.26	1.18-1.35	$\sim$10000
	`J_long`	1.34	1.26-1.43	$\sim$10000
	`H_short`	1.56	1.46-1.67	$\sim$10400
	`H_middle`	1.67	1.56-1.77	$\sim$10400
	`H_long`	1.76	1.66-1.87	$\sim$10400
	`K_short`	2.07	1.93-2.22	$\sim$11200
	`K_middle`	2.20	2.06-2.34	$\sim$11200
	`K_long`	2.33	2.19-2.47	$\sim$11200

Table 9: SPIFFIER grating parameters. Resolution values correspond to the 1.6 pixel line FWHM. For simplicity, throughout the document high resolution configurations are referred to as R$\sim$10000 and low resolution configurations as R$\sim$5000.

3.5   NIX modes

NIX has five different observing modes; one associated with imaging, three with high contrast modes, and one with spectroscopy.

The imaging mode has two pixel scales: 13 mas/pix and 27 mas/pixel, which provide respectively $\sim$26x26 and 55x55 arcsec fields of view. The smaller pixel scale is designed to fully sample the PSF in the J, H and K filters (1 to 2.5 μm), while the large field of view is a balance between reasonable sampling and as large a field of view as possible. In long wavelength imaging ($>$2.5 μm), only a 13 mas/pix configuration is available. The fine pixel sampling choice in this configuration is due to the high sky background in these wavelengths.

The optical design of the instrument means that a small border of $\sim$10 pixels will be vignetted around the outside edge of the detector for both aperture settings. This will help with alignment of the components and will reduce the amount of scattered light reaching the detector. It is possible this area of unexposed could provide additional input to the data reduction.

We note that NIX pipeline includes only basic (single exposure) image reduction steps for high contrast modes: dark subtraction, linearity correction, flat-fielding, and bad pixel interpolation. It does not provide

further support for scientific analysis beyond that point. For the high contrast modes, observers are responsible for requesting all the necessary calibrations beyond those given above.

3.5.1 Filter wheel

Filter	λ_c [μm]	FWHM$_\lambda$ [μm]	Average(Peak) Transmission [%]
J	1.28	0.20	82
H	1.66	0.31	93
Ks	2.18	0.39	87
Short-Lp	3.32	0.43	80
Lp	3.79	0.60	78
L-Broad	3.57	1.04	83
Mp	4.78	0.58	80
Pa-b	1.282	0.021	75(83)
Fe-II	1.644	0.020	86(94)
H2-cont	2.068	0.064	80(90)
H2-1-0S	2.120	0.020	67(77)
Br-g	2.172	0.020	65(75)
K-peak	2.198	0.099	83(89)
IB-2.42	2.420	0.049	71(82)
IB-2.48	2.479	0.051	65(78)
Br-a-cont	3.965	0.108	82(91)
Br-a	4.051	0.023	69(80)

Table 10: The table lists NIX filter wheel contents. FWHM$_\lambda$ is the width at half transmission. λ_c is the middle of this range. The average transmission is calculated within the half transmission limits. For narrow band filters, we also include the peak transmission inside parentheses.

There is a wide range of filters to choose from, most of which are mounted in the filter wheel. When the user selects a 'short' wavelength filter (i.e. $\lambda < 2.5\ \mu$m) or a 'long' wavelength filter, the associated pupil wheel mask is automatically selected for the pupil wheel. Two additional filters are mounted in the pupil wheel: the neutral density (ND) filter and the blocking filter. The blocking filter provides additional blocking of the long wavelength thermal background (see below). The full list of filters is given in Table 10; note that the L-Broad filter is designed solely for use with the LSS mode.

The Blocking filter in the pupil wheel (see Section 3.5.2) is included to block a potential long-wavelength leak in $< 2.5\ \mu$m observations at the cost of throughput (from 5% in J to 10-15% in K). During the commissioning, no problematic cases were observed which requires the use of this filter.

Filter transmission profiles are available on the ERIS website[2], and are used to compute the total instrument throughput reported in the ERIS ETC [3] which can be displayed if selected on the "Select Output" tab.

3.5.2 Pupil wheel

The pupil wheel of NIX contents a range of different elements that are relevant to the sections that follow, these are detailed in Table 11. For all settings, there is a trade-off to be considered between maximising throughput, while reducing the thermal background. For longer wavelength observations, more care has to be taken to limit the emission from the sky and structures surrounding the pupil. So, to optimise the observations two 'reduced stops' are available, a larger one for JHK to maximise throughput and a smaller one for LM that limits the background.

3.5.3 Possible modes and settings

The possible observing modes and the possible cross matches between the observations are shown in Table 12 and Table 13.

---

[2](https://www.eso.org/sci/facilities/paranal/instruments/eris/inst.html)
[3]https://etc.eso.org/observing/etc/eris

No.	Item	Obs. Mode	Description
1	`JHK-pupil`	imaging	The JHK reduced pupil stop is a metal plate with a circular aperture.
2	`Blocking`	imaging	A copy of the JHK reduced pupil stop with a filter that enhances blocking of out of band thermal background.
3	`LM-pupil`	imaging	The LM reduced pupil stop is a metal plate with a smaller circular aperture than the JHK stop, to reduce thermal background.
4	`Spider`	imaging	The spider mask blocks out thermal emission from the secondary mirror and the spiders at the expense of throughput ($\sim15\%$ reduction); only for pupil tracking.
5	`ND`	imaging	A copy of the LM reduced pupil stop with a neutral density filter.
6	`APP`	high contrast	An apodizing phase plate that produces a pair of offset images in which opposite halves of the PSF are suppressed, and a fainter central image as a photometric and astrometric reference.
7	`SAM-7`	high contrast	Sparse aperture masks with the specified number of mini-apertures for non-redundant and partially redundant interferometric imaging.
8	`SAM-9`		
9	`SAM-23`		
10	`Lyot`	high contrast	The Lyot stop is a spider mask with an undersized circular aperture, to be used in conjunction with AGPMs in the aperture wheel.
11	`Lyot-ND`	high contrast	A copy of the Lyot stop with a neutral density filter, useful when observing very bright objects.
12	`Grism`	spectroscopy	A grism for *L*-band spectroscopy with a copy of the LM reduced pupil stop, used with the slit mask in the aperture wheel
13	`Open`	–	An empty aperture; not user-selectable.
14	`Block`	–	A blocked aperture to stop any light reaching the detector; not user-selectable.

Table 11: NIX pupil wheel contents

	Aperture	Camera	Filter	Pupil wheel	Tracking
Short imaging	Large field	`27mas-JHK`	$<2.5\,\mu\mathrm{m}$	`JHK-pupil`, `Blocking`, `ND`	Field, Pupil
	Small field	`13mas-JHK`			
Long imaging	Small field	`13mas-LM`	$>2.5\,\mu\mathrm{m}$	`LM-pupil`, `ND`	Field
				`LM-pupil`, `ND`, `Spider`	Pupil
APP	Small field	`13mas-LM`	$>2.5\,\mu\mathrm{m}$	`APP`	Pupil
FPC	AGPM-L, AGPM-M	`13mas-LM`	$>2.5\,\mu\mathrm{m}$	`Lyot`, `Lyot-ND`	Pupil
SAM	Small field	`13mas-JHK` `13mas-LM`	Any Any Narrow	`SAM-7` `SAM-9` `SAM-23`	Pupil
LSS	Slit Mask	`13mas-LM`	`L-Broad`	`Grism`	Field

Table 12: Configuration combinations for observing modes with NIX.

		1	2	3	4	5	6	7	8	9	10	11	12	13	14	15	16	17
		J	H	Ks	Short-Lp	Lp	L-Broad	Mp	Pa-b	Fe-II	H2-cont	H2-1-0S	Br-g	K-peak	IB-2.42	IB-2.48	Br-a-cont	Br-a
1	JHK-pupil	✓	✓	✓					✓	✓	✓	✓	✓	✓	✓	✓		
2	Blocking	✓	✓	✓					✓	✓	✓	✓	✓	✓	✓	✓		
3	LM-pupil				✓	✓		✓									✓	✓
4	Spider				✓	✓		✓									✓	✓
5	ND	✓	✓	✓	✓	✓		✓	✓	✓	✓	✓	✓	✓	✓	✓	✓	✓
6	APP										✓	✓	✓	✓	✓	✓	✓	✓
7	SAM-7	✓	✓	✓	✓	✓		✓	✓	✓	✓	✓	✓	✓	✓	✓	✓	✓
8	SAM-9	✓	✓	✓	✓	✓		✓	✓	✓	✓	✓	✓	✓	✓	✓	✓	✓
9	SAM-23								✓	✓	✓	✓	✓	✓	✓	✓	✓	✓
10	Lyot				✓	✓		✓									✓	✓
11	Lyot-ND				✓	✓		✓									✓	✓
12	Grism						✓											

Table 13: All possible combinations for the filter and the pupil wheel.

4 ERIS performance overview

The following section is intended to give the user a rough idea of the expected ERIS performance. It provides an overview only, and the Exposure Time Calculator (ETC) should be used to estimate the feasibility of science observations. The ERIS ETC can be found at `http://www.eso.org/observing/etc/`.

4.1 Adaptive optics system performance

As already discussed, the ERIS provides two main observing AO modes namely NGS mode and LGS mode. Both require using a NGS, as a high order and tip tilt reference respectively. The following subsections detail the performances provided by these two modes. The performance for the seeing enhancer depends only on the seeing and airmass at the time of the observations, and not on the user's choice of NGS. The expected resolution is typically in the range 0.1–0.3″. For the LGS and NGS modes, the Strehl ratio (SR) achieved in nominal seeing of 0.87 arcsec along the line of sight, is given as a function of magnitude and distance of the NGS. Then, in order to give an idea of how the system performance changes, the on-axis performance is shown for each of three line-of-sight seeing values (0.7, 0.87 and 1.1 arcsec). The ETC provides more complete information.

4.1.1 AO system reference star
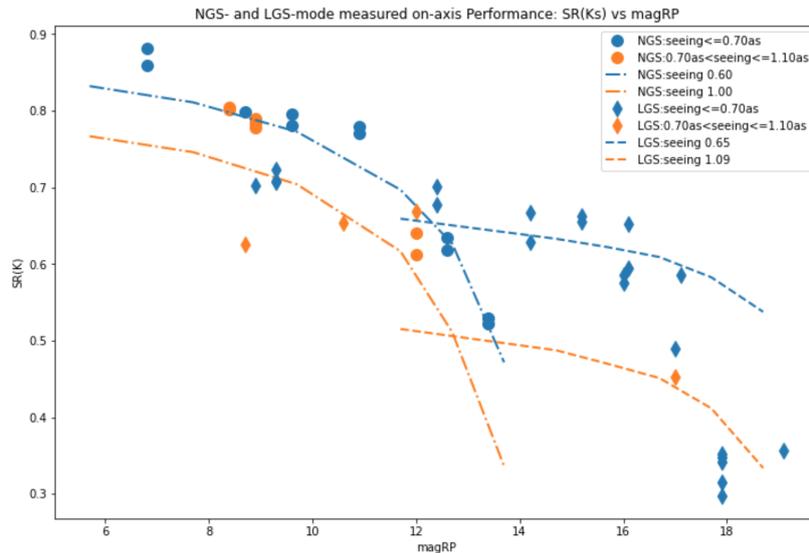
Figure 17: Simulated (lines) and measured (points) Strehl ratio in K band as a function of the reference star *Gaia* RP magnitude for NGS and LGS (Davies et al. 2023, Riccardi et al. *in prep*).

The ERIS AO module has a reference star acquisition FoV of circular shape with a diameter of 120 arcsec. The AO performances are reported in terms of SR as a function of reference star magnitude in R band. The star type is assumed G2V. Note that the NGS WFSs (both HO and LO) wavelength range is 600-1000 nm, so the user is encouraged to search for redder type star in the observation planning. The atmospheric parameters used in the simulations assume standard atmospheric conditions at Paranal and consider a seeing value of 0.87 arcsec, which is taken as the seeing along the line of sight at 30 deg of Zenith distance. Figure 17 summarises the AO performance on-axis for NGS and LGS versus reference star magnitudes (blue and red curves respectively) and the requirements (blue and red dots). These data show the interesting condition that when the NGS is fainter than a R~13.5 mag, the LGS option should be used all the time.

4.1.2 NGS mode performance

The general plot of SR vs. reference star magnitudes and off axis distances is reported in Figure 18. Since the simulations have been done with a given wind profile the SR pattern is not centro-symmetrical. The reported values are an average for off-axis targets located at 0, 90, 180 and 270 degrees with respect to the reference coordinate system of the simulations.
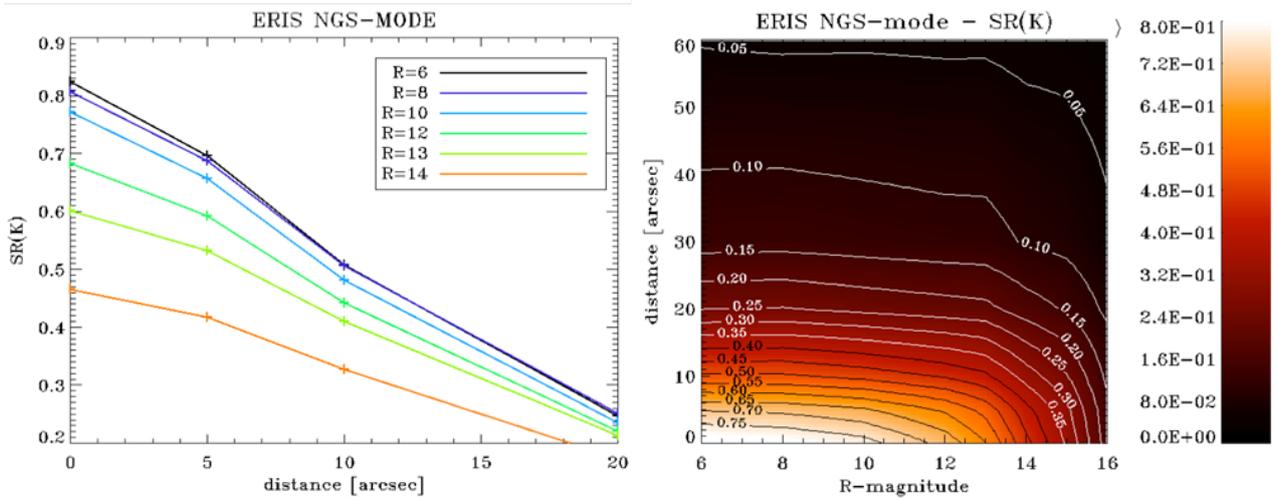
Figure 18: The NGS mode performance as a function of reference star magnitude and off-axis distance from scientific target.

With the help of this figure, the case of multiple reference star availability can be solved by comparing SR(mag, r) for the given reference stars. In the plot, NGS magnitudes below 14 mag has not been considered because for mag > 13 better performances are achieved by using the ERIS LGS mode irrespective of the off-axis distance.

4.1.3   LGS mode performance
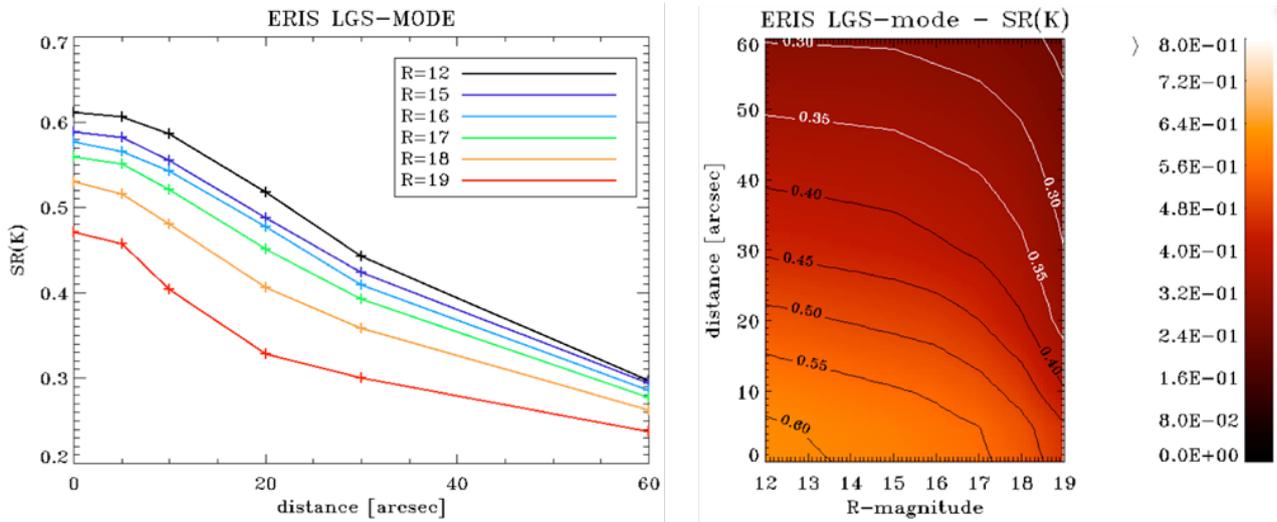
Figure 19: The LGS mode performance as a function of reference star magnitude and off-axis distance from scientific target.

The general plot of SR vs. reference star magnitudes and off-axis distance is reported in Figure 19. The simulations have been done with a given wind profile, so the SR pattern is not centro-symmetrical. The reported values are an average for off-axis target located at 0, 90, 180 and 270 degrees with respect to the reference coordinate system of the simulations.

With the help of this figure, the case of multiple reference star availability can be solved by comparing SR(mag,r) for the given reference stars.
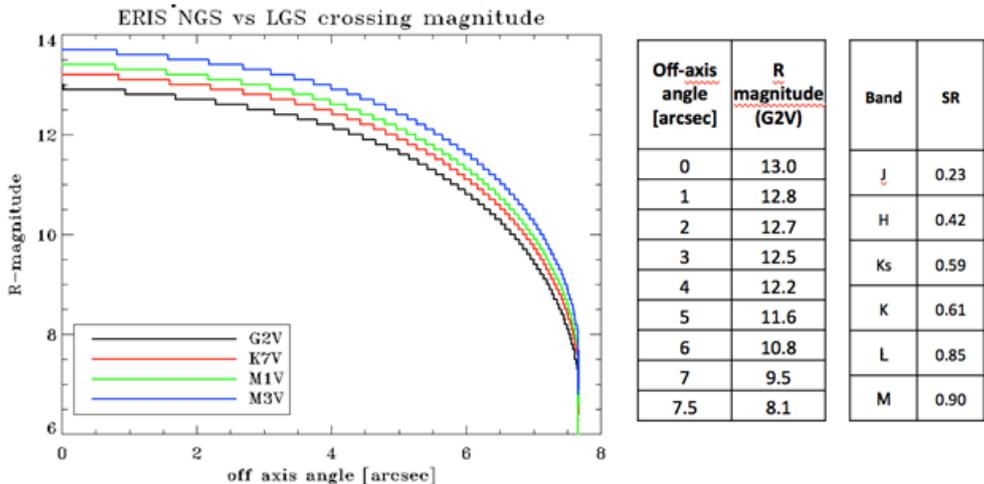
Figure 20: Identification of maximum off axis angle for the NGS WFS reference star for NGS and LGS mode equal performances. The table on the right side shows the limiting magnitude value for equal performances and the achieved SR in various bands. The magnitude is given for different star types. The ERIS specifications refer to the G2V type star.

4.1.4 NGS mode and LGS mode performance versus reference star spectral type

When a single reference star is found within 59″ of the science target (i.e. within the AO module's FoV), the NGS vs LGS mode performances can be compared easily. With the atmospheric parameters considered for ERIS, this comparison is reported in Figure 20.

The Figure shows the maximum off-axis angle at which one gets better performance with the NGS mode with respect to the LGS mode. If a reference star with a given (Rmag,r) values lies above (or to the right of) the line for its spectral type, then LGS mode provides better performance than the NGS mode. The plot shows tht for redder spectral types, there is a slight gain in the NGS performance, as expected for the WFS band-pass. But the important conclusion is that the LGS mode always leads to a better SR for stars fainter than 14 mag in R band.
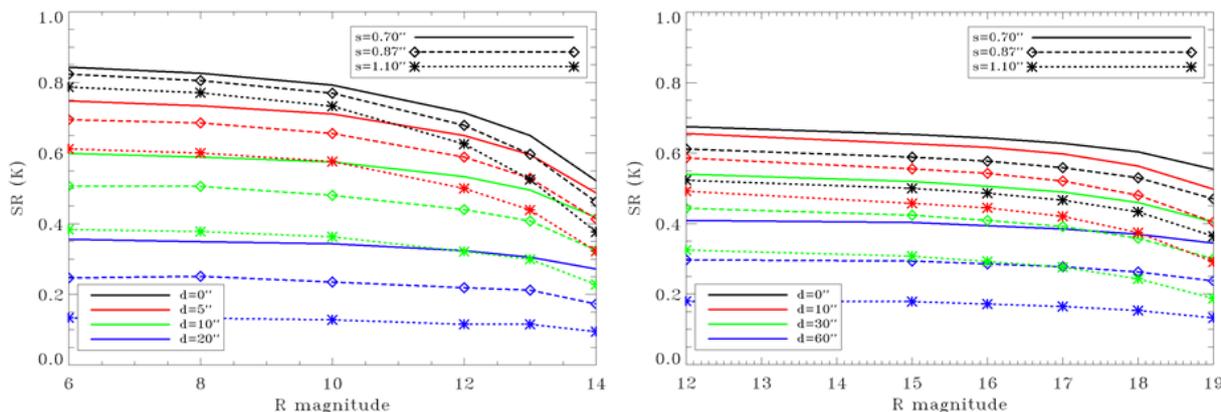
Figure 21: K band SR for 3 different seeing values for NGS (left) and LGS (right) respectively.

4.1.5 AO performance versus seeing value

Figure 21 shows the on-axis system performances for two additional seeing values (0.7 and 1.1 arcsec) to allow estimate the performances as a function of seeing. The different colour lines correspond to different off-axis distances for the star (i.e. indicating anisoplanatism). Performance values can be interpolated within the given ranges.

4.1.6 Performance vs average wind speed

The variation of the AO system performance (NGS and LGS modes) can be considered negligible within the 9.6-14.3 m/s range of wind speeds covered in the simulations.

4.1.7 Sky background from the Moon

The sky background in the LGS low-order wavefront sensor was measured at several angular separations from a half-Moon (FLI ~0.57) on the night of 2022-08-05. Simulations of the sky emission spectrum at each pointing were made using the ESO SkyCalc Model Calculator[4], which were converted into Gaia RP fluxes using the filter response curve. These were scaled to the counts measured in the low-order wavefront sensor, accounting for a bias level expected in the measured counts. Using this scaling factor and a large number of SkyCalc simulations, the sky background was predicted for a range of values of the Moon distance and fractional lunar illumination, as well as target altitude (Figure 22). An acceptable background level for a range of guide star magnitudes is shown, and these should be used to place constraints on both service and visitor-mode observations. The system has been tested in LGS mode with a 15th magnitude tip-tilt star at a distance of 15 deg from the full moon, however the telescope guide star was approximately 12th magnitude.
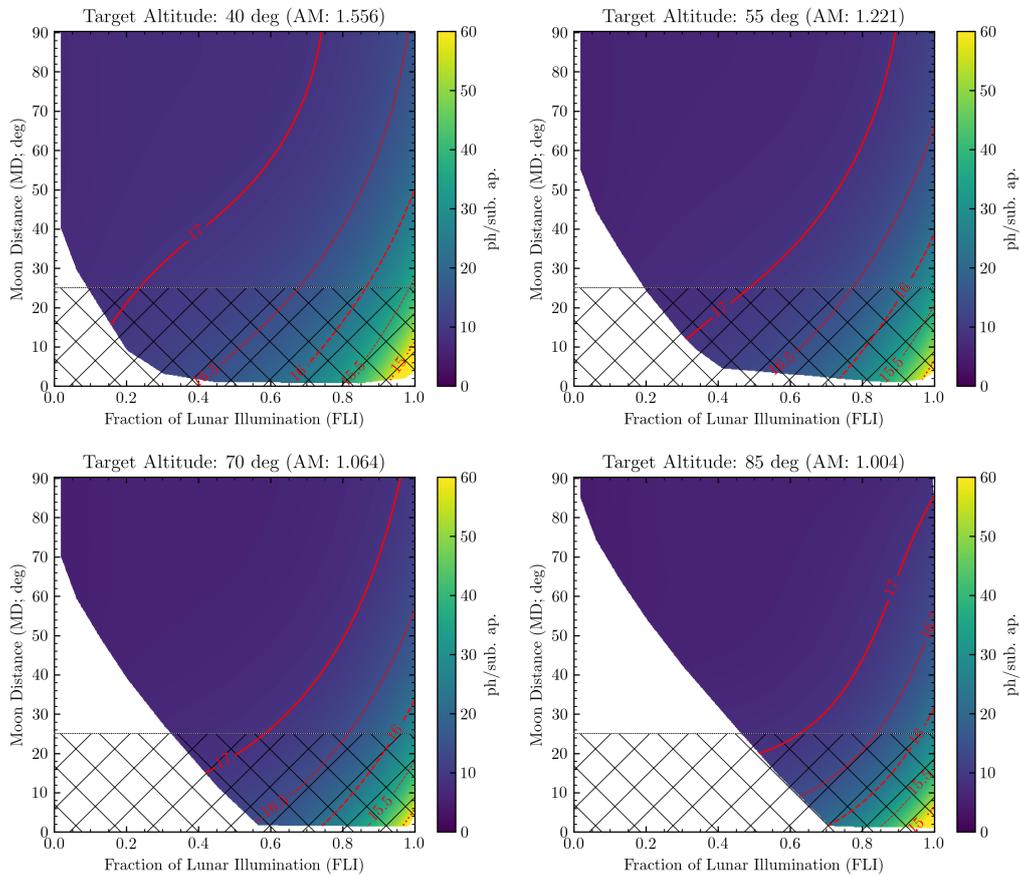
Figure 22: Estimated sky background in photons per sub-aperture in the LGS low-order wavefront sensor at 250Hz as a function of fraction of lunar illumination (FLI) and Moon distance (MD) for four different target elevations. Red contours denote recommended maximum Moon background levels for guide stars between 17th and 15th magnitude. The hatched region denotes Moon distances that are not permitted due to issues with telescope guiding. Due to geometry it is not possible for a Moon with FLI~0 to be close to the zenith at night.

The increased sky background from the Moon may also affect the quality of the adaptive optics correction. In particular, the numerical simulations of AO performances assume that the Moon on sky position is 90 degrees from the meridian where observations take place. In different conditions (Moon closer to the line of sight) some degradation of the AO performance may occur, especially in LGS mode with faint tip-tilt stars.

---

[4] https://www.eso.org/observing/etc/bin/gen/form?INS.MODE=swspectr+INS.NAME=SKYCALC

Even here, it is important not to over-specify the constraints, as this reduces the chances for the OB to be executed successfully.

4.1.8 PSF and ADI contrast in AO mode
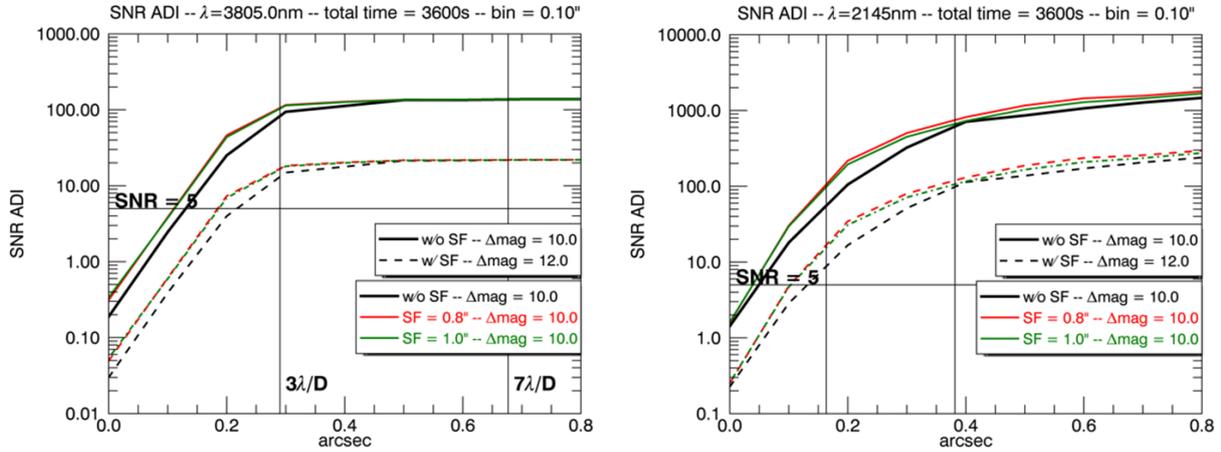
Figure 23: The signal-to-noise ratio for L' (left) and K band (right) computed with numerical simulations when AO corrected images are combined by using ADI technique. The signal-to-noise ratio saturates quickly in the L' case because of the large contribution from sky background.

Figure 23 plots the contrast achieved using the ADI technique in NGS AO mode in K and L′ bands. The total exposure time in this simulations is 3600s, made by combining 100 image pairs. The baseline mode results are shown with the black line while enhanced performance, using the focal plane Spatial Filter (SF) option in the SH sensor are shown as the red and green curves. This adjustable filter improves the high contrast performance. The difference between the two modes is quantified in the figure.

As an additional comparison of the baseline versus filtered SH option, Figure 24 is a plot of the PSF profiles in K and L′ bands for both options.
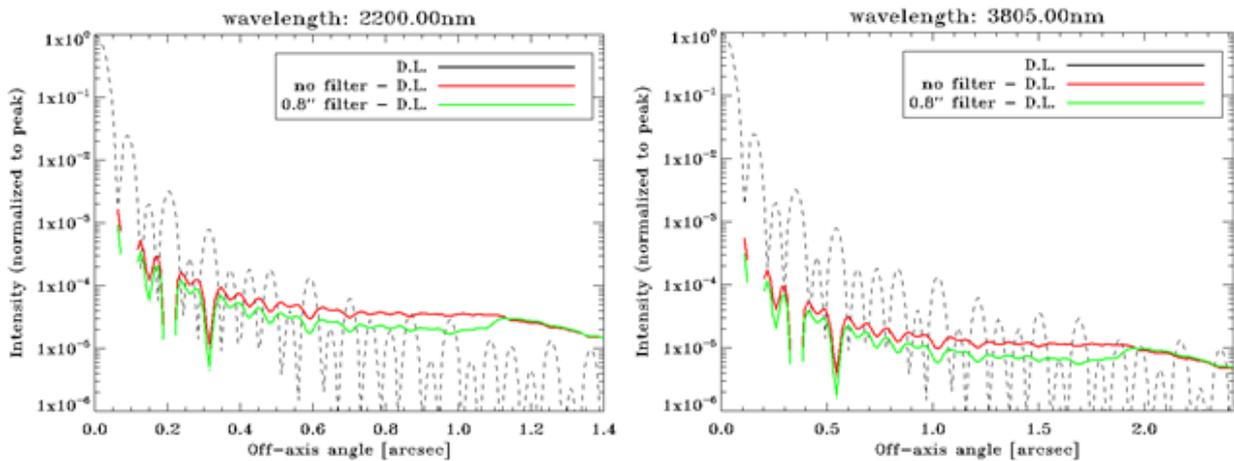
Figure 24: The corrected PSFs profiles at K and L' band for the two options baseline and filtered SH for the NGS WFS. Different behaviour is given by red and green line respectively. DL in the figure labels means Diffraction Limit.

4.2   NIX performance

The NIX performance for imaging is best assessed through the ETC, because the signal-to-noise that can be achieved depends on a number of details of the configuration – most obviously the filter, the exposure time, and the number of exposures. It also depends on the details of the source distribution, and on how well the background can be inferred either from the dithered science frames or from separate sky frames. The main purpose of this section is to provide additional useful information about the more complex modes.

4.2.1   Detector

4.2.1.1   Optimal DITs in long wavelength   Observations at longer wavelengths (3–5μm) are strongly affected by the high and variable background due to the thermal emission from the atmosphere. This can be somewhat mitigated by frequently measuring the sky background during your observations. As chopping is not possible with ERIS the background can only be sampled by offsetting the telescope. The overhead associated with this can be reduced if it is possible to keep the science target within the field of view at all times. For isolated regions we recommend using the `ERIS_nixIMG_obs_AutoJitter` template. More complex regions will require a carefully-constructed offset pattern. It is strongly recommended to frequently sample the sky during observations with the broadband long-wavelength filters (`Short-Lp`, `Lp`, `Mp`). Observations with these filters cannot exceed two minutes within a single exposure (i.e. $\text{DIT}\times\text{NDIT}\leq 120\,$s).

During the commissioning, recorded count levels for L' filter are 20k, 15k e- per 0.2 seconds respectively in April and June; 46k, 36k e- per 0.05 seconds for the M' filter. These count levels should be approached conservatively. In particular, there is no data recorded in warmer Chilean summers, where the count rates are expected to be higher with the warmer telescope.

In M-band, the background is by far the limiting factor even at the fastest full frame readout time. The read noise is about 50 e- rms in fast readouts. Hence, the detector can be read at full speed (DIT=0.034) to be conservative with the background level. There is no practical advantage for longer DITs (but see Section 4.2.1.2 for cube mode). In L-band, the situation is similar but there is no need to configure the detector to read at the fastest speeds. 0.1-0.2 DITs should serve well for most observing cases.

**4.2.1.2   NDIT limits in cube mode**   NIX has the potential to generate approximately 700 GB per hour when used at the fastest frame rate in cube mode. For operational reasons when using cube mode the maximum number of NDITs permitted within a single OB is limited to the equivalent of:

- 20,000 NDITs per hour for `windowF`

- 31,604 NDITs per hour for `window1`

- 40,000 NDITs per hour for `window2`

- 80,000 NDITs per hour for `window3` and `window4`

These limits are prorated to the total duration of the science templates within an OB, including overheads. For example, a science template with a 30m execution time using `windowF` can have at most 10,000 NDITs in cube mode. For OBs with science templates using different windows, the limit can be calculated by scaling the number of NDITs within each template by the size of the window relative to `windowF`, then comparing that sum to the limit for `windowF`. These limits are liable to be reduced without advanced warning if large data volumes cause too much congestion on either the internal network, or the internet link to the archive facility in Garching.

The maximum number of NDITs allowed per exposure in cube mode is limited to:

- 500 NDITs per exposure for `windowF`

- 800 NDITs per exposure for `window1`

- 1000 NDITs per exposure for `window2`

- 2000 NDITs per exposure for `window3` and `window4`

4.2.1.3 Saturation and persistence limits NIX has a variety of modes and some requiring deliberate saturation to work effectively. Hence, the restriction on count levels is more relaxed with respect to SPIFFIER. Detector saturation is currently permitted up to ten times the saturation level of the detector. This corresponds to a limit of 850k e- (163k ADU in SLOW mode, 327k ADU in FAST mode). The table below gives the brightest magnitude permitted for each readout mode, camera, and filter combination at the minimum exposure time. These limits were calculated using the ERIS ETC assuming:

- DIT=2 s, NDIT=1 for SLOW; DIT=0.034 s, NDIT=1 for FAST

- An A0V spectrum

- NGS on-axis, 50% turbulence category

- Airmass of 1.2, FLI of 0.5, and PWV of 2.5mm

These brightness limits assume that either the `JHK-pupil` or `LM-pupil` is being used. The attenuation of the ND filter and APP on the peak flux are also given.

	SLOW (DIT=2 s)		FAST (DIT=0.034 s)		Attenuation (mag)	
	13mas	27mas	13mas	27mas	ND	APP
J	$J = 9.7$	$J = 10.8$	$J = 5.5$	$J = 6.8$	6.00	-
H	$H = 9.3$	$H = 10.6$	$H = 5.0$	$H = 6.4$	5.50	-
Ks	$K = 7.4$	$K = 9.7$	$K = 3.0$	$K = 5.3$	5.06	-
Ls	†	-	$L = 1.5$	-	4.64	-
Lp	†	-	$L = 1.8$	-	4.57	-
Mp	†	-	$M = -0.3$	-	4.50	-
Pa-b	$J = 7.5$	$J = 8.8$	$J = 3.2$	$J = 4.5$	5.98	-
Fe-II	$H = 6.5$	$H = 7.9$	$H = 2.1$	$H = 3.5$	5.51	-
H2-cont	$K = 5.5$	$K = 7.8$	$K = 1.1$	$K = 3.4$	5.13	2.3
H2-1-0S	$K = 4.3$	$K = 6.6$	$K = -0.1$	$K = 2.2$	5.10	2.2
Br-g	$K = 4.2$	$K = 6.5$	$K = -0.2$	$K = 2.1$	5.06	2.2
K-peak	$K = 6.0$	$K = 8.3$	$K = 1.6$	$K = 3.9$	5.05	2.5
IB-2.42	$K = 4.7$	$K = 7.1$	$K = 0.3$	$K = 2.6$	4.94	1.3
IB-2.48	$K = 4.3$	$K = 6.6$	$K = -0.1$	$K = 2.2$	4.91	1.1
Br-a-cont	$L = 4.4$	-	$L = -0.1$	-	4.57	1.9
Br-a	$L = 2.5$	-	$L = -2.0$	-	4.56	2.2

† The sky background causes saturation in less than the minimum DIT.

Table 14: Maximum star brightness permitted for each filter, camera, and readout mode. Attenuation of the ND and APP are also given.

The `Blocking` filter in the pupil that can be used in conjunction with short-wavelength (<2.5um) filters has a small attenuation of between 0.05-0.25 magnitudes, larger at longer wavelengths.

The behaviour of saturated pixels differs between the two NIX readout modes. The `SLOW_GR_UTR` readout mode uses up-the-ramp sampling. This uses a pre-determined number of reads of the detector depending on the requested integration time, with a minimum of two reads required for the shortest integration time. This up-the-ramp sampling also employs a threshold above which reads of a given pixel are ignored when performing the final least-squares fit to the individual reads. This allows for an increased dynamic range between the brightest and faintest objects within a single image. For example, in a 60-s image with 31 reads, a bright star may exceed the threshold after the first few reads, whereas a faint star may stay below the threshold for all of the reads. The valid reads are then used to determine the count rate per pixel, which is multiplied by the integration time to produce the final image.

As a minimum of two reads are required for this sampling technique to measure the count rate from a least-squares fit to the ramp, pixels that exceed the saturation threshold in either the first or second read are flagged as saturated, and replaced with an extremely negative pixel value indicating that they are not reliable. At the shortest exposure times the effective saturation limit is reduced due to the requirement for a minimum of two reads, and can be estimated as $\sim 12000 \times \text{DIT}/(\text{DIT} + \text{MIN\_DIT})$ ADU. This is accounted for in the ERIS ETC. Figure 25 shows where the extrapolation or saturation occurs as a function of source brightness and integration time.
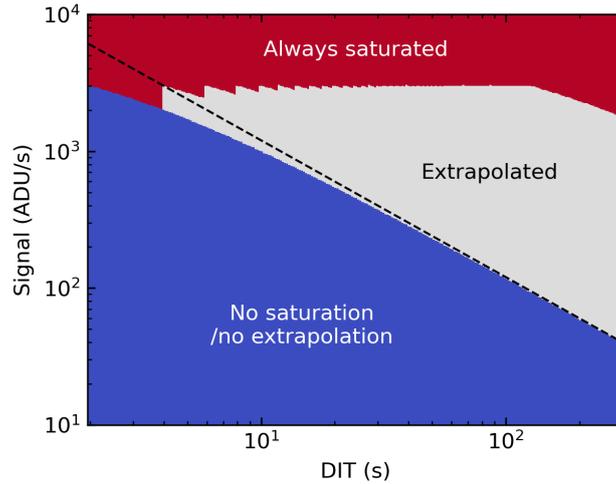
Figure 25: With the `SLOW_GR_UTR` readout mode the pixel value may be either extrapolated from valid reads (gray) or irrecoverably saturated (red). The blue region denotes where no saturation or extrapolation will occur, and the dashed line indicates the nominal well depth of ~12,000 ADU.

The `FAST_UNCORR` readout mode does not employ this type of sampling. Pixels will saturate at the full well depth, and there is no flagging of saturated pixels by an extremely negative value. The saturation level is also independent of the readout mode.

The user should consult the ETC to ensure that their instrument setup does not result in a count rate above the limit, and that it doesn't cause a saturation in the shortest DITs when the extrapolation of the up-the-ramp samples is not possible. These restrictions are put in to limit the effects of persistence in between consecutive OBs. Within a single OB, users are responsible for designing their observing strategy to minimise the impact in their data.

4.2.1.4 File transfer overhead in cube mode When operating in cube mode the individual NDITs are continuously transferred to disk via a network link. When the exposure time for each NDIT is short, there is insufficient time to transfer one frame before the next arrive, and the pending frames are buffered. This can lead to a significant overhead between exposures at the shortest DITs. The transfer overhead can be estimated from the DIT, NDIT, and the number of rows in the detector window (see Table 4) as:

$$\frac{(\texttt{NDIT} \times \texttt{NROWS} \times 2048 \times 2)}{52 \times 1024^2} - \texttt{DIT} \times \texttt{NDIT} \tag{1}$$

If this value is positive, the detector is accumulating data faster than it can be transferred, causing an additional overhead between exposures. For the full frame (`windowF`), this occurs for DIT < 0.154 s, and an additional overhead of 52 s is required for a DIT of 0.05 s and NDIT of 500. This overhead is described for each detector window in Table 22, and is incorporated into the calculation provided in P2.

4.2.2 Optical ghosts

All instruments suffer ghosting due to internal reflection within the filters, for which a faint (almost in focus) ghost image appears slightly offset from the true image. This is more noticeable with narrow band filters because their peak transmission is lower than for broad band filters. This section summarises the ghosting in NIX. The relative position and strength of the ghost for each filter in the centre of the field is indicated in Table 15 and Figure 26. The way in which the position of the ghost shifts across the field is also summarised in Figure 26. A more detailed mapping of the ghost in the `Br-g` filter shows that where $\delta(x, y)_{ghost}$ is the relative

$$\delta x_{ghost}/\Delta X_{source} = \delta y_{ghost}/\Delta Y_{source} = 0.0258$$

shift of the ghost with respect to the source, and $\Delta(X, Y)_{source}$ is the shift of the source on the detector. Thus it is possible to calculate the relative position of the ghost for any location in the field using the central offsets given in Table 15.

Ghosts can often be ignored, especially when dithering images of faint objects, because they remain below the noise level in the combined image. But they should be noted especially for high contrast imaging, since a ghost may appear in the dark region around the PSF.

Filter	X_{offset} (pix)	Y_{offset} (pix)	Peak ratio (%)	Total ratio (%)
J	4	-25	<0.1	0.2
H	3	-26	0.1	0.4
Ks	-1	-46	0.1	0.1
Pa-b	-3	-33	0.2	0.8
Fe-II	12	-20	0.1	0.4
H2-cont	5	-53	0.1	0.2
H2-1-0S	-1	-31	0.3	1.8
Br-g	0	-30	0.7	2.1
K-peak	2	-25	0.1	0.3
IB-2.42	30	-46	0.6	0.8
IB-2.48	7	-35	1.1	2.0

Table 15: Relative positions and strengths of ghosts at the centre of field with the `13mas_JHK` camera in NIX.
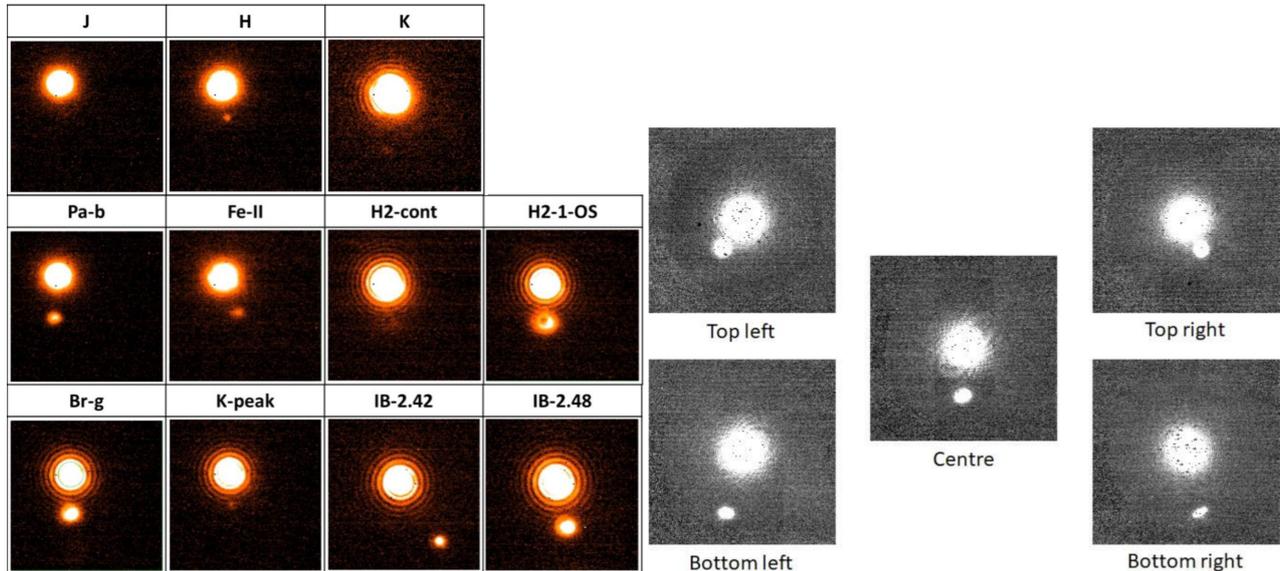
Figure 26: (left panel) Relative positions and strengths of ghosts in the centre of the field. (right panel) Dependency of relative ghost position on location in field, illustrated with the `Pa-b` filter.

4.2.3 High contrast imaging

High Contrast Imaging (HCI) is used in the imaging of faint circumstellar material or planetary companions, where the diffraction halo of the central star is the dominant noise source in the regions of interest. In nearly all cases the AO system uses the star as the NGS. In the context of NIX, both focal and pupil plane coronagraphy as well as sparse aperture masking, are considered high contrast techniques because they all aim to enable the user to measure characteristics of these targets as close as possible to their primary star.

All coronagraphs reduce the diffraction halo, and its associated speckle noise after post processing, at the expense of some loss in the throughput of the faint companion. This process is most effective when the target's primary star is bright enough that the AO performance is very good. In this case, the remaining speckles in the PSF halo are quasi-static because they originate from the instrument. As such, they can be separated from the source by tracking the pupil rather than the field, so that the speckle pattern remains fixed on the detector while the astrophysical source (e.g. the exoplanet) moves on the detector from one exposure to the next. The differential rotation can be maximised by observing the source as it crosses the meridian, The data
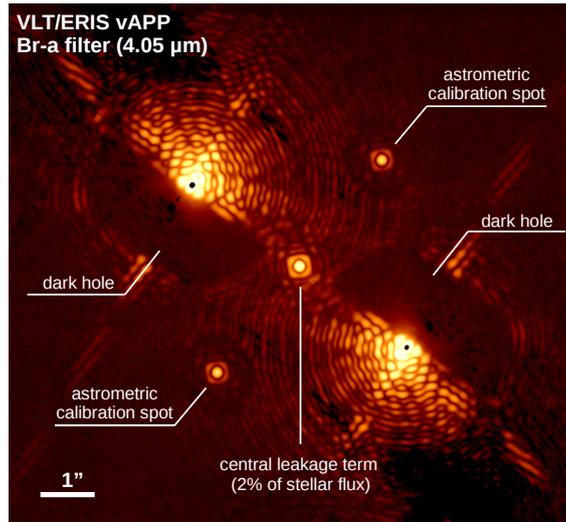
Figure 27: NIX on-sky APP PSF with `Br-a` filter.

can then be processed to remove the speckles with dedicated ADI techniques, which may differ according to the specific use case.

4.2.3.1 Pupil plane coronagraphy The pupil plane coronagraph is a grating vector Apodizing Phase Plate (APP, Otten et al. 2014, Optics Express, 22, 30287). The APP is a single optic that goes in the pupil plane. It generates three images of the star. The central image contains about 2% of the total flux from the star, and acts as a photometric and astrometric reference. The other two PSFs contain 49% of the transmitted flux each. Each of these two PSFs has a dark D-shaped region of suppression on one side of the star. The two D-shaped regions of both images are on opposite sides of the star, and so provide nearly 360 degrees of suppression when combined. As the orientation of the pupil mask relative to the telescope spiders must be fixed, the instrument rotator must be at a fixed angle of 36 degrees (`PUP_ANGLE`. It is not possible to set the instrument to an arbitrary rotation. For APP observations, which are always taken in pupil-tracking mode, North is at a position angle measured from vertical in a counter-clockwise direction of approximately `PARANG − PUP_ANGLE − 90.7` degrees (see also Section 7.2.4.2).

The APP works on all objects in the field of view simultaneously, providing suppression for single and multiple star systems. In these cases, care must be taken when dithering to define positions that will not cause overlapping PSFs in the subtracted image sets. The mode requires no special alignment in the focal plane, and is insensitive to tip-tilt motions and pointing errors in the telescope pointing. It is designed to work with any narrow band filter in K, L or M bands. In principle it can also be used with broad filters, but this will lead to radial smearing of the stellar PSFs.

The APP observations should be designed in a way that the central leakage term is not saturated in a single DIT since this serves as flux calibration. D-shaped components can be saturated to optimise achievable contrast. Table 16 provides guidance for the planning and users should refer to the ERIS ETC for the estimates of peak intensities in nominal PSFs at a given star magnitude, and Table 14 for the (un-attenuated) bright limit for each filter, camera, and readout mode. Peak intensities after attenuation by the APP must not exceed ten times the saturation level of the detector (see Section 4.2.1.3).

The leakage term of the APP PSF allows photometric calibration of an imaged faint companion. Indeed, since the side PSFs of the host star are usually saturated during a deep exposure, one can compare the planet flux in the dark zone to the leakage term of the star. This requires to carefully calibrate the flux ratio between the side PSFs and the central leakage term. During commissioning, the APP PSF was observed to be unstable depending on weather conditions, therefore we recommend to add a calibration exposure after each acquisition template to take an unsaturated APP PSF, and repeat this calibration every hour for extended observations. For such a calibration, one can use twice as long DITs as would be allowed for normal imaging without saturating, and use the same nodding (or dithering) positions as the science exposures to remove the sky background. We recommend a few minutes of total integration time for this calibration to obtain a good signal on the APP PSF.

During the commissioning, APP on-sky contrast curves are derived for `Br-g` and `Br-a` representing respectively a below and above 2.5 μm filter. These are shown in Figure 28. For `Br-g` case, γ Gru (K=3.5 mag)

Filter	Central [%]	Sides [%]	Background [%]
H2-cont	11.1	12.0	100.0
H2-1-0S	12.0	13.0	100.0
Br-g	12.8	13.0	100.0
K-peak	10.7	9.8	50.6
IB-2.42	2.8	27.0	31.9
IB-2.48	2.8	30.9	33.5
Br-a	1.4	16.1	29.1
Br-a-cont	1.2	12.9	22.5

Table 16: Relative peak intensities of various components in APP PSFs with respect to the nominal diffraction limited PSF. The central spot refers to the central leakage term from Fig. 27, while the sides refer to the average value for the North and South PSF.
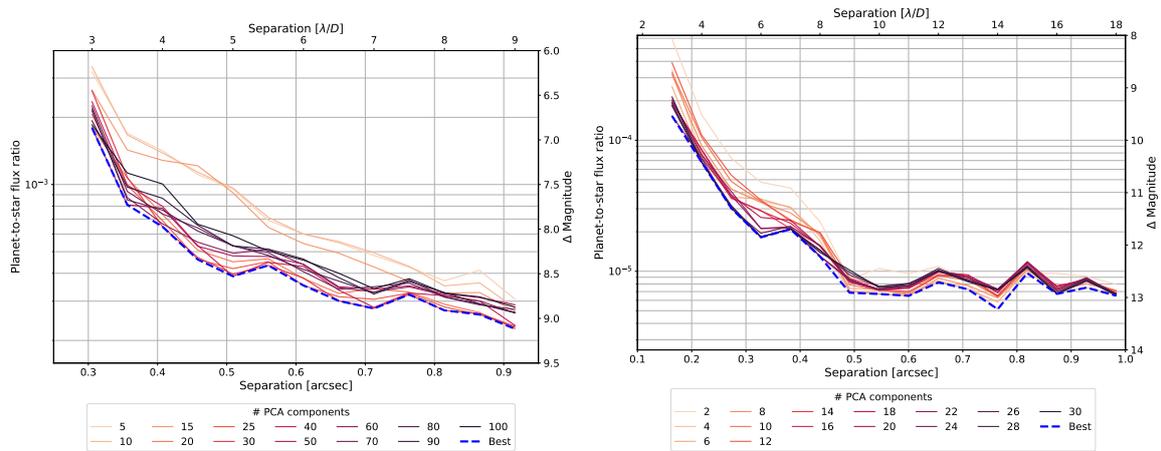
Figure 28: Representative APP on-sky contrast curves corresponding to 5σ fake source detection in `Br-a` (left) and `Br-g` (right) filters. For details refer to the text.

observed for 45 minutes (net exposure time) with an average seeing of 0.9" and PVW 6.9 mm. For `Br-a` case, ι Cap (L=2.2 mag) observed for 12 minutes with an average seeing of 0.6" and PVW 1.2 mm. The datasets are reduced with ADI-based Principle Component Analysis (PCA) (PYNPOINT; Amara et al., 2012, MNRAS, 427) and the limits are derived from fake planet injections. The resulting contrast will vary based on the post-processing technique used.

4.2.3.2 Sparse aperture aasking A Sparse Aperture Mask (SAM) is a pupil plane mask that has several smaller circular apertures cut out of it, typically with a combined throughput of 5 to 15% that of the full aperture. The distribution of the subapertures builds a series of non-redundant or partially redundant baselines and their associated Young's fringes in the focal plane.

For ERIS, there are three pupil mask choices for SAM imaging, yielding an inner working angle of 0.5 λ/D. They are briefly described below:

- The SAM-7 mask has the highest throughput, with a transmission of 14%, a total of 21 non-redundant baselines between the 7 apertures. It is designed to be used on faint targets, when looking for the highest dynamic range.

- The SAM-9 mask with 9 apertures has intermediate throughput of 10.6%, and a total of 36 non-redundant baselines. It will be used mostly to have many baselines for complex systems, with medium brightness.

- The SAM-23 mask has low throughput of 5%, but 253 baselines of which 173 are non-redundant. It is a partially redundant mask which can be used on bright targets for imaging purpose, at a resolution a factor two better than the diffraction limit of the telescope.
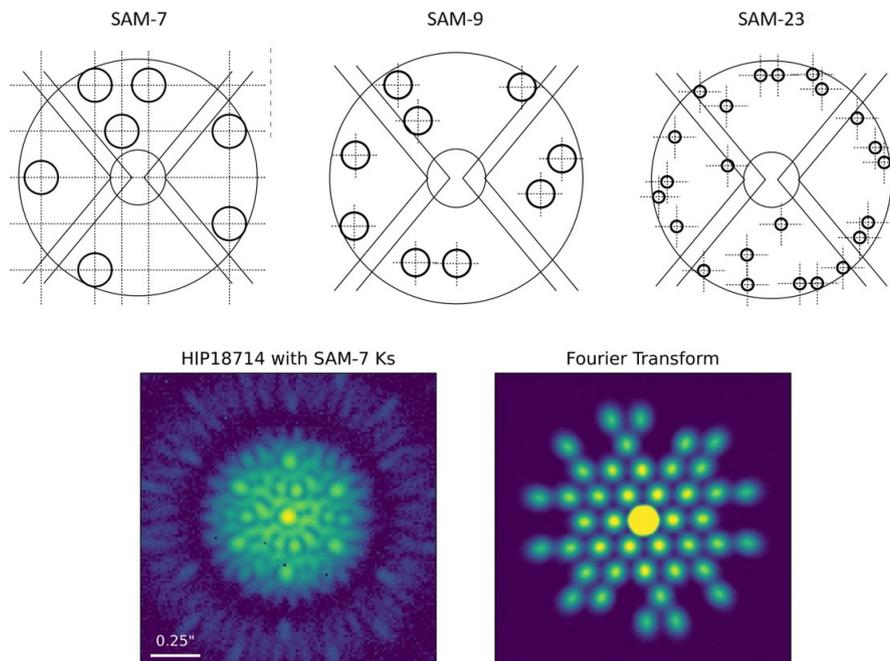
Figure 29: Top row: drawings of the SAM masks in NIX.These show the size and location of the apertures with respect to the full pupil. And illustrate how these can be fitted around the spider arms to avoid vignetting (note that the relative orientation of the spider and apertures may differ). Bottom row: an image of raw data taken with SAM-7 (left) and its Fourier transform (right).

A schematic of the three masks, and a representative PSF with the SAM-7 mask, are shown in Figure 29. The position and radius of the hole within each mask projected onto the telescope pupil are given in Tables 17, 18, and 19. Images of the SAM masks are taken monthly to monitor their position as a part of the calibration plan. These can be obtained from the archive by filtering for `DPR.TYPE = PUPIL,SKY`. Optimal exposure times are given for each valid mask and filter combination in Figure 30. All SAM observations are taken in pupil-tracking mode, with the rotator set to a fixed angle (`PUP_ANGLE`) of 34 degrees for observations with `NXPW=SAM-23` and `NXCW=13mas-JHK`, and of 136 degrees for all other combinations. North is at a position angle measured from vertical in a counter-clockwise direction of approximately `PARANG` − `PUP_ANGLE` + 90.7 degrees (see also Section 7.2.4.2).

The ERIS pipeline does not process these data. Instead they must be processed by the user's own scripts. Observations should include interleaved observations with a calibrator star in order to remove systematic effects within the telescope.
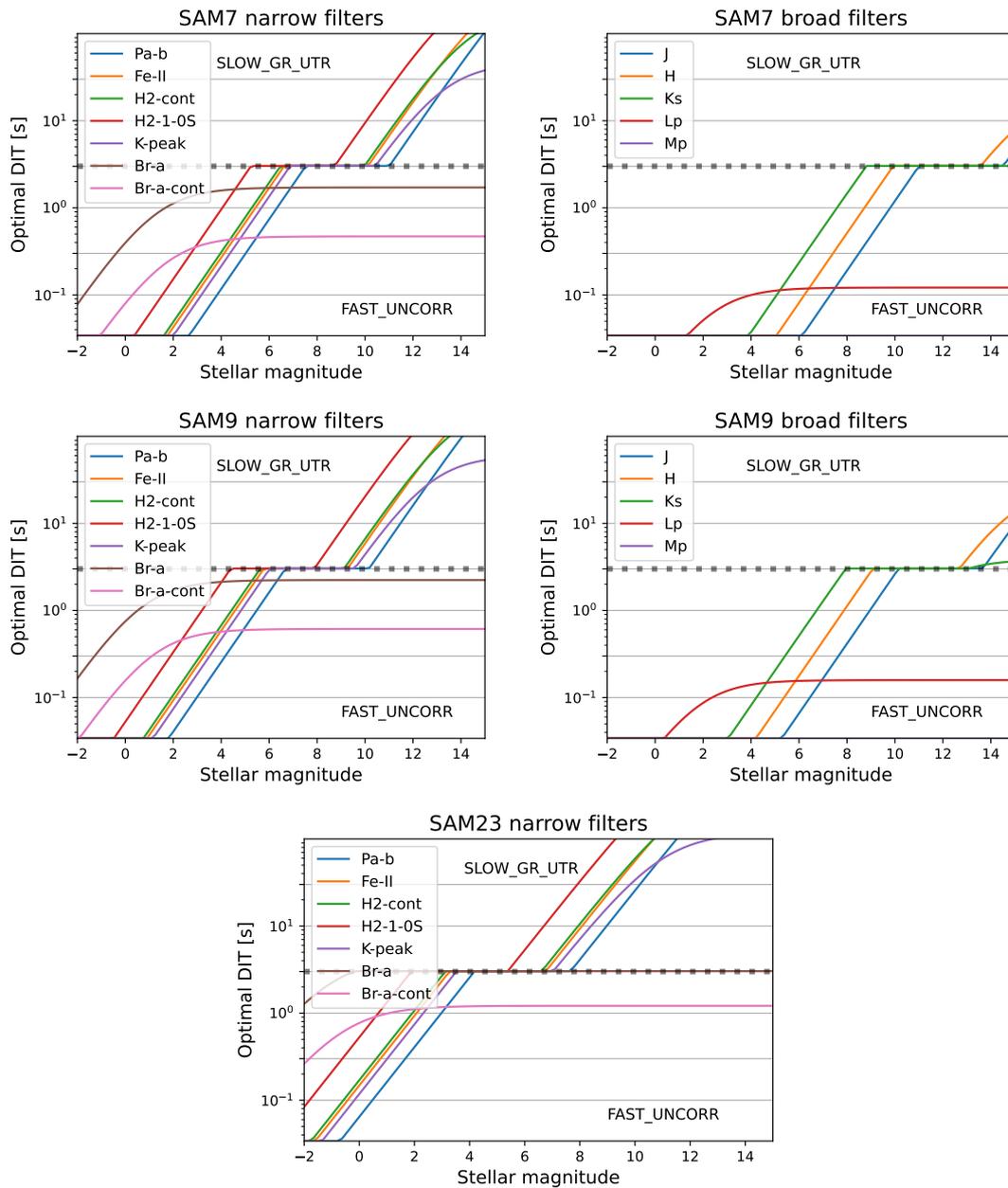
Figure 30: Optimal DIT used in combination with each SAM mask and each filter as a function of stellar magnitude of the target. These values were derived from the ERIS ETC.

Table 17: Positions and sizes of the holes of the SAM-7 mask.

13mas-JHK			13mas-LM		
X[m]	Y[m]	Radius[m]	X[m]	Y[m]	Radius[m]
−1.4321	−2.9013	0.5267	−1.4407	−2.9304	0.5331
2.8494	−1.5417	0.5267	2.8747	−1.5581	0.5331
−3.0371	0.0843	0.5267	−3.0703	0.0782	0.5331
−0.4643	1.4758	0.5267	−0.4661	1.4867	0.5331
−1.2777	2.9737	0.5267	−1.2894	3.0028	0.5331
0.4167	2.9323	0.5267	0.4210	2.9565	0.5331
2.9293	1.4017	0.5267	2.9550	1.4032	0.5331

Table 18: Positions and sizes of the holes of the SAM-9 mask.

13mas-JHK			13mas-LM		
X[m]	Y[m]	Radius[m]	X[m]	Y[m]	Radius[m]
−1.2914	−2.5043	0.4026	−1.2955	−2.5334	0.4082
−0.0565	−2.5538	0.4026	−0.0565	−2.5832	0.4082
−3.0791	−1.3526	0.4026	−3.1130	−1.3721	0.4082
2.5001	−0.5350	0.4026	2.5287	−0.5491	0.4082
3.1639	0.4926	0.4026	3.2022	0.5058	0.4082
2.0361	2.6913	0.4026	2.0580	2.7155	0.4082
−1.0850	1.7559	0.4026	−1.0932	1.7732	0.4082
−2.9773	0.7776	0.4026	−3.0116	0.7877	0.4082
−1.6554	2.8523	0.4026	−1.6715	2.8848	0.4082

Table 19: Positions and sizes of the holes of the SAM-23 mask.

13mas-JHK			13mas-LM		
X[m]	Y[m]	Radius[m]	X[m]	Y[m]	Radius[m]
−0.8436	−3.3059	0.1779	−0.8488	−3.3361	0.1801
0.7928	−3.3155	0.1779	0.8045	−3.3490	0.1801
1.3431	−3.3199	0.1779	1.3581	−3.3533	0.1801
−2.2067	−2.8298	0.1779	−2.2239	−2.8541	0.1801
−0.8362	−2.3534	0.1779	−0.8415	−2.3748	0.1801
2.1621	−2.8522	0.1779	2.1800	−2.8794	0.1801
2.7121	−1.9101	0.1779	2.7369	−1.9290	0.1801
−3.0063	−1.3964	0.1779	−3.0394	−1.4131	0.1801
0.2567	−1.4145	0.1779	0.2652	−1.4277	0.1801
2.9904	−1.4370	0.1779	3.0188	−1.4462	0.1801
−3.5477	−0.4468	0.1779	−3.5879	−0.4552	0.1801
−1.3553	0.4765	0.1779	−1.3749	0.4839	0.1801
−3.2635	0.0222	0.1779	−3.3074	0.0238	0.1801
−2.9880	1.4336	0.1779	−3.0248	1.4493	0.1801
3.5543	0.4506	0.1779	3.5896	0.4580	0.1801
3.2834	0.9234	0.1779	3.3114	0.9332	0.1801
2.7383	1.8732	0.1779	2.7630	1.8911	0.1801
−1.3463	2.3682	0.1779	−1.3549	2.3918	0.1801
−2.1647	2.8451	0.1779	−2.1835	2.8785	0.1801
1.6533	2.8264	0.1779	1.6716	2.8525	0.1801
−0.2525	3.3104	0.1779	−0.2511	3.3386	0.1801
0.2874	3.3068	0.1779	0.2919	3.3352	0.1801
1.3865	3.3031	0.1779	1.4013	3.3352	0.1801

4.2.3.3 Focal plane coronagraphy Focal plane coronagraphy is implemented in ERIS using an Annular Groove Phase Mask (AGPM, Mawet et al. 2005, ApJ 633, 1191), more commonly referred to as a vortex coronagraph (VC). This is followed by a Lyot stop in the pupil plane. The vortex coronagraph provides 360 degrees of suppression around a point source, whilst allowing light from circumstellar disks and companions to be transmitted through to the final focal plane. The total field of view in this mode is limited to a radius of 8.2″ (Figure 31, left panel).
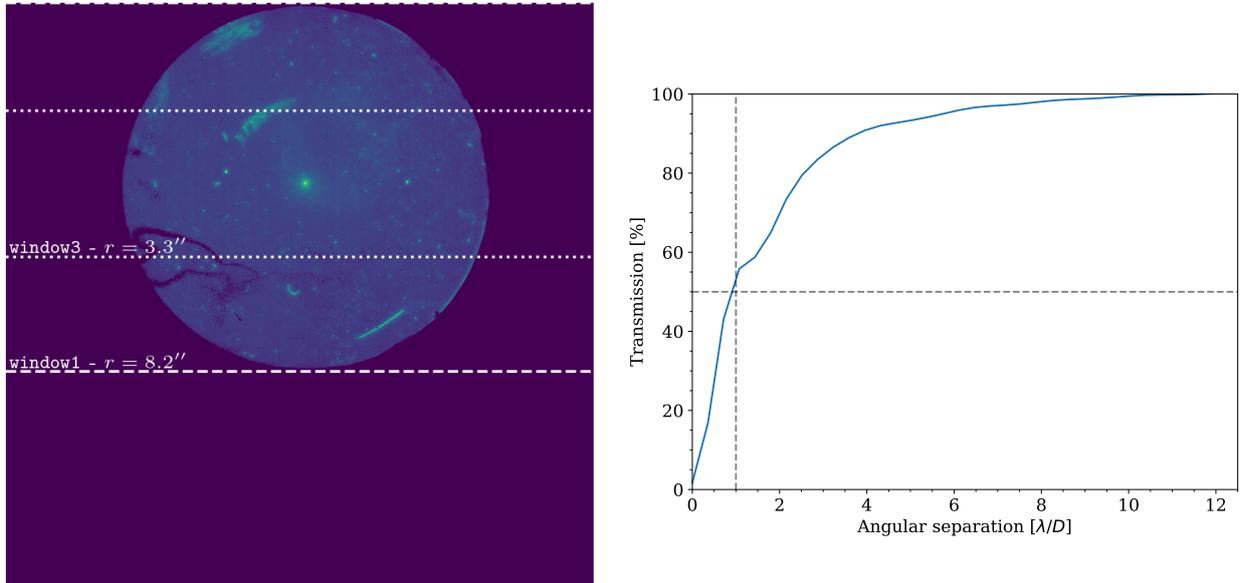
Figure 31: *(left):* The field-of-view with the vortex coronagraph is limited to an 8.2″ radius. The detector can be windowed to allow for shorter DITs for very bright targets. *(right):* Theoretical coronagraphic transmission as a function of radial distance to the vortex centre. The coronagraphic transmission of >50% which makes the vortex one of the most efficient in terms of inner working angle.

The VC is implemented as separate masks for L and M bands. The target star must be placed on the centre of the VC in the focal plane, corresponding to a specific location in the ERIS field-of-view. The positioning must be done precisely because the VC performance is highly dependent on pointing error and differential atmospheric refraction during the course of an observing block. When properly aligned, a doughnut-shaped pattern residual light can be seen around the centre of the vortex mask (Figure 36).

An initial alignment template brings the star close to the VC location, and then short cadence science exposures are used to provide active correction to the position of the star relative to the VC. This is achieved by monitoring the changes in brightness of the residual stellar light around the vortex centre, and by sending small corrections to the AO system using the QACITS algorithm (Huby et al. 2016, A&A, 600, A46).

The observations are typically set up to take sky background measurements every 1-10 minutes. And to provide photometric calibration of the VC, a short exposure with the star moved off the VC and imaged on another area of the detector is typically taken once every hour. Both of these are at the discretion of the observer, and are defined when the observing block is made.

The VC has a throughput of about 83% in L band and 68% in M band (substrate transmission). Together with the Lyot stop, the combined throughput is ∼62% in L band and ∼51% in M-band. The VC works at radial distances from ∼ 1λ/D and out to several arcseconds. More specifically the coronagraphic transmission is already > 50% at 1 $λ/D$, and increases at larger radial distance from the vortex centre. The synthetic transmission curve, computed via Fourier optics simulation and verified during commissioning, is given in Figure 31 (right panel).

Coronagraphic performance: During commissioning, the contrast curves with the vortex coronagraph were measured with the `Lp` filter on two different objects: i Vel ($K = 4$) and GQ Lup ($K = 7$). The details of the observations and the results are presented below.

GQ Lup was observed in a Object-Sky-Object-... sequence with 400×0.3 s on the O exposures and 10×0.3 s on the S exposures, providing a net exposure time of 52 m on target after frame selection. The total exposure time, including sky frame, was 61 m and the total execution time was 83 m. The total ADI sequence amounts

to 58.6 deg of parallactic angle rotation. The R-mag (AO guide star) of GQ Lup is 10.3.

The data reduction used the VIP package (Christiaens et al. 2023, JOSS, 8) and includes dark subtraction, flat-field correction, bad pixel removal, re-centring of frames, PCA sky subtraction, absolute re-centring, and median-subtraction or annular PCA for post-processing. The resulting contrast curves are given in Figure 32 (left). The contrast curves are the 5-sigma contrast corrected for small sample statistics (Student-t correction; Mawet et al. 2014, ApJ, 792). The companion, GQ Lup b, was first removed before computing the contrast curves. The contrast curves include the off-axis transmission of the vortex illustrated in Figure 31.

i Vel was observed following the same strategy as GQ Lup, with a net exposure time of 60 m on target. The data processing and post-processing also followed the same principle as GQ Lup. The resulting contrast curves are given in Figure 32 (right).

The performance obtained are similar to GQ Lup up to about 2.5 λ/D. At larger separation, the contrast is better with i Vel. A brighter star means improved AO performance, increased pointing accuracy with QACITS ($\sim$0.014 λ/D with i Vel instead of $\sim$0.02 λ/D for GQ Lup), and a deeper background-limited sensitivity in terms of contrast, which account for the difference in the contrast curves beyond 2.5 λ/D.
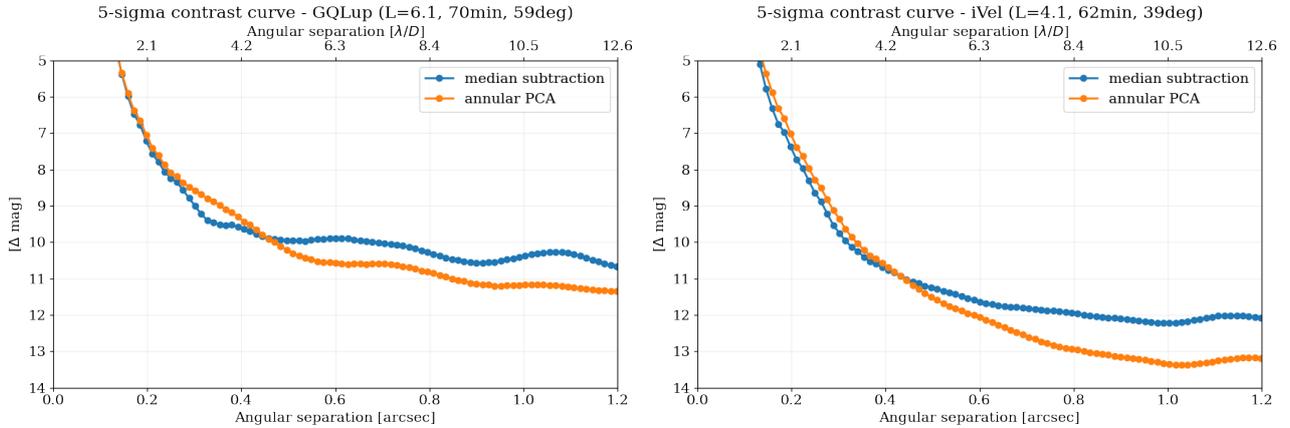
Figure 32: 5-sigma post-processed contrast obtained with the vortex focal plane coronagraph. (Left) GQ Lup, with a total ADI sequence of 70-min and a parallactic angle rotation of 59 degrees. (Right) i Vel, with a total ADI sequence of 62-min and a parallactic angle rotation of 39 degrees.

Magnitude limit: On the bright end, the limit is given by the saturation on the off-axis PSFs obtained during acquisition. With a minimum DIT of 0.034 s and a FPC throughput of $\sim$62%, this limit is reached for $L < 3.7$. Brighter targets require to use windowing and/or the Lyot-ND filter in acquisition. With windowing `window1` and `window3` one can reduce the minimum DIT to 0.022 s and 0.009 s, respectively, decreasing the magnitude limit by $\sim$0.5 and 1.5, respectively. The field-of-view is entirely preserved with `window1`, but it is reduced to $\sim$3.3″ in the `window3` mode. See also Section 2.4.1.2 for more details on windowing

The Lyot-ND filter, on the other hand, transmits about 1/66 of the light in the `Lp` filter and 1/62 in the `Mp` filter, which thus translates in a delta magnitude of $\sim$4.5. One can also combine the Lyot-ND filter in acquisition with windowing to reach in principle a magnitude limit of $L > -2$ (`window3` plus Lyot-ND filter).

On the faint end, observation of targets with $L > 7$ will become progressively more limited by QACITS, which currently measures the pointing error every five seconds. For a $L = 7$ star, the signal-to-noise ratio of the centring measurement (assuming a 1:100 rejection) is approximately 50, using the ETC with standard parameters. This drops to about 20 for $L = 8$ and <10 for $L = 9$. The QACITS performance (2-axis standard deviation) at $L = 7$ is 0.02 λ/D compared to the 0.014 λ/D on i Vel ($L \sim 4$), suggesting that the QACITS correction starts to be limited by the SNR at $L = 7$. We can conjecture that at $L = 8$ (drop of a factor $\sim$2 in SNR) QACITS would still be functional, although at a reduced pointing accuracy, but the control loop would eventually stop functioning between $L = 8$ and $L = 9$. We should stress however that the usefulness of coronagraphic observation for objects fainter than magnitude ~ 9 is questionable. Indeed in this regime, we expect the contrast to be limited by background noise at most separations, and normal imaging should be favored. Due to these considerations, the FPC mode is only offered for targets with $L < 8$ and $M < 7$ (Section 5.6.9).

4.2.4 Long slit spectroscopy

NIX can also take data in long slit spectroscopy mode over a wavelength range of $3.05 - 4.05\,\mu$m. There is single internal configuration of NIX which combines a slit mask in the aperture wheel (12 arcsec × 68 mas, on-sky), a grism suitable for L band that is mounted with an LM-reduced stop in the pupil wheel, and a special broadband `L-broad` filter. This configuration provides a spectral resolution of R∼900. The spectrum is dispersed in the vertical direction on the detector – as can be seen in the annotated example image in Figure 33 (left).
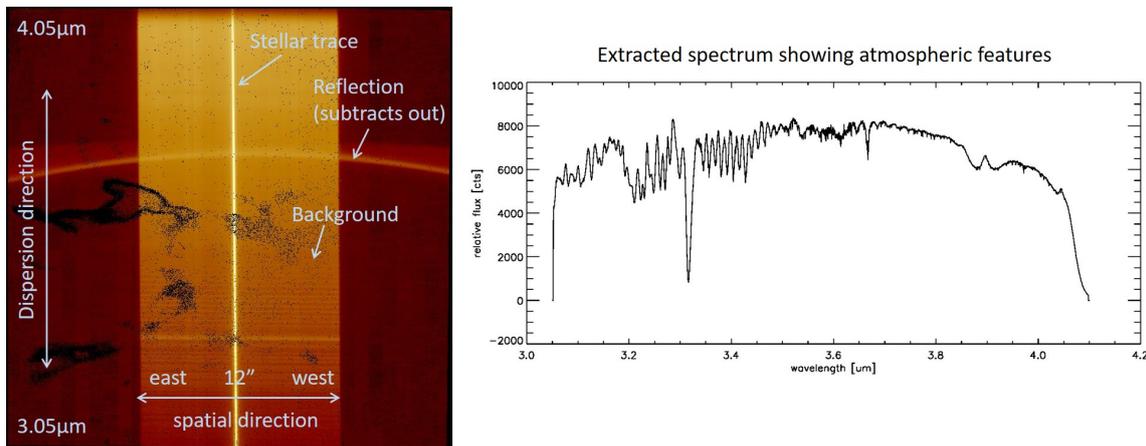
Figure 33: (Left) Image of a raw 2D L-band spectrum showing the background and a stellar trace. (Right) The extracted spectrum is dominated by atmospheric absorption features.

This slit is undersized relative to the diffraction limit of the telescope in the L band; this ensures that the wavelength dispersion is independent of the object's relative alignment to the slit. However, it does mean that accurate alignment of the object with the slit is essential to maximise transmission. Manual intervention by the instrument operator is therefore required during the acquisition to centre the star.

When running the acquisition template, the operator will initially see an image of the slit - which is recorded. The slit is then removed from the beam and a larger field of view is imaged. The RTD shows this larger field of view with the original slit image subtracted, this creates a dark 'stripe' on the detector. The target must be aligned with the slit to within a few pixels, otherwise the transmission of light through the slit will be greatly diminished.

The pipeline includes two sky subtraction techniques. The first of these requires a sky offset position, which can be achieved using the `ERIS_nixLSS_obs_GenericOffset` template, making a nod that deliberately takes the object out of the slit – either by a perpendicular movement or by a sufficiently large movement along the slit. If no dedicated sky offset position is specified, or when using the `ERIS_nixLSS_obs_AutoJitter`, sky subtraction is achieved by generating a median frame using the images from the different offset positions.

Internal instrument flexure can cause the exact location of the spectra on the detector to move for objects at different instrument orientations. The pipeline will the adjust the wavelength solution to account for this shift, using some the brighter skylines. Note this is not an issue within a single observation, but if combining data from different OBs the observer should be aware.

An example extracted spectrum is shown Figure 33 (right). Of note are significant number of atmospheric absorption features, especially at the shorter wavelengths. This makes it hard to quantify S/N at the shorter wavelengths, but for longer wavelengths example values are that S/N ∼100 can be reached in 20 s for an $L = 5$ object, or an equivalent S/N can reached for an $L = 7$ source in 600 s. Note for any exposures longer than this the sky background would approach saturation of the detector. Users are advised to consult the ETC calculator for more precise estimates of sensitivities.

There are a few other subtle features of the mode to keep in mind when planning certain observations:

- In the L-band the AO corrected PSF has very noticeable Airy rings. The slit effectively takes a cross section through these, so on the detector it appears as if there is dispersed flux from multiple sources – one central bright source, then pairs of increasingly feint sources on either side of this. The pipeline allows extraction of flux from a variable sized window, to ensure the flux from these wings is included if desired. These effects should be considered if attempting to take spectra in crowded fields.

- There is a ghost visible in all LSS images. This appears as a curved arc about two-thirds of the way up the image. The brightness of this feature is dominated by the sky – not the object. It is therefore removed by the subtraction of a sky frame. This of course leaves residual noise and any user especially interested in a spectral feature at around $3.7\,\mu$m, should be aware of this.

- There is some variation in transmission across the length of the slit, which is noticeable as apparent vertical banding in image. This effect is wavelength invariant and is removed as part of the pipeline.

4.3   SPIFFIER performance

This section provides a brief overview of the important information about SPIFFIER performance needed for planning observations. This should be used in conjunction with the information available in Section 4.1 on the AO performance.

Limiting magnitudes and sky background may differ based on observing conditions, hence we recommend users to use the ERIS ETC for proper estimates (see Section 6.3).

4.3.1   Detector

The detector characteristics (dark current, etc.) are shown in Table 5.

4.3.1.1   DITs and NDITs   For long exposures on faint targets, we recommend to work with NDIT=1 and a DIT to reach the desired SNR per pointing rather than using short DITs and many NDITs. For exposures with $DIT > 150$ s, it is mandatory in both service and visitor mode to use a DIT of either 180s, 300s, 450s, 600s or 900s. For exposures with $DIT \geq 60$ s you must use $NDIT = 1$ to reduce the daytime calibration activities. Multiple exposures can be taken at the same position by modifying the `SEQ.NEXP` parameter which can then be averaged using the pipeline, equivalent to the averaging that is performed when $NDIT > 1$ by the detector NGC. The detector overhead between each exposure at a given offset position is minimal.

For short exposures, we recommend DIT values of 2s, 5s, 10s, 15s, 20s, 30s, 60s, 90s or 120s to reduce the daytime calibration activities and to enable sharing of the calibration data with other projects.

4.3.1.2   Saturation and persistence limits   Persistence characteristics are reported in Section 2.5.6. In service mode observations the count level must not exceed 50% of the detector well depth. This corresponds to a limit of 40k e- (20k ADU). The table below gives the brightest magnitude permitted for each grating and plate scale configuration at the minimum exposure time. These limits were calculated using the ERIS ETC assuming:

- DIT=1.6, NDIT=1

- An A0V spectrum

- NGS on-axis, 50% turbulence category

- Airmass of 1.2, FLI of 0.5, and PWV of 2.5

	25mas	100mas	250mas
`J_low`	$J = 4.3$	$J = 6.9$	$J = 7.1$
`H_low`	$H = 4.5$	$H = 6.8$	$H = 7.1$
`K_low`	$K = 4.0$	$K = 6.3$	$K = 6.5$
`J_short/_middle/_long`	$J = 3.2$	$J = 5.8$	$J = 6.0$
`H_short/_middle/_long`	$H = 3.4$	$H = 5.8$	$H = 6.1$
`K_short/_middle/_long`	$K = 3.2$	$K = 5.4$	$K = 5.7$

Table 20: Maximum star brightness permitted for each grating and plate scale configuration.

SPIFFIER uses the same up-the-ramp sampling as used in the `SLOW_GR_UTR` readout mode of NIX. The same considerations regarding saturation and extrapolation of pixel values, and the reduced well depth at shorter integration times, as discussed for NIX in 4.2.1.3 apply for SPIFFIER. The user should consult the ETC to ensure that their instrument setup does not result in a count rate above the limit, and that observations of bright stars are not affected by the reduced well depth at the shortest exposure times.

The restrictions on observations of bright stars are put in to limit the effects of persistence in between consecutive OBs. Within a single OB, users are responsible for designing their observing strategy to minimise the impact in their data. These limits are relaxed by one magnitude in visitor mode, but the user should consider the effect of persistence when planning their observing run.
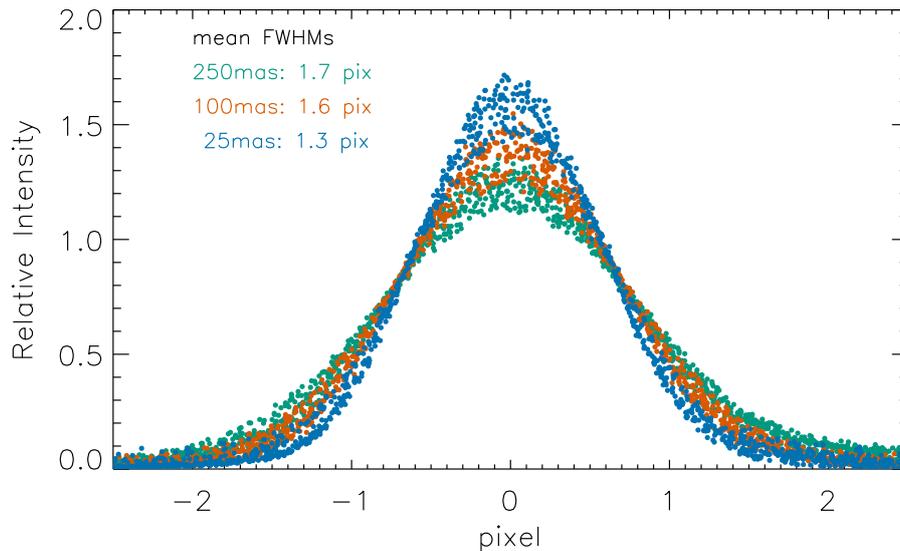
Figure 34: Fine sampled SPIFFIER line profiles in all grating configurations and pixel scales.

4.3.2 Spectral resolution and wavelength selection

Figure 34 presents SPIFFIER line profiles for all configurations. For a given configuration, the resolution is stable across the detector, varying only by a few percent. In all configurations, line profiles are under-sampled: line widths are between 1.3 and 1.6 pixels across different configurations. The data used in this analysis are available in the ESO archive facility for all combinations of gratings and pre-optics, and can be found by searching for `TPL.ID` of `ERIS_ifs_tec_BabySteps`.

For faint objects, there is a trade-off between spectral resolution and detectability. When observing at higher resolution, the continuum and spectrally resolved line emission are spread over more pixels, so the detector dark current and read noise become more important. Thus less observing time is needed to detect a line at lower resolution.. On the other hand, at lower resolution, especially in the H-band, OH-lines contaminate a larger portion of the spectrum. Spectrally unresolved emission lines and narrow velocity features can be measured more accurately and sensitively at higher resolution, but a single exposure covers a smaller wavelength range at higher resolution so not as many diagnostic lines may be present in the spectrum. It is up to the observer to weigh these trade-offs and decide whether to observe at R~5000 or R~10000. The ETC can be used to determine the observing time needed to obtain a certain S/N for emission lines and continuum in the various instrument setups.

4.3.3 Object-sky observation pattern

In practice, there are three ways to estimate the sky during SPIFFIER observations. We describe the concepts here using a few templates as a basis – for a definitive listing see Section 7.4.2.

- The template specifically tailored for this task is `ERIS_ifs_obs_FixedSkyOffset`. The template supports two different object-sky patterns: (1) O-S-S-O (`SEQ.ABBA=T`, `SEQ.NABCYCLES=2`) (2) O-S-O-O-S-O (`SEQ.ABBA=F`, `SEQ.NABCYCLES=2`). In the former option, object and sky frames are alternated with 50% of the total time spent on the object. The latter option, in which less time would be spent on the sky, is also commonly used when object exposures are well dithered. In this case, the nearest-in-time sky exposure is used to correct each object exposure.

- The template `ERIS_ifs_obs_AutoJitter` can be used to to estimate the sky background directly from the object frames for isolated sources (it does not inherently support dedicated sky frames). For example, offsets can be applied to place the source successively in the four quadrants of the SPIFFIER field of view. Then the empty quadrants can be used to estimate sky background. The object size should be considerably smaller than the selected field of view for optimal results, and the user should be sure that the rest of the field is suitable for sky background estimation.

- A more generic option is the `ERIS_ifs_obs_GenericOffset` template. This template provides full flexibility to the user. It is possible to assign each dither either an Object(`O`) or Sky(`S`) tag.

Among all three approaches the first one is a safer choice to obtain sky frames with SPIFFIER for less experienced users.

5 Observing with ERIS – Overview

5.1 Modes offered

The following modes are currently offered:

- AO modes: noAO, NGS, LGS, LGS-SE

- Sidereal and non-sidereal targets, including differential tracking

- Field tracking: IFS, nixIMG, nixLSS

- Pupil tracking: IFS, nixIMG, nixAPP, nixFPC, nixSAM

- SPIFFIER – all gratings and plate scales

- NIX imaging – 13mas and 27mas cameras, all filters

- NIX APP – 13mas camera, narrow-band K and L-band filters only

- NIX FPC – 13mas camera, L and M-band filters only

- NIX LSS – L-band low-resolution spectroscopy with only one setup

- NIX SAM – all SAM masks

- NIX – Fast and slow readout modes

- NIX – Detector windowing (sub-array)

5.2 Modes not offered

The following modes are not offered. Some of these modes may be offered in future periods contingent on successful implementation and commissioning.

- AO spatial filtering, the mechanism is fixed at the largest diameter aperture

- The `Blocking` NIX pupil wheel filters

5.3 Service mode

The majority of ERIS observations will be conducted in service mode (SM). It is important to carefully review the materials in this manual, as well as the information presented on the ESO website[5], when preparing ERIS observing blocks to ensure that they are feasible.

5.4 Visitor mode

Observations with ERIS can also be performed in visitor mode (VM) or delegated visitor mode (dVM). Information regarding visitor mode operations can be found on the ESO website[6]. Visitors are required to prepare backup targets in the event of poor conditions. Pointing restrictions can occur due to high winds from the north, so users are strongly encouraged to have backup targets in the south. Visitors should be aware that twilight time may be used by the observatory, and is not necessarily available for the visitor.

For more information, please refer to `https://www.eso.org/sci/facilities/paranal/sciops/vm_backup.html`

5.5 AO limits for service and visitor mode

Table 21 summarises the key limits and observing constraints that apply to either or both of service and visitor mode observations with ERIS. Particularly important are the Gaia BP and RP magnitude limits for the natural guide star (NGS mode) and tip/tilt star (LGS mode). Several of these parameters are automatically checked at Phase 1, and all are automatically checked at Phase 2. Observations exceeding these constraints/limits will not be accepted.

---

[5]`https://www.eso.org/sci/observing/phase2/SMGuidelines/SMRules.ERIS.html#InsSpec`
[6]`https://www.eso.org/sci/observing/phase2/VMGuidelines.ERIS.html`, `http://www.eso.org/sci/facilities/paranal/sciops/`

Table 21: Constraints in service and visitor mode

Constraint	Run Type	NGS	LGS	LGS-SE	noAO
Gaia BP	SM/VM	≤ 19	≤ 19	N/A	N/A
Gaia RP	SM/VM	≤ 11	7-18	N/A	N/A
Off-axis radius	SM/VM	$0''$-$59''$ ($< 30''$ rec.)	$0''$-$59''$	N/A	N/A
Airmass	SM/VM	< 1.9	< 1.9	< 1.9	< 2.9
TCAT	SM	$\leq 70\%$	$\leq 85\%$	$\leq 30\%$	Any
DIMM seeing	SM	$\leq 1.15''$	$\leq 1.4''$	$\leq 0.8''$	Any
Coherence time	SM	$> 2.2\,\mathrm{ms}$	$> 1.6\,\mathrm{ms}$	$> 4.1\,\mathrm{ms}$	Any
FLI	SM	N/A	≤ 0.5 for RP > 16	N/A	N/A

5.6 Observing constraints for service mode

All of the following constraints apply to service mode observations. Visitor mode observations must still respect the airmass constraint as this is a fundamental limitation of the instrument.

5.6.1 Image quality and turbulence category (TCAT)

The constraints and classification for ERIS OBs depends on what AO mode is being used.
For NGS, LGS, and LGS-SE observations:

- The TCAT specified at P1 corresponds to a specific threshold of the V-band seeing at zenith and coherence time.

- The same TCAT is used at P2 (with the image quality left at the default value).

- The OB is graded by comparing the DIMM-measured seeing and coherence time to the thresholds of the requested TCAT.

For no-AO observations:

- The TCAT specified at P1 corresponds to a specific V-band seeing at zenith threshold.

- The image quality specified at P2 is the predicted image quality (FWHM) given the requested TCAT, airmass, and central wavelength. The ETC calculates this value for all no-AO simulations.

- The OB is graded by comparing the requested image quality to the realised FWHM in the IFS/NIX images at the requested wavelength (or approximated from the DIMM if no obvious point source is present) over the course of the OB.

The maximum permissible turbulence category for each AO mode are:

- NGS: 70%

- LGS: 85%

- LGS-SE: 30%

- noAO: Any

5.6.2 Sky Transparency

The permissible sky transparency categories for each AO mode are:

- NGS, LGS, LGS-SE: photometric, clear, thin cirrus

- noAO: photometric, clear, thin cirrus, thick cirrus

Observations using faint NGS ($>$10th magnitude) or TT stars ($>$16th magnitude) are not recommended under thin cirrus conditions. Bright AO guide stars can be used under thin cirrus conditions, increasing the probability an OB is observable, unless stable conditions are needed for precise absolute photometry.

5.6.3 Airmass

Observations utilising NGS must be performed at airmass less than 1.9. Observations utilising LGS or LGS-SE must be performed at airmass less than 1.9. You should use the ETC to select an appropriate airmass constraint for your observations, considering the airmass of your target at culmination.

5.6.4 Moon

You should not over-specify the Moon constraints (MD: moon distance, FLI: fraction of lunar illumination) as this reduces the chances of the observation being executed. While the Moon does not directly affect infrared observations, it can cause issues when using faint NGS/TT stars (see Section 4.1.7). LGS observations using a tip-tilt star with a Gaia RP magnitude fainter than 16th magnitude are particularly affected. These OBs must have an moon illumination (FLI) constraint of 0.5 or less to ensure the background in the low-order wavefront sensor from scattered moonlight does not overwhelm the faint guide star.

For most other ERIS observations the moon illumination constraint can be entirely relaxed by selecting FLI=1. Only for the shortest wavelength filters (<1.2um) there is an increased contribution from the sky background, potentially degrading the sensitivity of your observations. The minimum moon distance permitted is 25 degrees. It is recommended to use a more stringent constraint of 40 degrees when using TT stars close to the faint limit.

5.6.5 Twilight

Observations of bright objects can be carried out in twilight, up to 45 minutes before the end of astronomical twilight. You should use the twilight constraint in the p2 tool to specify the number of minutes before the end of astronomical twilight that an OB can be started (e.g., −30 means the OB can be started at the earliest 30 minutes before the end of astronomical twilight).

5.6.6 Precipitable water vapour

The sky transmission and emission in the L and M-band vary strongly as a function of precipitable water vapour (PWV). You should use the ETC to select an appropriate PWV constraint for OBs with observations at these wavelengths.

5.6.7 Local sidereal time

Specifying a local sidereal time (LST) constraint may be desirable for observations using pupil tracking. The length of the LST interval must at the very least exceed the duration of the OB. Relaxing the interval further will make scheduling your observation easier. You should use at least the duration of the OB plus an additional 30 minutes. There are no limits on the maximum duration of the LST interval.

5.6.8 Wind speed

There are no specifications for maximum wind speed beyond those set by the observatory. Section 4.1.6 states that AO performance is not strongly affected by wind speed within the range 9.6-14.3 m/s. For service mode observations, the instrument operator will decide on whether the conditions are suitable for AO. For visitor mode observations, you are strongly encouraged to prepare backup OBs with targets in the south (as the wind is preferentially from the north) or with noAO in case the conditions are poor.

5.6.9 Faint limit for focal plane coronagraphy

Targets fainter than $L = 8$ ($M = 6$) cannot be observed with the FPC mode. Targets between $L = 7$ and $L = 8$ ($M = 5$ and $M = 6$) should request the best TCAT constraints for their observations.

6 Observing with ERIS – Phase 1: proposal preparation

This section will help you to decide whether ERIS is the right instrument for your scientific project, take you through a quick evaluation of the observing time needed, and guide you through the particularities of ERIS in the proposal form.

6.1 Is ERIS the right instrument for your project?

ERIS is, above, all, an adaptive optics instrument that is designed to provide diffraction limited observations at near infrared wavelengths. It has a variety of different observing modes and configurations that make it a very flexible single source instrument. These include with SPIFFIER:

- Integral field spectroscopy in J, H, and Ks bands. The field of view is between $0.8''$ and $8''$ depending on the pixel scale selected, and the spectral resolution is either R~5000 (covering a full single band in one setting) or R~10k (with half the coverage).

and with NIX:

- Imaging in J, H, and Ks bands with broad and narrow filters over a field of $26''$ or $55''$ according to the pixel scale selected; and in L', and M' bands over a $26''$ field.

- High contrast imaging in L' and M' bands using focal plane coronagraphs, pupil plane coronagraphs, or sparse aperture masks.

- Long slit spectroscopy at low ($R \sim 900$) resolution in a wide L band.

The AO system achieves excellent performance using a laser guide star and the adaptive secondary mirror of the Adaptive Optics Facility. It can still achieve some correction with tip-tilt stars that are as faint at R~19mag or up to $59''$ off-axis. And if no tip-tilt stars are available, the AO system can provide improved resolution with its 'seeing enhancer' mode; and seeing-limited observing is always possible although this is not the primary purpose of the instrument.

6.2 Targets and reference stars

Proposals requesting either NGS or LGS observations must specify the AO reference stars associated with each target (even if they are the same) in the "Observations" part of the proposal form. When the targets are too faint to act as AO reference stars it is recommended to query the Gaia DR3 catalogue via VizieR[7] to find suitable stars. The magnitude range should be limited appropriately using the constraint fields:

- `BPmag:` < 19, `RPmag:` < 11 for NGS,

- `BPmag:` < 19, `RPmag:` 7..18 for LGS,

and the target dimension should be limited to one arcminute. Checking compute distance, and "sort by distance" on the preference panel on the left can help you find a reference star not too close to the edge of the AO patrol radius. If a suitable reference star cannot be found using this query the observation of this target in this AO mode is not feasible. Add the selected reference star to your target list. The p1 tool will resolve the coordinates of stars with Gaia identifiers (e.g., Gaia DR3 528971921686611200), but it will only add magnitudes for stars in SIMBAD. Please manually add the Gaia BP and RP magnitude of the reference star (the form only accepts the name "B" and "R" in the "Band" field for now). These magnitudes will be used to confirm the feasibility of the observations. The reference star can then be associated with the observation of the target star in the "Observations" page of the p1 tool.

It is not necessary to select a telescope guide star at this stage. A check will be made at Phase 2 to confirm that there is a suitable telescope guide star in the vicinity of the target.

6.3 The exposure time calculator

The ERIS exposure time calculator (ETC) is available in `https://etc.eso.org/observing/etc/eris`. Users should plan their observing strategy based on the calculations in this web page. Particular attention should be made to the saturation limits described in this manual.

Describing the parameters used in the ETC to estimate the SNR of the observation in the "Time Justification" part of the proposal form would greatly help in assessing the feasibility of the proposed observations.

---

[7] `https://vizier.cds.unistra.fr/viz-bin/VizieR-3?-source=I/355/gaiadr3`

6.4 Instrument and telescope overheads

In addition to the required exposure time calculated using the ETC to achieve the desired SNR, estimates for the telescope and instrument overheads are required as a part of the proposal form. Table 22 gives estimates for the different overheads. These should be used to estimate the total telescope and instrument overhead for each observation. Make sure that the integration time and overheads for sky frames are accounted for, if these are required.

Action	Time (sec)
Telescope	
Telescope preset (first)	360
Telescope preset (subsequent in concatenation)	$100 + $ target_separation [deg]
Telescope offset ($\leq 0.5''$)	5
Telescope offset ($> 0.5''$)	15
AO	
Acquisition NoAO	60
Acquisition AO (NGS)	300
Acquisition AO (LGS)	360
Acquisition AO (LGS-SE)	300
IFS	
Acquisition (no interactive centring)	~ 45
Acquisition (interactive centring)	~ 90
Detector overhead per NEXP	$2.14 \times (\text{NDIT} + 1)$
Persistence recording overhead per NOFF	12
Change of grating (between high-res gratings)	5
Change of grating (all other)	160
NIX (nixIMG, nixAPP, nixSAM)	
Acquisition (no interactive centring)	~ 45
Acquisition (interactive centring)	~ 90
NIX (nixFPC, nixLSS)	
Acquisition (interactive centring)	~ 180
NIX (nixIMG, nixAPP, nixFPC, nixLSS, nixSAM)	
Detector overhead per NEXP (SLOW, windowF)	$2.37 \times \text{NDIT} + 2.47$
Detector overhead per NEXP (SLOW, window1)	$1.89 \times \text{NDIT} + 1.79$
Detector overhead per NEXP (SLOW, window2)	$1.69 \times \text{NDIT} + 1.59$
Detector overhead per NEXP (SLOW, window3/4)	$1.29 \times \text{NDIT} + 1.19$
Detector overhead per NEXP (FAST, windowF/1/2/3/4)	$10 \times \text{DIT} + 0.5$
Detector overhead per NEXP (FAST, windowF, cube, DIT>0.154 s)	$10 \times \text{DIT} + 0.5$
Detector overhead per NEXP (FAST, windowF, cube, DIT$\leq$0.154 s)	$10 \times \text{DIT} + 0.5 + \text{NDIT} \times (0.154 - \text{DIT})$
Detector overhead per NEXP (FAST, window1, cube, DIT>0.116 s)	$10 \times \text{DIT} + 0.5$
Detector overhead per NEXP (FAST, window1, cube, DIT$\leq$0.116 s)	$10 \times \text{DIT} + 0.5 + \text{NDIT} \times (0.116 - \text{DIT})$
Detector overhead per NEXP (FAST, window2, cube, DIT>0.077 s)	$10 \times \text{DIT} + 0.5$
Detector overhead per NEXP (FAST, window2, cube, DIT$\leq$0.077 s)	$10 \times \text{DIT} + 0.5 + \text{NDIT} \times (0.077 - \text{DIT})$
Detector overhead per NEXP (FAST, window3/4, cube, DIT>0.039 s)	$10 \times \text{DIT} + 0.5$
Detector overhead per NEXP (FAST, window3/4, cube, DIT$\leq$0.039 s)	$10 \times \text{DIT} + 0.5 + \text{NDIT} \times (0.039 - \text{DIT})$
Persistence recording overhead per NOFF	7
Change of camera (parallel with change of filter)	60
Change of filter (parallel with change of camera)	15

Table 22: Table of instrument overheads. In a single OB, the user will have overheads for either SPIFFIER or NIX. Note: Target centring takes variable amounts of time depending on the acquisition exposure times and instrument mode.

A more precise estimate of the total execution time can be made with the p2 demo environment[8], but this is not necessary for the proposal submission. The p2 tool takes into account the actual integration time for acquisition images, as well as the time taken to move the various mechanisms if multiple science templates are used.

---

[8] https://www.eso.org/p2demo/

6.5 Night-time Calibrations

Some observing modes require additional night-time calibrations. The time used to take these night time calibrations is charged to the user. Section 7.3 lists options and recommendations for night-time calibrations for the available observing modes. The user should ensure that their proposal includes adequate time for all required night-time calibrations that are not part of the standard calibration plan.

6.5.1 SPIFFIER - telluric standards

Telluric standard stars for IFS observations **must be requested by the user if required** as these will not be obtained automatically as a part of the observatory's calibration plan. If a telluric standard star is required then the time taken must be included in the total time request in the proposal. Finding a suitable telluric star is not required at Phase 1. Instead, it can be assumed that each observation of a telluric standard will take twelve minutes: six minutes for the telescope preset, one minute for the noAO acquisition, and five minutes for integration and associated overheads. If an AO acquisition is required, add an additional five minutes. This estimate should be appropriately increased if the standard has to be observed with multiple grating settings. At Phase 2 the telluric standard should be identified and included in a concatenation with the science target using the `ERIS_ifs_cal_StandardStar` template.

Additional details regarding the selection of suitable telluric standards can be found in Section 7.3.1.1.

6.5.2 NIX imaging - photometric standards

At the start of the night (or operations with NIX) a photometric standard will be observed at a low airmass in three of the broadband imaging filters (J, H, K_s) to measure the atmospheric transparency by comparing the measured zero point to a reference value. If the conditions are either "clear" (CLR) or "photometric" (PHO), a standard will be observed every two or three hours during the night to monitor the atmospheric transparency.

NIX broadband imaging OBs requesting PHO conditions must have a photometric standard observed within three hours before and after the OB is executed to confirm stability of the atmospheric transparency. If this condition is not met, the OB will be repeated. These standards will be observed as a part of the observatory's calibration plan, so it is not necessary for them to be requested by the user at either Phase 1 or Phase 2.

Dedicated photometric standards can be requested by the user. This may be desirable for an observation requesting PHO conditions if the very best photometric precision is required (i.e. $< 2\%$ variation in flux), for example. The time taken to observe these standards should be included in Phase 1, along with a justification of why they are required to achieve the science objectives. Finding a suitable photometric standard star is not required at Phase 1. Instead, it can be assumed that each observation of a photometric standard will take fifteen minutes: ten minutes for the telescope preset and AO acquisition, and five minutes for integration and associated overheads. This estimate should be appropriately increased if the standard has to be observed with multiple instrument configurations. At Phase 2 the photometric standard(s) should identified and included in a concatenation with the science target using the `ERIS_nixIMG_cal_StandardStar` template.

Photometric standards will not be observed in narrow-band filters, or with the blocking filter, as a part of the calibration plan. If these are required, they must be requested by the user as a part of their proposal and placed in a concatenation with the science target. Photometric standards will also not be observed in any of the APP, FPC, LSS, or SAM modes, regardless of the requested transparency. Users are strongly encouraged not to request PHO conditions for these modes as this significantly reduces the probability that their observations will be taken. Photometric standards observed as part of the observatory's calibration plan will only be observed in the `SLOW_GR_UTR` readout mode for short-wavelength filters (JHK_s), and in the `FAST_UNCORR` readout mode for long-wavelength filters. If photometric calibration is required in other readout mode/filter combinations, these must be requested by the user.

Additional details regarding the selection of suitable photometric standards can be found in Section 7.3.2.1.

6.5.3 NIX long-slit spectroscopy - telluric standards

Telluric standards for NIX long-slit observations **must be requested by the user if required** as these will not be obtained automatically as a part of the observatory's calibration plan. If a telluric standard star is required then the time required must be included in the total time request in the proposal. It is not necessary to find a suitable telluric standard at Phase 1. Instead, it can be assumed that the observation of a telluric standard will require fifteen minutes; approximately ten minutes for the preset and acquisition, and

five minutes for integration and associated overheads. At Phase 2 the telluric standard should be identified and included in a concatenation with the science using the `ERIS_nixLSS_cal_StandardStar` template.

7 Observing with ERIS – Phase 2: observation preparation

As with all other ESO instruments, users prepare their observations with the p2 web interface. Acquisitions, observations and calibrations are coded via templates and two or more templates make up an Observing Block (OB) (see Section 7.4.2). OBs contain all the information necessary for the execution of an observing sequence.

The web-based p2 tool is used to prepare ERIS observations for both service and visitor mode. The generic guidelines for Phase 2 and the p2 tool can be found at the following links:

- `http://www.eso.org/sci/observing/phase2/SMGuidelines.html`

- `http://www.eso.org/sci/observing/phase2/p2intro.html`

ERIS-specific information can be found at the following page:

- `https://www.eso.org/sci/observing/phase2/SMGuidelines/SMRules.ERIS.html#InsSpec`

The generic and ERIS-specific guidelines must be followed when preparing your observation in the p2 tool.

7.1 AO and instrument acquisition

7.1.1 Target and guide star coordinates

Having precise target and guide star coordinates can greatly improve the efficiency of the acquisition procedure, and are essential for IFS observations given the small field of view.

- The target coordinates and proper motions can be provided at any epoch and/or equinox in the p2 tool. These will be propagated to the correct epoch and reference frame at the time of observation by the telescope and instrument software.

- The NGS/TT star coordinates must be provided in the ICRS reference frame (closely aligned with the J2000 equinox) using the middle of the observing period as the epoch (epoch = 1968 + [observing period]/2, e.g. for P111 epoch = 1968 + 111/2 = 2023.5). Using any other equinox or epoch will degrade accuracy of the initial acquisition.

The propagation of the NGS/TT star coordinates is done automatically in the `ObsPrep` tab of the p2 tool when selecting a NGS/TT star. As such, it is **strongly recommended that this tool is used to select the AO guide star** rather than entering the coordinates manually. Precise coordinates for both the NGS/TT star and the target star will enable a rapid acquisition as the offset between the AO stage and two instruments is known precisely.

The telescope guide star must also be specified at Phase 2. It is strongly recommended to use the `ObsPrep` utility to select a telescope guide star that is compatible with your offset pattern. Telescope guide star coordinates can be entered manually, although this is strongly discouraged. OBs containing acquisition templates that do not specify a telescope guide star will be rejected.

7.1.2 Non-sidereal and differential tracking

General information regarding the format of ephemeris tables are given on the ESO web page[9]. Take great care when creating these ephemeris tables as there are very few automatic checks on their format and content.

Non-sidereal targets must have an OB name starting with "MOV_" such that they are easily identifiable by the operator. For observations where the target and the AO reference are the same, use the normal acquisition template for the instrument mode requested. The epehmeris table for the target should be uploaded using the "Ephemeris" tab in p2 (see Table 23). Use "00:00:00.000" for `TTS.ALPHA` and `TTS.DELTA` (or `NGS.ALPHA` and `NGS.DELTA`), but do specify the magnitude and color of the object in `TTS.MAG` and `TTS.COLOR` (or `NGS.MAG` and `NGS.COLOR`) so that the AO system is configured correctly. For observations of extended sources, set the appropriate extended keyword: either `EXTENDED` for point-like objects with a diffuse background (e.g., AGN), or `EXTENDED_FULL` for resolved objects with flat-topped brightness profiles (e.g., planets, moons, resolved asteroids).

For observations requiring differential tracking between the science target and AO reference (Section 3.2) you must use the differential tracking acquisition templates (those with suffix `_difftrack`). The OB must also have a name starting with "MOV_", as for simple non-sidereal observations. An ephemeris table for both

---

[9]`https://www.eso.org/sci/observing/phase2/SMSpecial/MovingTargets.html`

the target and the AO reference must be created (see Table 23). For sidereal objects that act as either target or reference star the ephemeris table should contain at least two entries spanning the date range of the period in which the observations are being conducted, giving the same coordinates for each entry. Correcting for proper motion is not relevant except for the closest stars. The ephemeris table of the target must be uploaded using the "Ephemeris" tab in p2. The ephemeris table of both the target and the AO reference must be uploaded into the acquisition template. Do not use the same file name for both tables. **Additionally, you must specify absolute time constraints that describe when the two objects are within 59″ of one another, the limit of the patrol radius of the AO system.** OBs using the differential tracking templates that do not specify absolute time constraints will be flagged for review. For observations of extended sources, set the appropriate extended keyword: either `EXTENDED` for point-like objects with a diffuse background (e.g., AGN), or `EXTENDED_FULL` for resolved objects with flat-topped brightness profiles (e.g., planets, asteroids).

Target	AO reference	Target is AO star?	Acquisition template	"Ephemeris" tab	Target tracking table (`SEQ.TRACK.TARG`)	AO tracking table (`SEQ.TRACK.REF`)
Sidereal						
Sidereal	Sidereal	Yes	`*_acq`			
Sidereal	Sidereal	No	`*_acq`			
Non-sidereal, no differential tracking						
Non-sidereal	Non-sidereal	Yes	`*_acq`	✓		
Non-sidereal, with differential tracking						
Sidereal	Non-sidereal	No	`*_difftrack`		✓	✓
Non-sidereal	Sidereal	No	`*_difftrack`	✓	✓	✓
Non-sidereal	Non-sidereal	No	`*_difftrack`	✓	✓	✓

Table 23: Ephemeris tables required for sidereal, non-sidereal, and differential tracking OBs

7.1.3 Interactive centring using the NGS/TTS

The keywords `SEQ.NGS_ACQUISITION` and `SEQ.TTS_ACQUISITION` in the NGS and LGS acquisition templates, respectively, for SPIFFIER and standard NIX imaging modes can be used to perform the interactive centring on the natural guide star or tip-tilt star rather than the science target. If you find that you need more than 30–60 s to detect your target at a low S/N, or your target has only a single emission line, **you are strongly recommended to perform the interactive centring using the AO star using this keyword**. It makes little sense to attempt a challenging acquisition on a faint object when a much brighter AO star could have been used in a fraction of the time. Having the image of the bright AO star at the start (and end, with a dedicated template) of your OB will also allow you to perform an absolute astrometric calibration of your observations.

If this keyword is set to true, the interactive centring will be done on the natural guide star or tip-tilt star, not the target. Once the centring is completed, the offset between the AO star and the target star will be calculated using the coordinates of the AO star provided by the user and the coordinates of the target propagated to the current epoch. As this calculation is done using mean coordinates, the effect of nutation is not included. However, the magnitude of this effect on the calculated offset is typically small, and depends on the target coordinates, the size of the offset, and the epoch of observation.

The telescope will then offset from the AO star to the target using these calculated offset, which are stored in the FITS header keywords `OCS.NGS/TTS.OFFSET.ALPHA/DELTA`. Note that it is essential that the AO star coordinates are provided close to the epoch of observations (see Section 7.1.1), as is done by the `ObsPrep` tool in p2. In a future period the full astrometric information of the AO star (e.g., proper motion, epoch) will be requested.

7.1.4 SPIFFIER/NIX acquisition position in service mode

For NIX observations the target indicated in the finding chart will always be acquired at following detector pixel coordinates (referenced to the full frame, see Figure 9):

- nixIMG:
    - `windowF`: $(960, 1050)$ (laser location on NIX detector)
    - `window2`: $(1024, 1536)$, or $(1024, 512)$ in the sub-array
    - `window4`: $(1024, 1536)$, or $(1024, 256)$ in the sub-array

- nixAPP (the coordinate of the central calibration spot), nixSAM:

  - `windowF`: $(800, 1536)$
  - `window2`: $(800, 1536)$, or $(800, 512)$ in the sub-array
  - `window4`: $(800, 1536)$, or $(800, 256)$ in the sub-array

- nixFPC (coordinate of the L-band vortex):

  - `window1`: $(1043, 1410)$, or $(1043, 660)$ in the sub-array
  - `window3`: $(1043, 1410)$, or $(1043, 256)$ in the sub-array

- nixFPC (coordinate of the M-band vortex):

  - `window1`: $(1062, 1411)$, or $(1062, 661)$ in the sub-array
  - `window3`: $(1062, 1411)$, or $(1062, 257)$ in the sub-array

- nixLSS (coordinate of the centre of the slit):

  - `windowF`: $(1022, 932)$

For IFS observations the target indicated in the finding chart will always be acquired at the centre of the selected field of view specified in the acquisition template. An offset can be used to re-centre the object for the science exposure if the field of view of the first science template is different from the acquisition template (see Section 3.4), if precise centring is required.

You must not request the target to be centred elsewhere in the field of view during acquisition. Instead, use an offset to move the target to the desired position for the first exposure of the science template.

7.1.5 Finding charts

Finding charts can be generated automatically with p2. If finder charts are uploaded to complement those generated by p2fc for more complicated acquisitions they must contain:

- The requested instrument field of view (and, for IFS, the requested field of view in the acquisition template)

- A scale bar and a compass

- A marker indicating the location of the science target

7.2 Observations

7.2.1 NIX observations

Some important considerations specific to NIX observations:

7.2.1.1 All NIX modes:

- The NIX detector has a lot of bad pixels, especially on the left side. The user should consider carefully how to minimise the impact of these on their observations. This can be done, for example, by rotating the instrument or defining a dither pattern so that the highest priority science targets are not placed in that region of the detector. A representative bad pixel map can be found on the ERIS website[10] to help prepare observations with dither patterns.

- When planning to use ADI for the high contrast modes, ensure that the expected field rotation is sufficient to enable good separation of the speckles and science target during post-processing. LST constraints should be used for service mode observations to ensure sufficient field rotation is achieved.

- It is possible to specify an arbitrary instrument rotation angle for observations taken in field-tracking mode by varying `TEL.ROT.OFFANGLE` in the acquisition template (e.g., see Figure 37). For APP, FPC, and SAM observations, the instrument rotator cannot be changed and North will be at a position angle measured from vertical in a counter-clockwise direction of approximately `PARANG` − `PUP_ANGLE` + 90.7 degrees (see also Section 7.2.4.2), where:

---

[10]https://www.eso.org/sci/facilities/paranal/instruments/eris/inst.html

- PUP_ANGLE = 36 degrees for all APP observations,
- PUP_ANGLE = 135 degrees for all FPC observations,
- PUP_ANGLE = 34 degrees for SAM observations with NXPW=SAM-23 NXCW=13mas-JHK,
- PUP_ANGLE = 136 degrees for all other SAM observations.

- For standard imaging (nixIMG) observations taken in pupil tracking mode, an arbitrary angle can also be specified. North will be at a position angle of approximately PARANG − PUP_ANGLE − TEL.ROT.OFFANGLE + 90.7 deg, where PUP_ANGLE is 135 degrees (see also Section 7.2.4.2). If the Spider pupil mask is used, TEL.ROT.OFFANGLE must be zero to ensure the mask covers the telescope structure.
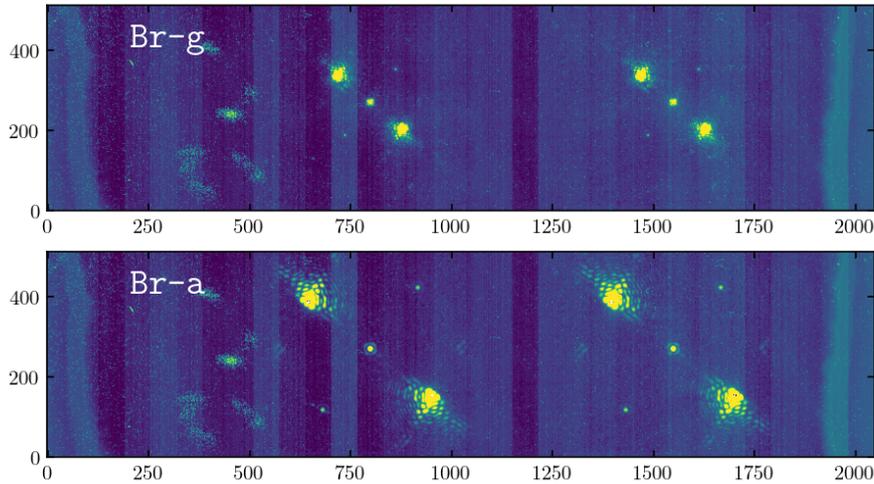
Figure 35: A composite image of the acquisition position for APP observations (800, 1536), and the recommended offset position at (1550, 1536) within the recommended window4 sub-array for K-band (top) and L-band (bottom).

7.2.1.2 nixIMG

- When the best photometric precision is required, and there are suitable 2MASS sources within the field, it is recommended to take short exposures in which the 2MASS sources are not saturated before and after the science exposures are taken.

7.2.1.3 nixAPP

- It is recommended to use an observing strategy with small random jitters plus nodding. The former serves purpose to clean up systematics (such as bad pixels) with efficient closed loop dithers and the latter to estimate the sky background at regular intervals (depending on the weather conditions, typically ~ 3, 10 minutes respectively in L and K bands). It is important to leave enough distance in between nodding positions so that alternating APP PSFs do not overlap (see Figure 35). Nodding between the acquisition position (800, 1536) and (1550, 1536), a $\pm 9.75''$ DETECTOR offset in X, will avoid the large clusters of bad pixels. As described in Section 7.2.4.3, a DETECTOR offset of $-9.75''$ will move the centre of the PSF from (800, 1536) to (1550, 1536). Do not use SKY offsets for these nods as the field will rotate over the course of the observation. Small dithers ($\sim 0.05''$) around each nodding position will further mitigate the effect of bad pixels. The acquisition position is the same for both window2 and window4, however the number of rows read out is different, see Figure 9 and Section 7.1.4. It is strongly recommended to use the window4 sub-array to reduce the total data volume.

- It may be desirable to position a faint companion at a given position angle relative to the dark hole. An LST constraint can be used to ensure service mode observations are only scheduled with a specific range of parallactic angles.

- Do not forget to take an unsaturated image of the APP PSF after the acquisition, and after each hour for extended OBs, as described in Section 4.2.3.1.

7.2.1.4   nixFPC   The focal plane coronagraph observing mode is the most complex of those offered, requiring additional keywords to ensure the secondary guiding loop (QACITS) runs correctly. The detector integration times during both the acquisition and initial optimisation, as well as during the observations themselves, must be selected carefully.

Acquisition: The vortex effect reprocesses the sky background producing a detectable glow that defines the centre. The star will be brought close to this vortex centre during the interactive centring step of the acquisition. After centring, the QACITS acquisition starts. This automatically takes a set of background measurements, an off-axis flux measurement, and performs an initial optimisation of the centring before the science template is started. The acquisition sequence is described in detail in Table 24, and an example of the optimisation loop in action is show in Fig. 36.

Table 24: nixFPC acquisition procedure

Step	Description	Template parameters	DPR.TYPE
1	Initial centring onto vortex. `DET.DIT` must match the science template.	`DET.DIT` `DET.NDIT`	
2	Open AO loops and offset to sky	`TEL.SKY.OFFSETALPHA` `TEL.SKY.OFFSETDELTA`	
3	Acquire sky frame for PSF measurement	`SEQ.PSF.DIT` `SEQ.PSF.NDIT`	`SKY,PSF`
4	Set `NXPW` to `Lyot`, if using `Lyot-ND`		
5	Acquire dark frame for coronagraph centring	`SEQ.VORTEX.DIT`† `SEQ.VORTEX.NDIT`†	`DARK`
6	Acquire sky frame for coronagraph centring	`SEQ.VORTEX.DIT`† `SEQ.VORTEX.NDIT`†	`SKY,CORO`
7	Revert `NXPW`, if necessary		
8	Acquire sky frame for QACITS at start of science template. `DET.DIT` must match the science template.	`DET.DIT` `DET.NDIT`	`SKY`
9	Acquire sky frame for initial optimisation loop.	`SEQ.OPTIMIZE.DIT` `SEQ.OPTIMIZE.NDIT`	`SKY,OPT`
10	Offset target to coronagraph, AO loops closed		
11	Offset target slightly off-axis for flux measurement		
12	Acquire PSF frames. The flux is used by QACITS during the initial optimisation and the science template.	`SEQ.PSF.DIT` `SEQ.PSF.NDIT`	`OBJECT,PSF`
13	Offset target back to coronagraph		
14	Close initial QACITS optimisation loop. Finishes after tip-tilt error less than `SEQ.OPTIMIZE.THRESHOLD`† or number of iterations exceeds `SEQ.OPTIMIZE.NITER`†.	`SEQ.OPTIMIZE.DIT` `SEQ.OPTIMIZE.NDIT`	`OBJECT,OPT`

† – hidden parameter

Observation: During the observing template, QACITS will continually measure the tip-tilt residual, sending a pointing correction every few seconds. During a sky offset, a dedicated sky exposure (`DPR.TYPE=SKY,CORO`) will be taken with a pre-defined DIT and NDIT to re-measure the coronagraph centre position by fitting the vortex centre glow. If the science template is using `NXPW=Lyot-ND`, the pupil wheel is temporarily changed to `Lyot` to ensure a high S/N measurement of the vortex centre.

DITs: When choosing the DIT, one should avoid any saturation. For the off-axis PSF, the user should refer to the ERIS ETC[11] to select an appropriate integration time for their target. When the target is close or onto the vortex centre, the stellar flux is rejected by a factor that depends mostly on the quality of the centring.

The `DET.DIT` used for the initial interactive centring in the acquisition template must match the `DET.DIT` used in the science template; `NDIT` can be different, and should be much shorter for the acquisition. These

---

[11]`https://etc.eso.org/observing/etc/eris`
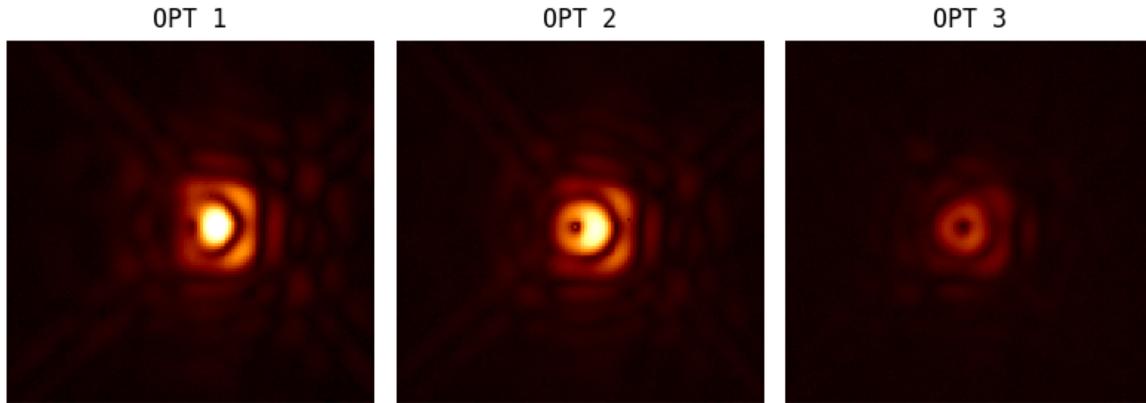
Figure 36: Improvement of the rejection of the on-axis star as the centring is improved at the end of the QACITS acquisition sequence. Sky subtracted and sqrt stretch

two template parameters also set the `DIT` and `NDIT` for the background measurement used by the QACITS algorithm during the the first "O" frames of the science template. To ensure a good S/N on this background, set `DET.DIT`×`DET.NDIT` to be ∼2s in the acquisition template. This background is updated at every "S" frame in the science template. This behaviour may change in upcoming periods to allow for a more appropriate `DIT` to be used for the interactive centring.

The exposure time for the off-axis PSF measurement (`SEQ.PSF.DIT/NDIT`) should be set well below the saturation threshold, but high enough to ensure an excellent S/N on the PSF for post-processing of the reduced data. Setting `SEQ.PSF.NDIT` to reach a total integration time of a few seconds is recommended. Additional off-axis PSF measurements can be obtained at the end of an OB, or during a long OB, using a dedicated `ERIS_nixFPC_obs_GenericOffset` template with `OBSTYPE=F` (see Section 7.2.1.4).

After the initial interactive centring and off-axis PSF measurement, the position is not yet optimised and the stellar light rejection will be moderate. For a position accuracy of $< 1\ \lambda/D$ (or ∼$0.1''$ in L-band), the rejection is a factor two or better. Hence the integration time for the optimisation images (`SEQ.OPTIMIZE.DIT`) can be a factor of two higher with respect to that of the off-axis PSF. Again, setting `SEQ.OPTIMIZE.NDIT` to reach a total integration time of a few seconds is recommended to ensure a high S/N.

During the observations taken during the science template, the stellar light rejection should reach a much better level, and the peak intensity can decrease by up to > 100 times. A safe value—to avoid any saturation due to drift and other effect—is to use a maximum DIT of 10-20x higher than the off-axis PSFs. Note that it is not necessary to use the same `NDIT` for the "O" and "S" frames. For example, a valid strategy is to use `NDIT=500` for the object frames and `NDIT=50` for the sky frames.

Finally, overhead between exposures can impact the QACITS algorithm. Hence we advocate to ensure those are kept to a minimum by using the smallest sub-array available for this mode. In the largest usable sub-array for this mode (`window3`) the overhead reaches a minimum for integration times of >0.1 s. For more details, please refer to section 4.2.1.4. Due to the volume of data produced in this mode, the use of the full frame (`windowF`) is not permitted. Unless the full field of view offered by the `window1` sub-array is needed, the smaller sub-array `window3` should be used. See Section 2.4.1.2 for more details regarding the available sub-arrays, and Section 4.2.1.2 for the restrictions on the data volume within a single OB.

Additional recommendations for NIX FPC observations:

- It is strongly recommended to use the smallest sub-array (`window3`), unless the full FPC field of view offered by the larger sub-array (`window1`) is required. The full frame (`windowF`) cannot be used in this mode.

- An off-axis image of the PSF can be obtained at the end of the OB, or during a long OB, by adding a dedicated `ERIS_nixFPC_obs_GenericOffset` template. The offset to move the star from the coronagraph must be specified in the template. A small offset of 1–$2''$ is recommended for the F frame and, if used, a larger offset of ∼$30''$ for the S frame, being careful to avoid nearby stars. An alternative approach for obtaining a background measurement is to take two F frames offset by a few arcseconds. It is not permitted to mix `OBSTYPE=O` and F within a single template.

- A software bug that introduced a five degree offset to offsets in FPC mode at the start of the second and subsequent observing templates was fixed on the 25th of May 2025.

7.2.1.5 nixLSS

- The target will always be acquired at the centre of the slit. The offset coordinate system is aligned with the slit.

7.2.1.6 nixSAM

- The same acquisition position as for APP observations is used, (800, 1536). The same dithering strategy and `window4` sub-array used for APP observations is strongly recommended.

7.2.2 SPIFFIER observations

The offset between the AO system and the centre of the SPIFFIER field-of-view is calibrated to an accuracy of around $0.5''$, and interactive centring is not required if you are using the 250mas pixel scale. For observations requiring the 100mas and 25mas scales, it is recommended to use interactive centring such that the target is well-centred within the field of view. The acquisition strategy depends on the brightness of the target.

For a bright target that is visible with `DIT` < 10 s (e.g., $K < 13$ for the K_low grating and the `100mas` scale) it is best to perform interactive centring on the target itself. Use the ERIS ETC [12] to determine an appropriate integration time for your acquisition images, keeping in mind that it is only necessary to detect the target at a low S/N in the wavelength-collapsed image. In general, never set `NDIT` to anything other than 1. The marginal gain in S/N between `DIT=30`, `NDIT=1` and `DIT=30`, `NDIT=2` ($\sqrt{2} = 1.4$), for example, is not worth the additional overhead incurred when the target will be detectable with a single integration.

If you find that you need more than 30–60 s to detect your source at a low S/N, or your target has only a single emission line, **you are strongly recommended to perform the interactive centring using either the natural guide star or the tip-tilt star**, depending on the observing mode. See Section 7.1.3 for more information.

ERIS has a residual drift that is not corrected by the flexure model, which is of order $0.2''$ per hour at zenith angles > 50 deg. This drift is caused by the differential flexure between the AO bench and the two scientific cameras. If it is possible to measure the position of a source within the field of view on every exposure, this drift can be corrected in the pipeline. However, if you do not expect to detect your source in individual exposures, then we recommend the use of the `ERIS_ifs_cal_PSF` template immediately after acquisition and at the end of the OB. This will provide a direct measure of the drift during OBs that are executed at larger zenith angles. The AO guide star (or tip-tilt star) can be used for this and, since the aim is only to measure the position of the star, the exposures typically do not need to be longer than 10 sec for a single object and sky observation. Work is ongoing to improve the quality of the flexure model so such measurements are no longer needed.

Some other important considerations specific to SPIFFIER observations:

- The `ERIS_ifs_cal_PSF` template must be used if calibration observations of a PSF star are required. This star can either be the AO guide star or a different star of suitable brightness.

- Choice of plate scale should be done carefully: are the observations driven by the available field of view, by signal-to-noise per pixel, or by achieving the highest possible spatial resolution?

- For pupil tracking mode, North will be up at an hour angle of zero, however this can be adjusted by using a non-zero value for `TEL.ROT.OFFANGLE` in the acquisition template. The position angle of North will be approximately `TEL.ROT.OFFANGLE` $-$ `PARANG` $+ 180$ deg for Northern targets, and `TEL.ROT.OFFANGLE` $-$ `PARANG` deg for Southern targets. When observing more widely separated companions in service mode, a judicious use of local sidereal time constraints will ensure that the companion stays on the detector throughout the observation. Keep in mind the rectangular spaxels in the reconstructed image result in a higher spatial sampling along the detector x axis.

7.2.3 Observations in pupil tracking mode

When using pupil tracking the following restrictions apply:

- The target must be either the natural guide star (NGS mode) or the tip-tilt star (LGS mode).

- Sidereal tracking only; no differential tracking.

---

[12]`http://www.eso.org/observing/etc/`

- Any offset to a sky (`OBSTYPE=S`) must be within the AO patrol radius (59″) as these offsets are done in closed-loop to ensure an accurate return offset to the object (`OBSTYPE=O`).

- Offsets must be performed in `DETECTOR` coordinates.

- `ERIS_ifs_obs_AutoJitter`, `ERIS_ifs_obs_FixedSkyOffset`, and `ERIS_nixIMG_obs_AutoJitter` cannot be used.

7.2.4   Detector coordinate and offset conventions

ERIS Coordinate Convention 1 - SPIFFIER, NIX Wide Field (27mas-JHK)

TEL.ROT.OFFANGLE=0 (PA=0 deg)   TEL.ROT.OFFANGLE=45 (PA=-45 deg)

ERIS Coordinate Convention 2 - NIX Small Field (13mas-JHK, 13mas-LM)

TEL.ROT.OFFANGLE=0 (PA=0 deg)   TEL.ROT.OFFANGLE=45 (PA=-45 deg)
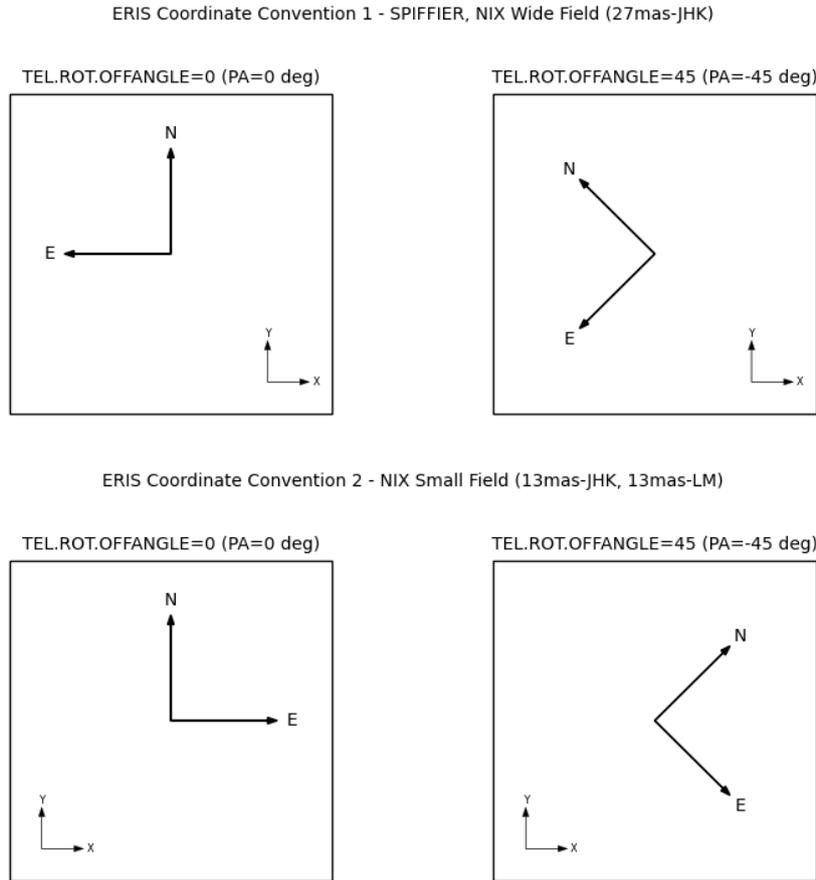
Figure 37: Coordinate system definitions for ERIS.

7.2.4.1   Coordinates   In Figure 37, we depict the coordinate system definitions for ERIS. There are two configurations depending on the direction of East with respect to the X-axis on the detector when the position angle is zero. The first configuration, when the East points in the opposite direction of the detector X-axis, applies to all SPIFFIER modes and wide field imaging with NIX. The second configuration applies to the all modes of NIX except the wide field imaging configuration.

The convention on the rotation is the same. When the user requests `TEL.ROT.OFFANGLE` of 45 degrees via acquisition templates, the instrument will be configured at a position angle of −45 degrees on-sky using the standard definition. *Note the minus sign.*

7.2.4.2   Position angle of North   The position angle of North on the detector for both field and pupil-tracking observations can be estimated from the information provided in the header.

For SPIFFIER:
$$\theta_{\text{North}} = -\left(\texttt{TEL.PARANG} - \texttt{ADA.ABSROT} - 41.07\right) + \delta \tag{2}$$

where $\delta = 1.23 \pm 0.57\,\text{deg}$, estimated from observations of the calibration binary λ^1 Scl taken simultaneously with VLTI/GRAVITY on the night of 2024-12-22 ($\theta = 26.4151 \pm 0.001\,\text{deg}$).

For NIX, for the `27mas-JHK` camera:

$$\theta_{\text{North}} = \texttt{TEL.PARANG} - \texttt{ADA.ABSROT} + 90.7 + \delta \tag{3}$$

and, after flipping the image to put East in the correct direction, for the `13mas-JHK` and `13mas-LM` cameras:

$$\theta_{\text{North}} = -(\texttt{TEL.PARANG} - \texttt{ADA.ABSROT} + 90.7) + \delta \tag{4}$$

where δ is an offset depending on the specific instrument mode used. These were estimated for each NIX mode using observations of the wide binary HD 69130 taken on the night of 2025-01-30 that had a position angle of $\theta = 46.5734 \pm 0.0017$ deg estimated from *Gaia* astrometry propagated to that epoch, and are listed in Table 25. These measurements were made directly in the raw images, with a correction for the anamorphic distortion of a 0.2% reduction in the plate scale in the vertical direction, and a 0.2% increase in the horizontal direction.

Mode	Setup	δ (deg)
`nixIMG`	`27mas-JHK`	-3.218 ± 0.008
`nixIMG`	`13mas-JHK`	1.821 ± 0.006
`nixIMG`	`13mas-LM`	1.037 ± 0.017
`nixAPP`	`13mas-JHK`	0.279 ± 0.021
`nixAPP`	`13mas-LM`	0.601 ± 0.020
`nixFPC`	`13mas-LM` (L')	4.670 ± 0.016
`nixFPC`	`13mas-LM` (M')	4.663 ± 0.038
`nixSAM`	`13mas-JHK`	1.820 ± 0.018

Table 25: Position angle of north offset for the different NIX observing modes.

Observations of globular clusters are only routinely taken in the standard `nixIMG` modes. Given that the relative offset between the various NIX modes should be stable, routine observations of neither globular clusters nor calibration binaries are taken in the other modes. Instead, the offsets in Table 26 can be added to the position angle of North measured in the astrometric calibration of the corresponding `nixIMG` mode derived from the globular cluster observations to properly calibrate observations in the other modes.

		nixIMG setup used for astrometric calibration		
Mode	Setup	27mas-JHK	13mas-JHK	13mas-LM
`nixAPP`	`13mas-JHK`	$\cdots$	-1.541 ± 0.022	$\cdots$
`nixAPP`	`13mas-LM`	$\cdots$	$\cdots$	-0.437 ± 0.026
`nixFPC`	`13mas-LM` (L')	$\cdots$	$\cdots$	3.633 ± 0.023
`nixFPC`	`13mas-LM` (M')	$\cdots$	$\cdots$	3.626 ± 0.042
`nixSAM`	`13mas-JHK`	$\cdots$	-0.001 ± 0.019	$\cdots$

Table 26: Offsets to apply to the `nixIMG` calibration for other NIX modes

For observations using either the `13mas-JHK` or `13mas-LM` cameras, this assumes that the astrometric calibration accounts for the flip of the East direction (i.e. the calibration provides the position angle of North on the detector measured in a counter-clockwise direction from vertical after the image has been flipped). For example, if an astrometric calibration with the `13mas-LM` camera yielded a position angle of North of 0.5 deg counter-clockwise from vertical (after flipping the image to correct the East direction), the position angle of North within a `nixAPP` observation would be at $0.5 - 0.437 = 0.063$ deg counter-clockwise from vertical (again, after flipping the image).

7.2.4.3 Offsets In all observing templates of ERIS, the unit of offsets are standardized to arcseconds. The reference system can either be in `SKY` (RA, DEC) or in `DETECTOR` (x, y) coordinates. **Both `SKY` and `DETECTOR` offsets move the telescope (i.e. the source moves in the opposite direction)**. For example, a `DETECTOR` offset of $(+1, +1)$ moves the object $-1''$ in x and $-1''$ in y on the detector. Similarly, a $(+1, +1)$ `SKY` offset moves the object $-1''$ East and $-1''$ North. Keep in mind that the orientation of the sky coordinate system for NIX depends on which camera is being used (see Section 7.2.4). It is strongly recommended to use `DETECTOR` offsets for APP, SAM, and any pupil-tracking observations, such that the offset pattern on the detector is known in advance. This is critical for observations using the detector windows where the change in parallactic angle may result in an offset moving the star off the sub-array as the field rotates. `SKY` offsets should only be used for these modes when performing large sky offsets to avoid nearby, bright stars in the sky frame.

The offsets in the templates are always defined as *relative* offsets. For example, a series of offsets $(0, -10, 0, 10)$ brings the object back to the origin. The offset given in an observing templates may end at any arbitrary position (ending on a SKY position, for example); the telescope will always return to the origin at the end of a template regardless of the stated offset pattern, returning the object back to the acquisition position. Subsequent templates will start with the object in the acquisition position, regardless of any offset pattern in previous templates.
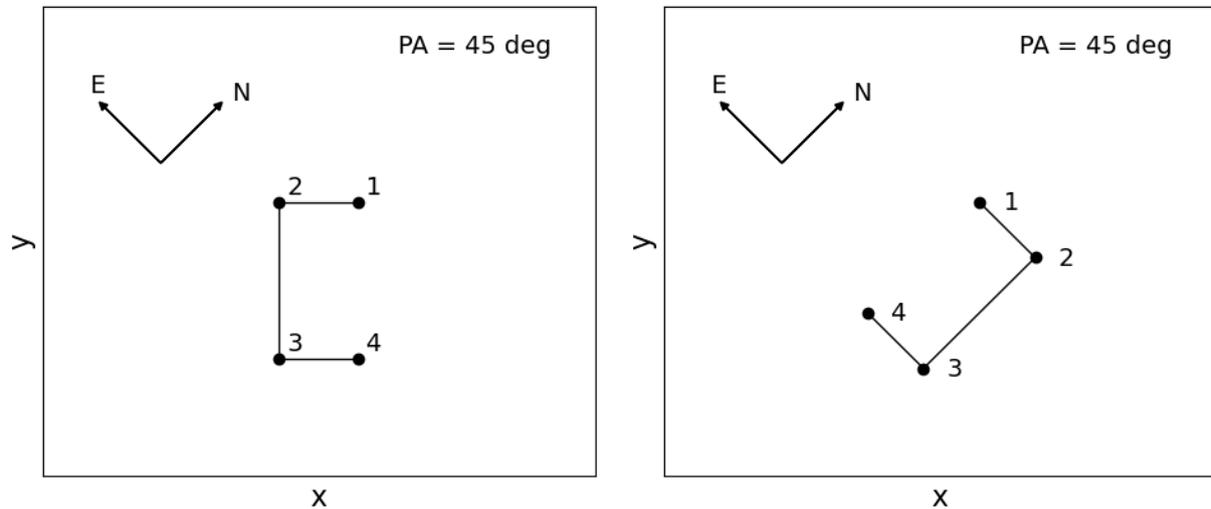

Figure 38: An illustration of the offset sequence for a point source with the on-sky position angle of 45 deg taken with the `ERIS_ifs_obs_GenericOffset` template. Left side: Offset coordinate type `DETECTOR`; Right side: Offset coordinate type `SKY`. This figure is meant to illustrate where on the detector the image of a point source is showing up, if the telescope is doing the following offset sequence: $(0, +1, 0, -1)$ in x or `RA` and $(0, 0, +2, 0)$ in y or `DEC`. The numbers illustrate the order of the offsets.

7.3   Calibrations

The details of all the calibrations required for ERIS are given in the ERIS Calibration Plan[13] (RD1). Table 27 and 28 summarise the calibration templates respectively for SPIFFIER and NIX.

When possible, calibrations are done internally to the instrument using the calibration unit during day-time. However, there are a few exceptions to this. For example, the 3-5 μm modes for NIX cannot be calibrated internally. Flat-fielding in L and M bands will have to be performed on the sky during twilight. The day-time and twilight calibrations and are provided by default by the observatory, and do not need to be requested by the user. In each of the following two tables, calibrations listed among the upper set are part of the standard calibration plan and do not need to be requested by the user.

In addition to these, there are a number of calibrations that are performed on sky during night-time. *These night-time calibrations are charged to the observing time of the user.* In each of the following two tables, calibrations listed among the lower set must be specifically requested by the user and will be charged to their observing time. Note that not all of these are required for all types of observations. It is not possible to take calibrations with the CU without moving the telescope to zenith and as such attached arc and flat-field calibrations are not offered. The following sections provide recommendations for what calibrations are generally requested for various observing modes to help you decide which calibrations to request.

7.3.1   Recommended night-time calibrations for SPIFFIER

In general, on-sky calibrations for SPIFFIER observations are limited to spectroscopic standard stars for atmospheric correction `ERIS_ifs_cal_StandardStar` and PSF standards `ERIS_ifs_cal_PSF`.

7.3.1.1   Telluric standards   There are two classes of stars that are typically used as telluric standards in the near-infrared. Either single hot stars (spectral type <A0, <B4 preferred) that are relatively featureless

---

[13]https://www.eso.org/sci/facilities/paranal/instruments/eris/doc.html

SPIFFIER Calibration Templates

standard calibration plan:	
`ERIS_ifs_cal_Arcs`	Take internal arc frames during daytime
`ERIS_ifs_cal_Darks`	Take dark frames during daytime
`ERIS_ifs_cal_LampFlats`	Take internal flat-field frames during daytime
charged to user:	
`ERIS_ifs_cal_StandardStar`	Observe a standard star for telluric and flux calibration.
`ERIS_ifs_cal_PSF`	Take an image of a different star to use as PSF reference

Table 27: Summary of calibration templates for SPIFFIER

NIX Calibration Templates

standard calibration plan:	
`ERIS_nix_cal_Darks`	Take dark frames during daytime.
`ERIS_nixIMG_cal_LampFlats`	Take flat-field frames during daytime using calibration unit.
`ERIS_nixIMG_cal_TwFlats`	Take flat-field frames during twilight.
`ERIS_nixIMG_cal_SkyFlats`	Take flat-field frames night time (three sets at varying airmasses)
`ERIS_nixIMG_cal_StandardStar`	Only if photometric conditions requested for broad-band imaging, otherwise must be requested by the user
charged to user:	
`ERIS_nixIMG_cal_StandardStar`	Standard star observation in imaging mode.
`ERIS_nixLSS_cal_StandardStar`	Standard star observation in LSS mode.

Table 28: Summary of calibration templates for NIX

in the near-IR, or single solar analogues (G0–G4) for which the solar spectrum can be used to remove stellar absorption lines. Binary stars are avoided; resolved systems complicate the extraction of the spectrum, while unresolved companions may contribute significant flux at longer wavelengths.

A curated list of potential telluric standards, as well as a utility to select a suitable one given the target coordinates and observation duration, is available on the ERIS website [14].

7.3.2 Recommended night-time calibrations for NIX

7.3.2.1 Photometric standards In case accurate photometric calibrations are required, the template `ERIS_nixIMG_cal_StandardStar` can be used on a star that is known to be a stable photometric reference. Photometric standards stars were selected from a variety of sources, e.g. van der Bliek (1996, A&AS, 119, 547), Persson et al. (1998, AJ, 116, 2475), Leggett et al. (2003, MNRAS, 345, 144), Leggett et al. (2006, MNRAS, 373, 781). The curated list of photometric standard stars that are be used to measure zero points in each of the five standard broadband filters is available on the ERIS website[15].

7.3.2.2 High-contrast imaging For observations with the APP it is recommended to take an unsaturated image of the APP PSF immediately after the acquisition, and after each hour for long OBs. These measurements can be used to calibrate the flux ratio between the side PSFs and the central leakage term which has been seen to vary on short timescales under variable observing conditions (see Section 4.2.3.1).

For SAM observations, the most critical aspect is to identify and observe suitable reference stars ('calibrators') so that the interferograms can be calibrated. These calibrators should be determined by the observer using a utility like JMMC's SearchCal[16] to obtain the best possible results. The templates for the observations

---

[14]https://www.eso.org/sci/facilities/paranal/instruments/eris/tools.html
[15]https://www.eso.org/sci/facilities/paranal/instruments/eris/tools.html
[16]https://www.eso.org/sci/facilities/paranal/instruments/eris/tools.html

of the calibrators are identical to those of the science targets.

7.3.2.3 Telluric standards for long-slit spectroscopy. It may be desirable to obtain a spectrum of a telluric standard immediately before or after a science observation, depending on the type of science being done. Observations of a telluric standard with the template `ERIS_nixLSS_cal_StandardStar` must be requested by the user in concatenation with their science OB.

A sample of 36 bright ($V < 6$) A0V stars was selected from SIMBAD, filtered to exclude those that show evidence of binarity or infrared excess. This sample of stars will be regularly observed to monitor the health of the instrument, and is available on the ERIS website[17]. Fainter A0V stars can be selected if none of these are suitably close in airmass to the science target.

7.3.3 Recommended night-time calibrations for AO

The only relevant calibration is to acquire the DSM best flat, which is part of the standard calibration plan and so carried out by observatory staff as part of routine operations.

7.4 Observing blocks and templates

7.4.1 Observing block

Any ERIS science OB should contain one acquisition template, followed by a small number – often just one – of science and optionally night-time calibration templates. The available templates are listed in the following subsections, and possible night-time calibrations are listed in Section 7.3. Note that it is not possible to mix NIX and SPIFFIER templates in a single OB.

7.4.2 Templates

A full list and description of the templates, including their input parameters, is given in the ERIS Template Manual[18] (RD2). To prepare your observations, you will need to look in this manual for a description of the template keywords.

All acquisition, observing, and calibration templates for NIX and SPIFFIER will be visible to users of p2 when configuring OBs. These can easily be separated by the naming convention (which always includes either 'ifs' for SPIFFIER or 'nix' for NIX). Mixing of inappropriate combinations (e.g. noAO acquisition with the smallest plate scale in SPIFFIER) are not permitted, and will generate an error in p2.

SPIFFIER Acquisition Templates

`ERIS_ifs_acq_NGS`	Acquisition using NGS-AO
`ERIS_ifs_acq_LGS`	Acquisition using LGS-AO and seeing enhancer modes.
`ERIS_ifs_acq_NGS_difftrack`	Same as `ERIS_ifs_acq_NGS` but additional information on the non-sidereal motion of the target/reference star can be provided
`ERIS_ifs_acq_LGS_difftrack`	Same as `ERIS_ifs_acq_LGS` but additional information on the non-sidereal motion of the target/reference star can be provided
`ERIS_ifs_acq_noAO`	Applicable to seeing limited observations.

SPIFFIER Observing Templates

`ERIS_ifs_obs_AutoJitter`	Automatically generates a pseudo-random sequence of (object only) dither positions within a defined range.
`ERIS_ifs_obs_FixedSkyOffset`	Similar to the above template, but with an equal number of matching sky positions at a single relative offset.
`ERIS_ifs_obs_GenericOffset`	Freely definable sequence of object and sky positions.

Table 29: Summary of acquisition and observing templates for SPIFFIER

---

[17]https://www.eso.org/sci/facilities/paranal/instruments/eris/tools.html
[18]https://www.eso.org/sci/facilities/paranal/instruments/eris/doc.html

7.4.2.1 SPIFFIER science templates The summary of SPIFFIER acquisition and observing templates is given in Table 29, and a few additional details are provided here. The common parameters for all templates are: `DET.DIT` (detector integration time in seconds), `INS.SPXW.NAME` (pixel scale either 25mas, 100mas or 250mas), `INS.BAND.NAME` (instrument band configuration, refer to Table 9). The templates will set both filter and grating wheel to appropriate positions for a given configuration.

SPIFFIER acquisition templates:

- The NGS acquisition template is `ERIS_ifs_acq_NGS`. It requires information on the NGS star, target, and the telescope guide star. The position angle on-sky can be set (keyword `TEL.ROT.OFFANGLE`).

- The `ERIS_ifs_acq_LGS` template is for acquisition in LSG mode. Configuration is similar to NGS mode.

- The template `ERIS_ifs_acq_noAO` is for acquiring the target without the use of the AO system, i.e. seeing limited observations.

SPIFFIER observing templates:

- The `ERIS_ifs_obs_AutoJitter` template provides `SEQ.NOFF` number of random offsets inside a square box of size `SEQ.JITTER.WIDTH` arcseconds. `DET.NDIT` and `SEQ.NEXPO` can be used to specify number of DITs and exposures per offset position. Random dithers are useful to average out the effects of the flat fielding. Note that this template does not provide dedicated sky exposures because it is expected that the sky background can be derived from the object exposures. In the following example, SPIFFIER is configured in K_low and in 100mas. The telescope will perform five dithers within a 4x4 arcsecond box. In each offset, the detector will be integrated 3 times for 20 seconds.

ERIS_ifs_obs_AutoJitter

Parameter	Value	p2 label
DET.DIT	20	Detector integration time
DET.NDIT.LIST	3	Number of detector integrations
SEQ.JITTER.WIDTH	4	Jitter width
SEQ.NEXPO	1	Number of exposures per offset position
SEQ.NOFF	5	Number of offset positions
INS.BAND.NAME	K_low	SPIFFIER wavelength band name
INS.SPXW.NAME	100mas	SPIFFIER scale size (arcsec)

- The `ERIS_ifs_obs_FixedSkyOffset` template is similar to that above but also provides random dithers for sky exposures centred around a fixed offset from the original pointing of `SEQ.SKY.OFFSETALPHA`, `SEQ.SKY.OFFSETDELTA` (RA,DEC). If `SEQ.ABBA` is `T`, a (OS)→(SO) pattern will be used, otherwise a (OSO)→(OSO) pattern is adopted. Here, `O` is for object and `S` is for sky frames. `SEQ.NABCYCLES` can be used to specify the number of cycles. Note that one full (OS)→(SO) pattern counts as two cycles, as does one (OSO)→(OSO) pattern. The number of integrations that are averaged needs to be set individually by `SEQ.NDIT.OBJECT` and `SEQ.NDIT.SKY` respectively for object and sky. `SEQ.NEXPO` defines the number of separate exposures per offset, and it is common to both sky and object offsets. Finally, the AO loop state is tied to `SEQ.OBSTYPE.LIST`, where the AO loops are closed for `O` exposures and open for `S` exposures. The example is the same as for `ERIS_ifs_obs_AutoJitter` with the exception of sky frames which are centred 20 arcsec east and 10 arcsec south of the science target. The template will perform (OS)→(SO)→(OS) offsets in this case with `SEQ.NABCYCLES=3`.

ERIS_ifs_obs_FixedSkyOffset

Parameter	Value	p2 label
DET.DIT	20	Detector integration time
SEQ.ABBA	T	Implement ABBA object/sky sequence
SEQ.JITTER.WIDTH	4	Jitter width
SEQ.NABCYCLES	3	Number of AB/BA cycles or ABA cycles
SEQ.NDIT.OBJECT	3	NDIT for the OBJECT positions
SEQ.NDIT.SKY	3	NDIT for the SKY positions
SEQ.NEXPO	1	Number of exposures per offset position
SEQ.SKY.OFFSETALPHA	20	telescope offset to sky in RA
SEQ.SKY.OFFSETDELTA	-10	telescope offset to sky in Dec
INS.BAND.NAME	K_low	SPIFFIER wavelength band name
INS.SPXW.NAME	100mas	SPIFFIER scale size (arcsec)

- `ERIS_ifs_obs_GenericOffset` is the most advanced template and gives full flexibility to the observers. The observers are expected to provide a list of offsets along two axes with `SEQ.OFFSET1.LIST` and `SEQ.OFFSET2.LIST`, while the total number of offsets is defined by `SEQ.NOFF`. The keyword `SEQ.OFFSET.COORDS`

identifies whether the offset coordinate system is on `SKY` or on the `DETECTOR`, see Section 7.2.4.3 for details. Additionally, the number of DITs (`DET.NDIT.LIST`) and the observation type (`SEQ.OBSTYPE.LIST`, either `O` for object or `S` for sky) needs to be defined for each offset. The example configuration performs a four point dither around the object, following a square box of size 4 arcseconds. Note that the offsets are *relative to the previous position* in all ERIS observing templates.

`ERIS_ifs_obs_GenericOffset`

Parameter	Value	p2 label
DET.DIT	20	Detector integration time
DET.NDIT.LIST	3 3 3 3	List of NDITs
SEQ.NEXPO	1	Number of exposures per offset position
SEQ.NOFF	4	Number of offsets
SEQ.OBSTYPE.LIST	O O O O	List of observation types (O or S)
SEQ.OFFSET.COORDS	DETECTOR	Offset coordinate type selection
SEQ.OFFSET1.LIST	-2 4 0 -4	List of telescope offsets in RA or X
SEQ.OFFSET2.LIST	-2 0 4 0	List of telescope offsets in DEC or Y
SEQ.RETURN	F	Return to origin? (T/F)
INS.SPXW.NAME	25mas	SPIFFIER scale size (arcsec)
INS.BAND.NAME	K_low	SPIFFIER wavelength band name

NIX Acquisition Templates

ERIS_nixIMG_acq_NGS	Standard acquisition for all closed-loop AO modes using a natural guide star
ERIS_nixIMG_acq_LGS	Standard acquisition for all closed-loop AO modes using a laser guide star or for seeing enhanced observations
ERIS_nixIMG_acq_NGS_difftrack	Same as ERIS_nixIMG_acq_NGS but additional information on the non-sidereal motion of the target/reference star can be provided
ERIS_nixIMG_acq_LGS_difftrack	Same as ERIS_nixIMG_acq_LGS but additional information on the non-sidereal motion of the target/reference star can be provided
ERIS_nixIMG_acq_noAO	Standard acquisition for seeing limited observations.
ERIS_nixAPP_acq_NGS ERIS_nixAPP_acq_LGS ERIS_nixFPC_acq_NGS ERIS_nixLSS_acq_NGS ERIS_nixLSS_acq_LGS ERIS_nixSAM_acq_NGS	These templates are similar to nixIMG acquisition templates. Distinct templates are necessary to ensure correct keyword associations. Slight nuances exist if a given mode requires additional steps during acquisition. For example, the target must be along the slit for LSS mode.

NIX Observing Templates

ERIS_nixIMG_obs_GenericOffset ERIS_nixAPP_obs_GenericOffset ERIS_nixFPC_obs_GenericOffset ERIS_nixLSS_obs_GenericOffset** ERIS_nixSAM_obs_GenericOffset	Freely definable sequence of pointing positions.
ERIS_nixIMG_obs_AutoJitter	Automatically generates a pseudo-random sequence of (object only) dither positions within a defined range.
ERIS_nixLSS_obs_AutoJitterOnSlit	Similar to above but only jitters parallel to the slit.

**The offsets within this template are parallel and perpendicular to the slit.

Table 30: Summary of acquisition and observing templates for NIX.

7.4.2.2 NIX science templates In general, NIX observing templates follow similar concepts to those for SPIFFIER. There are, however, a different set of parameters specific to NIX. They are described below:

- `DET.READOUT` is either `SLOW_GR_UTR` or `FAST_UNCORR` for the slow and fast modes respectively (see Section 2.4.1).

- `INS.NXCW.NAME`, `INS.NXFW.NAME`, and `INS.NXPW.NAME` are used to set the camera wheel, filter wheel, and pupil wheel positions respectively. Available setups are given in Section 3.5. If there is only single compatible option for a given mode, one or more parameters may be hidden (e.g. `INS.NXPW.NAME=APP` and hidden in APP templates)

- `SEQ.NIX.DET.WINDOWING` is used to specify the sub-array configuration for the detector readouts from among the pre-defined configurations given in Section 2.4.1.2.

- `SEQ.CUBE.ST` (`T/F`) is another keyword specific to NIX, which determines the data format. If set to `T`, the number `NDIT` of exposures are taken and tiled along the third axis of the fits cube. The default behavior (`F`) is to take an average of the individual exposures, then as single mean combined image is saved instead. `NDIT` limits in cube mode are given 4.2.1.2.

We provide below a set of selected NIX template configurations for completeness and to illustrate relevant detector setups.

- `ERIS_nixIMG_obs_AutoJitter` is similar to `ERIS_ifs_obs_AutoJitter` except for the specific details of the NIX configuration. The following example is representative of observations with the `Lp` filter. Thirty random offsets are requested within a jitter box limited to about half of the FOV. At each dither, an effective exposure of 20 seconds will be taken (`DITxNDIT`, `0.2x100`).

ERIS_nixIMG_obs_AutoJitter

Parameter	Value	p2 label
DET.DIT	0.2	Detector integration time
DET.NDIT	100	Number of detector integrations
DET.READOUT	FAST_UNCORR	Detector readout mode
SEQ.CUBE.ST	F	Store Data Cube? (T/F)
SEQ.JITTER.WIDTH	13	Jitter width
SEQ.NEXPO	1	Number of exposures per offset position
SEQ.NIX.DET.WINDOWING	windowF	NIX Detector windowing
SEQ.NOFF	30	Number of offset positions
INS.NXCW.NAME	13mas-LM	NIX camera wheel
INS.NXFW.NAME	Lp	NIX filter wheel
INS.NXPW.NAME	LM-pupil	NIX pupil wheel

- `ERIS_nixIMG_obs_GenericOffset` is similar to `ERIS_ifs_obs_GenericOffset` except for the specific details of the NIX configuration. In the example, NIX is configured to observe a target with a 5-point dither with the `Ks` filter and the 13 mas/pix pixel scale. Large offsets may be necessary to avoid the overlap of bad pixels in the final stacked images.

ERIS_nixIMG_obs_GenericOffset

Parameter	Value	p2 label
DET.DIT	20	Detector integration time
DET.NDIT	1	Number of detector integrations
DET.READOUT	SLOW_GR_UTR	Detector readout mode
SEQ.CUBE.ST	F	Store Data Cube? (T/F)
SEQ.NEXPO	1	Number of exposures per offset position
SEQ.OFFSET.COORDS	SKY	Offset coordinate type selection
SEQ.OFFSET1.LIST	0 -7 14 0 -14	List of offsets coordinates in RA or X
SEQ.OFFSET2.LIST	0 -7 0 14 0	List of offsets coordinates in DEC or Y
SEQ.NIX.DET.WINDOWING	windowF	NIX Detector windowing
SEQ.NOFF	5	Number of offset positions
INS.NXCW.NAME	13mas-JHK	NIX camera wheel
INS.NXFW.NAME	Ks	NIX filter wheel
INS.NXPW.NAME	JHK-pupil	NIX pupil wheel

- `ERIS_nixAPP_obs_GenericOffset` is equivalent to `ERIS_nixIMG_obs_GenericOffset`. The following example is designed to use two alternating positions on the detector and slightly jitter around each one. At each dither, data is recorded continuously for about two minutes with DIT=0.5s in cube mode. Jittering would allow averaging detector effects and alternating nodding positions (with large enough offsets) to monitor skies at each position.

ERIS_nixAPP_obs_GenericOffset

Parameter	Value	p2 label
DET.READOUT	FAST_UNCORR	Detector readout mode
SEQ.CUBE.ST	T	Store Data Cube? (T/F)
SEQ.NEXPO	1	Number of exposures per offset position
SEQ.NIX.DET.WINDOWING	window4	NIX Detector windowing
SEQ.NIX.DIT.LIST	0.5	List of detector integration time
SEQ.NIX.NDIT.LIST	240	List of number of detector integrations
SEQ.OBSTYPE.LIST	O O O O O	List of observation types (O or S)
SEQ.OFFSET.COORDS	DETECTOR	Offset coordinate type selection
SEQ.OFFSET1.LIST	0 0.05 15 -0.1 -15	List of offsets coordinates in RA or X
SEQ.OFFSET2.LIST	0 0.05 0 -0.1 0	List of offsets coordinates in DEC or Y
INS.NXCW.NAME	13mas-LM	NIX camera wheel
INS.NXFW.NAME	Br-a	NIX filter wheel

- ERIS_nixFPC_obs_GenericOffset is equivalent to ERIS_nixIMG_obs_GenericOffset. In the example NIX is configured to observe a target in *L*-band at and perform regular 15″ sky offsets.

ERIS_nixFPC_obs_GenericOffset

Parameter	Value	p2 label
DET.READOUT	FAST_UNCORR	Detector readout mode
SEQ.NEXPO	1	Number of exposures per offset position
SEQ.NIX.DET.WINDOWING	window3	NIX Detector windowing
SEQ.NIX.DIT.LIST	0.3	List of detector integration time
SEQ.NIX.NDIT.LIST	400 10 400 10	List of number of detector integrations
SEQ.NOFF	4	List of offset positions
SEQ.OBSTYPE.LIST	O S O S	List of observation types (O or S)
SEQ.OFFSET.COORDS	DETECTOR	Offset coordinate type selection
SEQ.OFFSET1.LIST	0 0 0 0	List of offsets coordinates in RA or X
SEQ.OFFSET2.LIST	0 15 -15 15	List of offsets coordinates in DEC or Y
INS.NXFW.NAME	Lp	NIX filter wheel
INS.NXPW.NAME	Lyot	NIX pupil wheel

- ERIS_nixLSS_obs_AutoJitterOnSlit is unique to NIX long slit spectroscopy mode. There is no need for explicitly specifying the instrument configuration since there is a single allowed combination of NIX mechanisms. The template will offset the object along the slit in random movements. The range of offsets is given by SEQ.JITTER.WIDTH (note this is total range centred around the first position), the number of offsets is set by SEQ.NOFF. While using fast readout mode, observers are requested to combine multiple fast exposures to obtain a single exposure of at least 2 sec, in order to reduce the data rate and improve the observing efficiency. For example, with the following setup, observers can obtain three images (SEQ.NEXPO) per offset position and each image is equivalent to the mean of 20 images (SEQ.NDIT) of DIT=0.2', seconds.

ERIS_nixLSS_obs_AutoJitterOnSlit

Parameter	Value	p2 label
DET.DIT	0.2	Detector integration time
DET.NDIT	20	Number of detector integrations
DET.READOUT	FAST_UNCORR	Detector readout mode
SEQ.CUBE.ST	F	Store Data Cube? (T/F)
SEQ.JITTER.WIDTH	10	Jitter width
SEQ.NEXPO	3	Number of exposures per offset position
SEQ.NOFF	2	Number of offset positions

- ERIS_nixLSS_obs_GenericOffset is very similar to ERIS_nixLSS_obs_AutoJitterOnSlit. All comments about mechanism setup, exposure times and windowing also apply for this template. The main difference is that the user can request a list of offsets. The template uses a similar keyword convention to other NIX imaging generic offset templates, with the user specifying the number of offset positions, the type of offset and the scale of the movement. The offsets are defined either parallel or perpendicular to slit, they are in units of arcsec and are cumulative.

ERIS_nixLSS_obs_GenericOffset

Parameter	Value	p2 label
DET.DIT	0.2	Detector integration time
DET.NDIT	20	Number of detector integrations
DET.READOUT	FAST_UNCORR	Detector readout mode
SEQ.CUBE.ST	F	Store Data Cube? (T/F)
SEQ.OBSTYPE.LIST	O O	List of observation types (O or S)
SEQ.OFFSET1.LIST	-2 4	List of offsets coordinates parallel to the slit
SEQ.OFFSET2.LIST	0 0	List of offsets coordinates perpendicular to the slit
SEQ.NEXPO	3	Number of exposures per offset position
SEQ.NOFF	2	Number of offset positions

- ERIS_nixSAM_obs_GenericOffset is equivalent to ERIS_nixIMG_obs_GenericOffset. In the example NIX is configured to observe a target with a 2-point dither with the Pa-b filter and the 13 mas/pix pixel scale with the SAM-23 mask.

ERIS_nixSAM_obs_GenericOffset

Parameter	Value	p2 label
DET.READOUT	SLOW_GR_UTR	Detector readout mode
SEQ.CUBE.ST	T	Store Data Cube? (T/F)
SEQ.NEXPO	1	Number of exposures per offset position
SEQ.NIX.DET.WINDOWING	window4	NIX Detector windowing
SEQ.NIX.DIT.LIST	1	List of detector integration time
SEQ.NIX.NDIT.LIST	20	List of number of detector integrations
SEQ.NOFF	2	List of offset positions
SEQ.OBSTYPE.LIST	O O	List of observation types (O or S)
SEQ.OFFSET.COORDS	DETECTOR	Offset coordinate type selection
SEQ.OFFSET1.LIST	-2 4	List of offsets coordinates in RA or X
SEQ.OFFSET2.LIST	0 0	List of offsets coordinates in DEC or Y
INS.NXCW.NAME	13mas-JHK	NIX camera wheel
INS.NXFW.NAME	Pa-b	NIX filter wheel
INS.NXPW.NAME	SAM-23	NIX pupil wheel

7.4.3   OB naming rules

In addition to the general naming rules, ERIS OBs must have a prefix indicating the instrument setup and AO mode used by the OB. For example:

- IFS_NGS_[OB name]

- IFS_LGS_[OB name]

- IFS_LGS-SE_[OB name]

- IFS_noAO_[OB name]

- ...

- nixIMG_NGS_[OB name]

- nixAPP_NGS_[OB name]

- nixFPC_NGS_[OB name]

- nixLSS_NGS_[OB name]

- nixSAM_NGS_[OB name]

- ...

- MOV_nixIMG_LGS_[OB name]

or, in general: [observatory prefix]_[instrument mode]_[AO mode]_[OB name]. More information can be found on the ESO website page[19].

---

[19]https://www.eso.org/sci/observing/phase2/SMGuidelines/OBNaming.ERIS.html

8 Data reduction

This section summarises the templates, data, and recipes necessary for the processing of NIX/SPIFFIER observations.

8.1 SPIFFIER

8.1.1 Day-time calibrations

The following items are necessary calibrations for SPIFFIER to generate a reconstructed cube corrected for detector and instrumental signatures.

Master Dark
Template: `ERIS_ifs_cal_Darks`
Data: Five dark images (DIT).
Purpose: Generate master dark for a given DIT and locate hot pixels.

Master Flat
Template: `ERIS_ifs_cal_LampFlats`
Data: five lamp-on and five lamp-off flat images.
Purpose: Generate master flat for a given band and pre-optics in order to correct the pixel-to-pixel sensitivity of the detector.

Wavelength Maps
Template: `ERIS_ifs_cal_Arcs`
Data: Pre-defined number of calibration spectra with combinations of Ne, Ar, Kr and Xe pen ray lamps and additional exposures with all lamps off.
Purpose: Wavelength calibration solution for a given band and pre-optics.

Distortion
Template: `ERIS_ifs_tec_NorthSouth`
Data: Pre-defined number of images of the triple slit mask (slits oriented along the detector columns) with back illumination on and off.
Purpose: Measure the relative positions of the slitlets with respect to each other on the detector and determine distortion correction map.

Gain and Linearity
Template: `ERIS_ifs_tec_GainLinearity`
Data: A series of flat images with increasing DIT (two of each) followed by a series of darks for the same DITs (two of each).
Purpose: Determine read-out noise, gain, detector linearity, bad pixel map.

8.1.2 Night-time calibrations

The following items list on-sky calibrations for SPIFFIER to correct for the atmospheric transmission and provide photometric and PSF calibrations.

Standard star
Template: `ERIS_ifs_cal_StandardStar`
Data: A set of object and sky exposures of a telluric standard star.
Purpose: Correct for the atmospheric (and instrument) transmission in the observed science data. Photometric calibration is achieved by using telluric standards of known magnitudes.

PSF star
Template: `ERIS_ifs_cal_PSF`
Data: A set of object and sky exposures of a PSF standard.
Purpose: Determine instrument/AO point spread function.

8.1.3 Recipes

In this subsection, methods used by the pipeline to generate calibration and science products are briefly described.

Detector linearity determination
Recipe: `eris_ifu_detlin`
A series of flat images with increasing DIT are used to determine non-linear pixels on the detector.

Bad pixel map and master dark determination
Recipe: `eris_ifu_dark`
A set of dark calibration frames is stacked to produce master dark frame. For each pixel, the standard deviation of intensity is computed to detect bad pixels and generate bad pixel map.

Master flat determination
Recipe: `eris_ifu_flat`
The lamp-off frames are subtracted from the lamp-on frames. The frames are combined via stacking into a master flat image.

Spectral distortion determination
Recipe: `eris_ifs_distortion`
Arc lamp and slit images are used to calculate the distortion of the slitlets on the detector. The information will then be used to map raw data to proper coordinates.

Wavelength calibration
Recipe: `eris_ifu_wavecal`
Using reference line tables, various lines are detected on arc lamp images. A polynomial fit on the detected lines allows to generate a wavelength calibration map.

Standard star data reduction
Recipe: `eris_ifu_jitter`
A series of object-sky frames of telluric standard are reduced and collapsed into data cubes. Standard star spectrum is optimally extracted from the cube to be used as scientific calibration input.

PSF star data reduction
Recipe: `eris_ifu_jitter`
A series of object-sky frames of the PSF reference are reduced and collapsed into data cubes. The PSF file is generated and strehl is computed.

Science data reduction
Recipe: `eris_ifu_jitter`
A series of object-sky frames of a science target are reduced and collapsed into data cubes. When a normalised telluric spectrum is given as input frame it will be used to correct the telluric features.

8.2 NIX

The approach to NIX data reduction is slightly different to SPIFFIER. The first step is to correct each exposure for detector signatures. Dark and gain-linearity are common calibrations for all observing modes,

- **Master Dark**
  Template: `ERIS_nix_cal_Darks`
  Recipe: `eris_nix_dark`
  Data: Five dark exposures with matching (DITxNDIT)
  Purpose: Generate a master instrumental dark and detect hot pixels.

- **Gain Linearity**
  Template: `ERIS_nix_tec_GainLinearity`
  Recipe: `detmon_ir_lg`
  Note: This recipe was developed by ESO, for details see `https://www.eso.org/sci/software/pipelines/detmon/detmon-pipe-recipes.html`
  Data: Set of dark and illuminated exposures with increasing DIT up to or near full well. Two of each.
  Purpose: Estimate the pixel-wise linearity curve, detect non-linear cold pixels.

8.2.1 Imaging

8.2.1.1 Master flats There are two options for flats in the imaging mode. Lamp flats at <2.5 μm will be taken with CU flat lamp. In >2.5μm, sky flats will be used for flat-fielding purposes. The corresponding recipes provide; low-frequency flat-field (optical flat-field), high-frequency flat-field (pixel-to-pixel sensitivity) and a bad pixel map. Alternatively, twilight flats can be used in conjunction with lamp flats to replace the low frequency flat-field.

Lamp Flats
Template: `ERIS_nixIMG_cal_LampFlats`
Recipe: `eris_nix_flat_lamp`
Data: Five illuminated and five dark frames at the same configuration of science observations.

Sky Flats
Template: `ERIS_nixIMG_cal_SkyFlats`
Recipe: `eris_nix_flat_sky`
Data: Seeing limited sky observations with 5 dithers at least two airmasses.

Twilight Flats
Template: `ERIS_nixIMG_cal_TwilightFlats`
Recipe: `eris_nix_flat_twilight`
Data: Sky exposures while the telescope is at zenith during twilight time as the background decays.

8.2.1.2 On-sky calibrators `ERIS_nixIMG_cal_StandardStar` and `ERIS_nixLSS_cal_StandardStar` can be used to observe a standard star at selected configurations. If requested, it is charged to the user. Reduction of this data follows the description in Section 8.2.1.3.

8.2.1.3 Data reduction The workflow for the NIX imaging data reduction is `eris_nix_img_cal_and_stack`. In a nutshell, this involves five steps each associated with their corresponding recipe:

1. `eris_nix_cal_det` – Removes detector signatures from each frame.

2. `eris_nix_img_skysub` – Calculates and removes sky background from each frame.

3. `eris_nix_img_cal_wcs` – Find catalogue sources in each frame to refine WCS coordinates

4. `eris_nix_img_cal_phot` – Calculates photometric zeropoint of each frame.

5. `eris_nix_img_hdrl_stack` – Stacks all processed object frames.

8.2.2 High-contrast modes

In high contrast imaging modes, corresponding dark, gain linearity and flat field calibrations (with nominal imaging pupil and aperture) will be provided. The data can be reduced in the same manner discussed in Section 8.2.1 up to `eris_nix_cal_det` step. NIX pipeline does not provide any post-processing option from here onwards.

8.2.3 Long slit spectroscopy

The reduction of long-slit spectroscopic data is fully supported by the pipeline, up to the extraction of a calibrated one-dimensional spectrum.

8.3 Useful FITS header keywords

The header contains a large number of keywords containing information regarding the instrument and telescope at the time the image was recorded. This section describes some of the more useful keywords when reducing ERIS data.

8.3.1 Ambient conditions

- `TEL.AMBI.FWHM.START/END` - DIMM seeing at start/end of exposure.

- `TEL.AMBI.TAU0` - τ_0 queried at end of exposure.

Time series of these parameters can be obtained from the ESO archive[20].

8.3.2 Telescope

- `RA/DEC` - Mean RA/Dec at the current epoch in the specified `EQUINOX` and `RADECSYS`, accounting for proper motion, if specified.

- `TEL.PARANG.START/END` - Parallactic angle at start/end of exposure. This is calculated from the telescope altitude and azimuth at the current pointing, corrected for misalignment. The algorithm converts the corrected topocentric observed altitude and azimuth into geocentric apparent RA/Dec using `slaOap`, and then into mean-of-date RA/Dec using `slaAmp`. This procedure is repeated for a simulated pointing $0.2''$ lower in altitude. The parallactic angle, computed using `slaDbear` with these mean-of-date coordinates, is the angle between the local vertical and the mean north celestial pole of date. For the purposes of ERIS observations, this is functionally equivalent to the standard definition of the parallactic angle with respect to the true north celestial pole of date, differing by at most $0.01°$ for altitudes above $30°$. To re-compute the parallactic angle at intermediate times, e.g., for cube-mode observations, the mean coordinates (`RA/DEC`) must be precessed to the equinox of the observations for consistency.

- `TEL.ROT.ALTAZTRACK` - Keyword present and "T" if pupil tracking, absent if field tracking.

- `TEL.TARG.ALPHA/DELTA` - RA/Dec at the specified `TEL.TARG.EPOCH/EQUINOX`, supplied by the user.

- `TEL.TARG.PMA/PMD` - Proper motion at the specified `TEL.TARG.EPOCH/EQUINOX`, supplied by the user.

- `ADA.ABSROT.START/END` - Absolute rotator angle at start/end of exposure.

8.3.3 AO

- `AOS.NGS/LGS.FREQ` - High-order loop frequency.

- `AOS.LO.LO_FREQ` - Low-order loop frequency.

- `AOS.NGS/LGS.LOOP_MATRICES` - Matrices generation date, and number of modes corrected.

- `AOS.NGS/LGS/LO.WFS.FLUX` - Average wavefront sensor flux.

- `OCS.AASALARM` - If "1" an aircraft alarm was triggered causing the laser propagation to be temporarily paused during this exposure.

8.3.4 NIX

The keywords for NIX are in the `INS2` group. These include keywords describing the mechanism positions and temperatures.

8.3.5 SPIFFIER

The keywords for SPIFFIER are in the `INS3` group. These include keywords describing the mechanism positions and temperatures.

---

[20]`https://archive.eso.org/cms/eso-data/ambient-conditions/paranal-ambient-query-forms.html`